1-2008

Electrical Imaging Hydro chemical and isotope investigation of Mubazarah area in UAE (AL-Ain)

Faris Mirghani Mahgoub

United Arab Emirates University
Deanship of Graduate Studies
M. Sc. Water Resources Program

Electrical Imaging , hydrochemical and isotope investigation of Mubazarah area, Al-Ain, (U.A.E).

By

Faris Mirghani Mahgoub

A Thesis Submitted to

Deanship of Graduate Studies
United Arab Emirates University

In the Partial Fulfillment of the Requirements for the M.Sc. Degree in

Water Resources

Deanship of Gradate Studies
United Arab Emirate University
January, 2008

United Arab Emirates University
Deanship of Graduate Studies
M. Sc. Water Resources Program

Thesis Title

Electrical Imaging, hydrochemical and isotope investigation of Mubazarah area, Al Ain, United Arab Emirates, (U.A.E)

Author's Name

Faris Mirghani Mahgoub

Supervisors

No	Name	Position
1	Dr. Ahmed Murad	Head of Geology Department, Assistant professor of Hydrogeology, Geology Department, College of Science, United Arab Emirates University
2	Dr. Ahmad El-Sayed El-Mahmoudi	Associate Professor of Geophysics, Water Studies Center, King Faisl University, KSA
3.	Dr. Haydar A. Baker	Professor of Applied Geophysics, Department of Geology, College of Science, United Arab Emirates University

Thesis of Faris Mirghani Mahgoub
Submitted in Partial Fulfillment for the Degree of
Master of Science in Water Resources

Chair of Examination Committee
Dr. Ahmed Murad, Assistant Professor of Hydrogeology .....
Geology Department
United Arab Emirates University.

External Examiner
Prof. Alan E. Kehew .....
Department of Geosciences
Western Michigan University

Internal Examiner
Prof. Abdulrazag Y. Zekri .....
Chemical & Petroleum Engineering Department
United Arab Emirates University

Assistant Chief Academic Officer for Graduate Studies
Prof. Ben Bennani .....

United Arab Emirates University
2007/2008

To
To the lovely memory of my father

"O Lord, bestow on them the Mercy even as they cherished me in childhood." (The Holy Quran 17: 24)

ACKNOWLEDGMENT

All praise and thanks are due to Almighty Allah, Most Gracious; Most Merciful, for the immense mercy which have resulted in accomplishing this research. May peace and blessings be upon prophet Muhammad (PBUH), his family and his companions.

I have to thank my thesis Committee Chairman, Dr. Ahmed Murad for guiding me through the writing of the thesis, and for all the corrections and revisions made to text that is about to be read. It became a lighter and more concise thesis after his suggested improvements. I also acknowledge with enormous gratitude the inspiration, encouragement, valuable time and guidance showed by my other supervisor, Dr. Ahmed Almahmoudi. Without his substantial knowledge of Geophysics and Groundwater Exploration I would not have been able to complete this work. I have learned so much from working with Ahmed Murad and Ahmad Almahmoudi over the years.

I am also greatly indebted to my thesis committee member Dr. Haydar Baker for his valuable comments which have increased the value of my research. I would also like to thank Dr. Mohsin Sherif, the director of Water Resources Master Program for his support during the duration of the research.

I would like also to acknowledge UAEU for the support extended towards my research through its remarkable facilities and for providing me the opportunity to pursue graduate studies.

My sincere thanks go to Mr. Mohammed Khalifa for helping and providing me his valuable papers and articles.

I would like also to extend my deep thanks and appreciation to the staff of Al-Ain Municipality, Agricultural Department for their help in water sampling for my study.

All parents are a gift to their children. In that sense, my parents have always been there for me in my good and difficult times. They have supported me in everything that I have endeavored and their continual encouragement has lifted my confidence whenever I encountered problems. Their wisdom and knowledge have made me into a better person. Words fall short in conveying my gratitude towards them. A prayer is the simplest means I can repay them. This thesis is dedicated to the memory of my father. He has been wonderful father and has shown a genuine interest in and concern for my life, my work and my well-being.

Finally, I would like to thank everybody who was important to the successful realization of this thesis, as well as expressing my apologies that I could not mention everyone personally.

ABSTRACT

In the last few decades, the United Arab Emirates has experienced extraordinary development. Such fast development imposes great pressure on natural resources, including water. Regardless of the severe shortage in the natural water resources, the per capita water consumption in the UAE is 500 liters a day, which is among the highest in the world.

Al-Ain, like many other cities in UAE, is promoting tourism and the recently formed Al-Ain economic and Tourism Board is looking to Mubazarah and its surrounding area as major site for tourism. The recently published Jabal Hafit development master plan Report (Town Planning Department, Al-Ain, 2001) suggests designation of the massif and surrounding area as a National Park.

The focus of the study is Mubazarah area. It lies in a valley about 2 kilometers long by 0.5 kilometer wide at the north end of Jabal Hafit near Al-Ain. Fifteen large diameter wells have been completed in the well field, with about 10 wells capable of producing large quantities of water. Because of its high mineral content and high temperature, the water from the Mubazarah well field should be curative and therapeutic. The Municipality has constructed a spa resort that uses this water to benefit its citizens and visitors. The water is also used for irrigation of salt tolerant forest plantings. However, it is not suitable for drinking because of the high TDS concentration.

This study is devoted to the investigation of the water potentiality and quality of Mubazarah area. It defines the hydrogeological parameters of Mubazarah using different techniques. To that end, detailed geophysical, hydrogeological and hydrochemical investigations were conducted. To achieve this aim, previous studies were reviewed. The required information and data about geology, hydrogeology, climatology, hydrochemistry and geoelectric investigations were collected.

In the hydrogeological aspects of this study, the groundwater bearing formations encompassing Jabal Hafit fractured limestone aquifer, the Quaternary aquifer and gypsum aquifer are presented. The spatial extent and petrophysical

characteristic of these aquifers are the primary factors controlling storage and movement of groundwater. Informations about the aquifers geometry in space, petrophysical parameters, hydrology and drainage basins network are vital to understand the flow regime, recharge mechanism and the boundary conditions of the hydrogeological systems.

One of the new developments in recent years is the use of Electrical Imaging (EI) techniques to provide a cost effective characterization of the subsurface in characterizing on the groundwater conditions of the region. The EI method has been successful in identifying features of concern, in particular sinkholes, fractures, and voids.

The 2-D Electrical Imaging surveys were also utilized nine 2-D resistivity profiles were conducted and oriented along the strike direction of the limestone exposure west of Jabal Hafit area to intersect the maximum possible number of geologic features. Each profile consisted of 30 electrodes spaced 20m apart which penetrate to about 120m depth. The Wenner array was used in this survey and apparent resistivity data was collected and inverted using Res2dinv, ver. 3.54 to create a model of subsurface resistivity that approximated the true subsurface resistivity distribution and displayed this as a cross section. Resistivity data interpretation was constrained by the available borehole lithologies and groundwater salinity data.

In the hydrogeochemical aspects, the physical properties including the hydrogen ion concentration (pH), electrical conductivity (EC), total salinity distribution, temperature and chemical properties including the major cations and anions are discussed. The distribution of various physical and chemical elements and the ion dominance in the groundwater are detailed. To demonstrate the spatial distribution of each hydrochemical parameters, contour maps of each parameter have been created using Surfer mapping system software Ver.8. This hydrogeochemical concluded with an assessment for the suitability of groundwater for irrigation purposes based on SAR and EC. Selected water samples were also analyzed for environmental isotopes including deuterium (δD) and oxygen -18 ($\delta^{18}O$) to provide clues about the genesis and flow path of groundwater.

The conclusions and main findings of the study are presented. Recommendations for future development of the study area are also prepared. Such results will guide planners, decision makers, and researchers to seek solution for groundwater development in the basin and implement ground water resources managing plans.

Table of contents

LIST OF FIGURES

LIST OF TABLES

ABBREVIATIONS

mm	Millimeter
cm^2	Centimeter square
mwh	Million watt per hour
km^2	Kilometer square
hr	Hour
yr	Year
ET	Evapotranspiration
Mm^3	Million Cubic Meters
NDC	National Drilling Company
USGS	United States Geological Survey
EAD	Environmental Agency Department
µS/cm	Micro Siemens per centimeter
GWRP	Groundwater Resources Program
GWAP	Groundwater Assessment Program
Km^3	Cubic Kilometer
m^3	Cubic Meter
mg	milligram
µmhos	Micromohs per centimeters
°C	Degree Centigrade
ppm	Part per million
TSE	Treated Sewage Effluent
TDS	Total Dissolved Solids
EC	Electrical Conductivity
d	Day
l	Liter
ha	Hectare=10,000 Square Meters
gal	Gallon
min	minute
Ω-m	Ohm.meter
ft	Feet
TW-1	Test Well
EI	Electrical Imaging
epm	Equivalent per milliliter
DC	Direct Current
TH	Total Hardness
SAR	Sodium Adsorption Ratio
pH	Hydrogen Ion Concentration
2 D	Two Dimensional
3D	Three Dimensional
V	Voltage
ρ	Resistivity
R	Resistance
I	Current
L	Length
AGI	Advanced Geosciences, Inc
EC	Electrical Conductivity

pH	Hydrogen Ion Concentration
ppm	Part per million
µg/l	Micro gram per liter
SAR	Sodium Adsorption Ratio
SMOW	Standard Mean Ocean Water
VSMOW	Vienna Standard Mean Ocean Water
LGWL	Local groundwater line

CHAPTER 1
INTRODUCTION

Introduction

1.1General Outline

Since the mid 1960s, the Emirate of Abu Dhabi has undergone major development, driven by large oil revenues and the commitment of the former ruler Sheikh Zayed to agriculture and to policy of 'greening of the desert'. Pre-development, a small population relied entirely upon groundwater within shallow aquifers. In the east of the Emirate, fresh groundwater was exploited by shallow wells and by natural falajes for potable use and for traditional agriculture. Westwards, the aquifer contained brackish to saline groundwater.

Abu Dhabi Emirate relies on conventional and non-conventional water resources to meet the ever increasing water demands .The main sources of water in the Emirate are groundwater (Al-Ain, Liwa), desalination plants, and sewage treatment plants (recycled wastewater) . Over the last two to three decades, however, rapid economic development, associated with sharp population increases and the development of a large agricultural sector, considerably supported from government subsidies, has meant an increasing reliance on unconventional water resources, such as desalination and also the development of alternative conventional water supply measures, such as recharge dams, storage dams, recharge wells, interception of groundwater losses, re-use of wastewater and water transfers.

Demand now far exceeds the capacity of the shallow aquifers and Abu Dhabi must increasingly use new water sources, specifically desalinated Arabian Gulf seawater and desalinated water imported from Fujairah on the Gulf of Oman. Development has led to environmental concerns in particular, the local over-abstraction from the surficial aquifer, aquifer salinisation and possible aquifer contamination from chemicals used in the agriculture sector. On the other hand, the proliferation of desalination plants along the Arabian Gulf, and the Emirate increasing reliance upon desalination, leads to both environmental and supply security concerns.

In this chapter a review of the water resources in Abu Dhabi's Emirate in general and a special emphasis was given to Al-Ain area in the eastern region is presented.

1.2 Physical Settings and Climatic Conditions

Abu Dhabi Emirate, one of the seven Emirates which comprise the United Arab Emirates (UAE), occupies an area of 67,340 km², or about 80% of the total area of UAE (Figure 1.1). It comprises the Eastern, Central and Western Regions of Abu Dhabi .It is bounded on the north by the Arabian Gulf and the Northern Emirates (Dubai Emirate), on the east by Sultanate of Oman and on the south and west by Kingdom of Saudi Arabia.

Abu Dhabi Emirate lies within the area of the hot desert climate; its climate is characterized by two main seasons: a long and dry summer, with temperatures rising to about 48°C between May and September; and a short, moderate winter between December and March, where temperatures rarely drop below 6°C. January is considered the coolest month in the year, while July is the hottest month. The yearly mean temperature is estimated at 27°C (Often the maximum temperature reaches 50°C in the southern desert in the summer, and in winter the minimum temperature drops to around 2°C, (Rizk,1999). In addition, the area is semi-permanently dominated by subtropical high pressure cells. The subsiding air results in heating and expands the hot weather conditions. This keeps the annual average of temperature high and makes the area as one of the hottest areas of the world.

Straddling the Tropic of Cancer in the southern part of the Emirate, Abu Dhabi Emirate coincides with the area of the high radiation input, the highest solar radiation is in June (796 mwh/cm^2) and the lowest in December (425 mwh/cm^2) with a monthly average radiation of 664.9 to 798.4 mwh/cm^2 during summer months. A general increase in radiation amount occurs from December to June, and decreases from July to September. The average annual hours of sunshine in the Emirate is 10 hours per day, with a maximum 11.5 hours in May and a minimum of 8.4 hours in December (Al-Shamsi, 1993).

The relative humidity in the Emirate reaches its maximum value during the November-March period and its minimum value in May. Relative humidity is high in the coastal areas, where its average reaches 60% in Abu Dhabi, however, this rate declines sharply with distance inland from the coastline, where its annual average reaches 45% in Al-Ain and 25% in Liwa (Garmoon, 1996).

The Emirate faces two types of wind conditions, winter depressions which descend from the Arabian Gulf to the north and northwest, and the summer monsoonal low which is developed over Rub Al Khali (Rizk, 1999). The wind speed varies between, light to moderate. The annual mean wind speed is less than 18.5 Km/hr, and it decreases from north-northwest to south-southeast (Al Shamsi, 1993).

Rainfall fluctuates widely from year to year and from one area to another. It is noticeable that the mountainous area receives the highest rainfall, followed by the eastern region, and the gravel plain. The amount of rainfall declines as we move towards the desert and western coast areas. The annual average rainfall for UAE was recorded at 110.2 mm. Most of the rainfalls in winter, as a result of atmospheric depressions accompanied with north westerly winds coming from the Mediterranean or by orographic effects. Some of the rain events in the country are accompanied by thunder and lightning, and the event may continue for one and at times up to three days. Summer rain is observed mainly in mountain areas especially in the eastern region, and the southeastern region (Al-Ain) (Ministry of Agricultural and Fisheries, 1993).

Mean annual rainfall within the Abu Dhabi Emirate varies from 46 mm at Jabal Dhana in the Western Region to 119 mm at Al Wigan, south of Al-Ain, in the Eastern Region. The mean annual rainfall at Al-Ain 1971-1994 was 96.4 mm, with a maximum of 303 mm/yr. The mean annual precipitation for Abu Dhabi Island is 87 mm, with a maximum of 227 mm/yr (Brook, 2003).

The evaporation rate is relatively high all over the Emirate. The coast has the lowest annual average pan evaporation between 7.5-8 mm/day, whereas in the western

Figure (1.1): Location Map of Abu Dhabi Emirate, United Arab Emirates.

gravel plain and desert foreland, the evaporation ranges between 10-11 mm/day (Al Nuaimi, 2003).

The average evapotranspiration (ET) value in the Abu Dhabi Emirate changes from one location to the other. In general, annual (ET) ranges between 1,909 mm and 2,124 mm. The minimum value can be observed along the eastern coast while the maximum value can be observed in interior parts. Evapotranspiration is generally high during summer (Al Nuaimi, 2003).

1.3 Water Resources in Abu Dhabi Emirate

Historically, all the Emirate's water requirements were met solely from groundwater obtained from shallow hand dug wells and the traditional falajes system. Pre-development, a small population relied entirely upon groundwater within shallow aquifers. In the east of the Emirate, fresh groundwater was exploited by shallow wells and by natural falajes, for potable use and for traditional agriculture; westwards, the aquifer contained brackish to saline groundwater. At that time, total abstraction did not exceed 200 Mm^3/yr (including falaj flows) of which agriculture consumed 163 Mm^3/yr and forestry, less than 1 Mm^3/y (NDC & USGS, 1996). By contrast, in year 2002 water use is estimated at over 3200 Mm^3/yr (EAD, 2002).

According to Dawoud et al, (2005), the reasons for this massive increase in demand are:

- Very high per-capita potable water consumption. Potable demand is increasing by 8% per annum, concurrently with a 6% per annum population growth.
- Continued expansion in the area under irrigation, comprising amenity planting, forestry and agriculture farms.
- Few, if any constraints on water use.

Groundwater constitutes 79% (78.5% brackish, 0.5% fresh) of all the Emirate's sources, followed by desalinated seawater (17%) and treated wastewater (4%) (EAD, 2003). Figure (1.2) shows the water resources of Abu Dhabi Emirate in 2003, and Figure (1.3) shows the locations of main water resources in the Emirate.

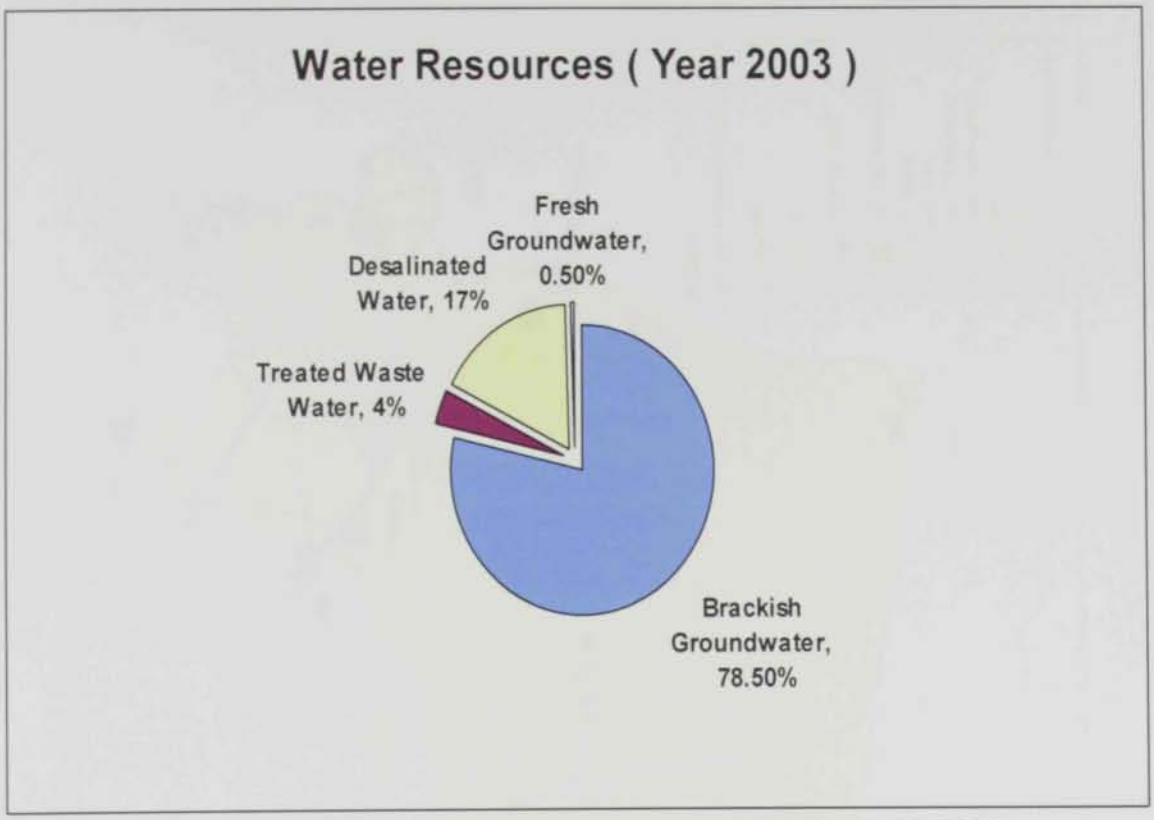

Figure (1.2): Water Resources in Abu Dhabi Emirate in 2003, (EAD, 2003).

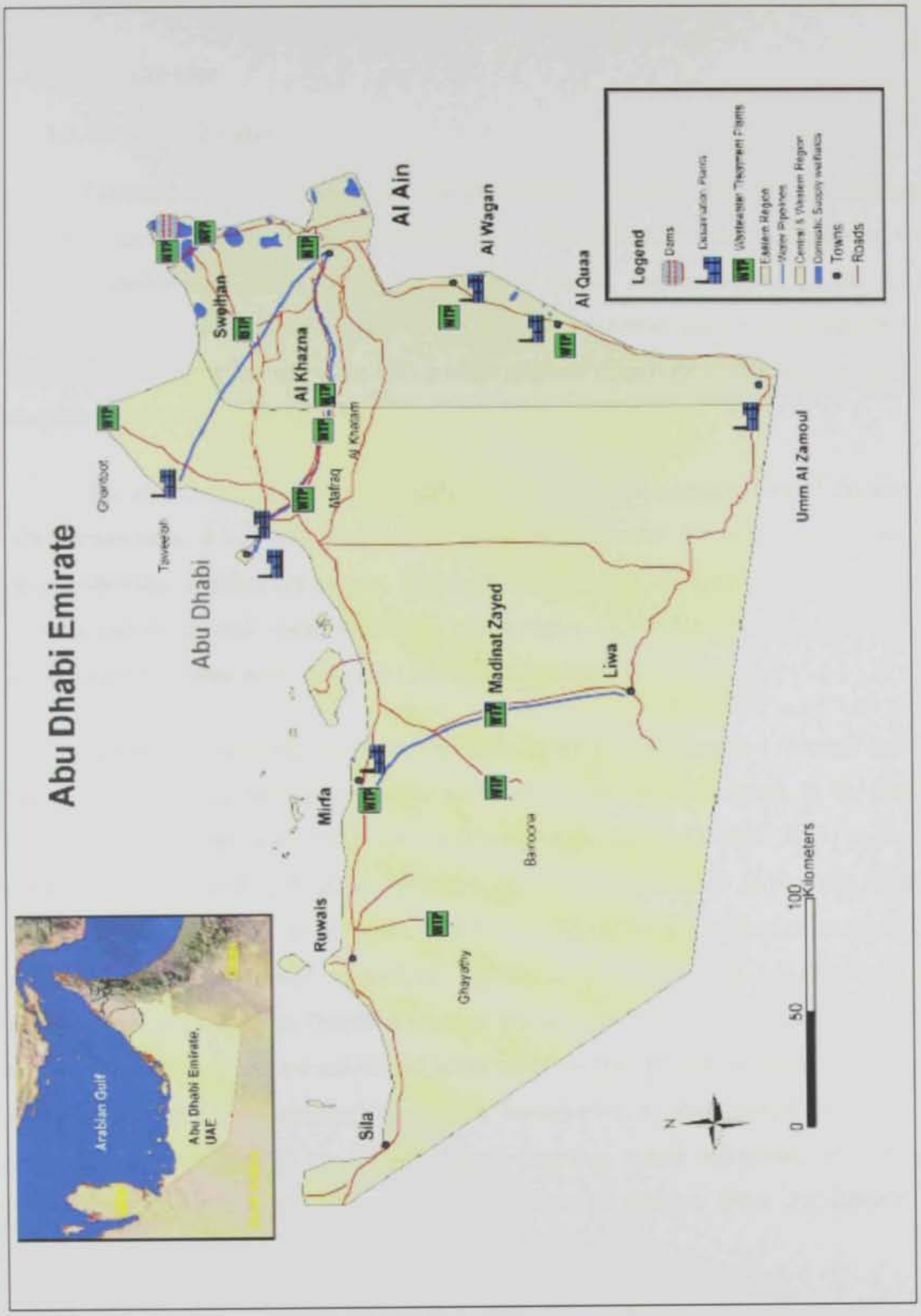

Figure (1.3): Location map of main water resources of Abu Dhabi's Emirate, (EAD, 2001).

1.3.1 Groundwater

1.3.1.1 Groundwater

Groundwater is mostly used in agriculture, forestry and amenity/recreation irrigation. Only a small amount of groundwater is abstracted for municipal drinking water supply (potable well fields are now found only in the eastern region. In the Al-Ain region, 15 well fields contribute only 4% of the total domestic water supply requirements (EAD, 2003). However, there are still a large number of private household wells which abstract water for domestic use.

The shallow aquifer contains freshwater storage in the eastern part of the Emirate while elsewhere, it contains brackish to saline groundwater. No regionally significant deep freshwater aquifers are known. The freshwater storage has long been over-exploited in particular by potable water wellfields in the region of Al-Ain; its use is increasingly constrained by falling well yields and increases in salinity (EAD, 2003).

Brackish to saline groundwater is found in the shallow aquifers through much of the Emirate, and it is utilized for almost all irrigation of farms and forest. In the Eastern Region of Abu Dhabi, year 2002 farm well surveys (Mott MacDonald, 2004) show that agriculture is irrigated with mostly brackish water; of over 24,000 farm wells sampled, 65% of wells have water of EC more than 6,000 μS/cm, while in some areas forests are irrigated with groundwater exceeding 30,000 μS/cm. This use of brackish-saline groundwater in farms and forests irrigation leads to increasing difficulties in soil/salt management, crop yield reduction and constraints on tree growth. Continued expansion of agriculture and forestry may require the introduction of desalinated water into the irrigation systems, yet to do so will clearly involve major infrastructure costs and government policy support. The total groundwater production from the Eastern and Central Regions is about 1,430 Mm^3/yr (Dawoud et al, 2005).

Groundwater, in spite of its heavy exploitation over the last 30 years, still provides the majority of the water supply for Abu Dhabi Emirate. The aquifers developed to date are primarily unconsolidated, Quaternary sands and alluvium found at depths of

generally less than 50 -100 m below ground level. A total of 253,000 Mm^3 occurs as a resource, but only 7% is fresh, the remainder is brackish or saline. Fresh groundwater, with salinity of less than 1,500 mg/l TDS, occurs in belts along the Eastern Region on the border with the Sultanate of Oman and also as a large basin in the Liwa–Beda Zayed area. Figure (1.4) summarizes the groundwater resources (fresh & brackish) of Abu Dhabi Emirate (EAD, 2003).

The Groundwater Resources Program (GWRP) (USGS/NDC, 1996) and Groundwater Assessment Project (GWAP) (GTZ et al, 2005) have used different methods to calculate the groundwater in storage in the Emirate, but both have ultimately calculated average saturated aquifer thickness and specific yield to estimate stored volumes. The volume of fresh groundwater calculated differs by only 8%.

Table (1.1): Abu Dhabi Emirate Groundwater Reserves Estimate from GWRP (NDC & USGS, 1996).

Salinity Zone	Area (m^2x10^6)	Average saturated thickness (m)	Average specific yield (%)	Volume Stored (Km^2)
Fresh – Eastern Region	1,440	20	14%	4
Fresh – Western Region	2,400	26	23%	14
Fresh- Emirate	3,840	-	-	18
Brackish below Fresh Water – Eastern Region	1,440	40	14%	8
Brackish below Fresh Water – Western Region	2,400	69	23%	38
Brackish – Remaining areas	29,983	42	15%	189
Brackish- Emirate	-	-	-	235
Total Fresh Brackish Emirate	-	-	-	253 Km^3

The GWRP calculated a total groundwater reserve of 253 Km^3 (7% fresh, 93% brackish– see Table 1.1).The most striking feature of this estimate is that the amount of

fresh groundwater remaining in storage is very small, and according to the GWRP assessment, at current groundwater abstraction rates, it is projected that the fresh and brackish groundwater resources will be depleted in 50 years.

1.3.1.2 Recharge Dams and Reservoir Projects.

Abu Dhabi topography is not generally suitable for the construction of recharge dams. In fact, only one recharge structure, a diversion bund with several downstream recharge basins, exists in the Emirate. The more mountainous terrain of the Northern Emirates is far more suitable for their construction; more than 100 dams have been constructed with a combined capacity of greater than 100 Mm^3 (EAD, 2001). Table (1.2) shows a total capacity of the Shwaib Dam and its reservoirs.

Table (1.2): Capacity of Shwaib Dam and Reservoirs (EAD, 2001)

Name of the Project	Facility:	Capacity (Mm^3)
Shwaib Dam	Length 3000 m, height 11m	5
Approach Channel	Length 3600 m, width 150 m	5.5
Shwaib Reservoirs	Seven reservoirs	21
Total Shwaib Dam and Reservoir project		31.5

1.3.2 Treated Wastewater

As a substitute for freshwater in agriculture and industry, treated wastewater has an important role to play in water resources of the Emirate .The economic feasibility for the treatment of sewage water and its usage depend on many factors such as the cost of treatment and the degree of required treatment in comparison to the cost of producing alternative water source for the same usage. The cost of producing one m^3 of desalinated water is 5 Dirhams, whereas the cost of producing one m^3 of treated sewage water is 2 Dirhams (Rizk, 1999)

The total treated sewage effluent production is currently about 87.3 Mm^3/yr and this is all used in the irrigation of amenity and road verges plantations both in the cities and along major highways (EAD, 2002). The largest sewage treatment plant is located at Mafraq, 40 km from Abu Dhabi City, which treats all domestic and industrial sewer

mains waste for Abu Dhabi Island and surroundings, serving for a population in excess of 500,000. Generally, a large proportion of all domestic & industrial wastewater is treated and re-used, but this forms only about 4% of all water produced (EAD, 2003).

1.3.3 Seawater Desalination & Imports

The total desalinated water use in the Eastern and Central Regions is about 365.0 Mm^3/yr. Out of this quantity about 132.4 Mm^3/yr in 2004 is imported from the Fujirah plant to Al-Ain City. Desalinated seawater is largely used for domestic supplies and its current use in farming is limited. Potable water supply deficits in Al-Ain will shortly be alleviated with desalinated supplies to be piped from the Fujairah (I) desalination plant (effectively imports to the area) (EAD, 2003)

Using groundwater as a source for the desalination process has been limited to the Al-Ain region. Several reverse osmosis plants have been operated in the Eastern Region, south of Al-Ain city at Um Al Zumol, Al Quaa and Al Wigan. Recently, however, dependence on groundwater for potable water production has been decreased and all plants have been abandoned due to the depletion of the saline water source; the one exception is the Um Al Zumol plant, where the production is 36,000 gallons per day (Brook, 2005).

1.4 Water Consumption in Abu Dhabi Emirate

Water of drinking quality, which meets the Abu Dhabi Emirate standards (2004), as specified by the Regulation and Supervision Bureau, is supplied for domestic, industrial and commercial use and accounts for 15.5 % of the total water resource consumed (EAD .2003). See Table (1.3) for the water consumption in the Eastern and Western Regions of Abu Dhabi Emirate in 2003.

By far, the largest user (58%) of water is the agricultural sector, comprising nearly 25,000 small citizens farms and a few, large state farms whose numbers have been declining in recent years (EAD, 2003). Water used in this sector is mostly brackish in quality, and almost exclusively groundwater Figure (1.5).

The second largest user of water is the forestry sector (18%) comprising over 300,000 hectares distributed between 250 separate plantations. Like agriculture, most of the water used is brackish groundwater, but in some cases, higher than seawater salinity groundwater is used for irrigation. The overall percentage of the total water resources used in this sector has increased from 16% in 2002 to 18% in 2003 (EAD, 2003).

Amenity irrigation for parks, gardens and recreational areas e.g. golf courses etc. accounts for just over 7% of total consumption, slightly less than the previous year. This sector relies mostly on treated effluent as a source, but wells are also utilized. Finally, the Industrial/Commercial sector, even as expanding, still accounts for only 1.72% of all water consumed. Industries are located in a small number of dedicated industrial cities (EAD, 2003).

Table (1.3): Water Consumption in Abu Dhabi Emirate in 2003 (EAD, 2003).

	REGION EASTERN (Mm^3)	%	REGION WESTERN (Mm^3)	%	TOTAL (Mm^3)	TOTAL %
Domestic	136.87	9.16	385.13	20.41	522.00	15.44
Industry	15.21	1.02	42.79	2.27	58.00	1.72
Agriculture	1109.07	74.19	840.29	44.54	1949.36	57.64
Forestry	122.85	8.22	484.45	25.68	607.30	17.96
Amenity	111.00	7.42	134.04	7.10	245.04	7.25
TOTAL	1495	10	1886.70	100	3381.70	100

1.5 Supplies-Demand Balances & Water Use Estimates

Dawoud et al (2005) have been derived a model to estimate the water demand for eastern and central regions of Abu Dhabi Emirate by the year 2020. Table (1.4) shows the modeled results for year 2002, 2010, 2015 and 2020. The results indicated an increase of about 100%, 132%, 136% and 269% in water demand due to future developments in agriculture, forestry, amenity and domestic sectors respectively. This increase in water demand will increase the pressure for using desalination water in agriculture and amenity sectors.

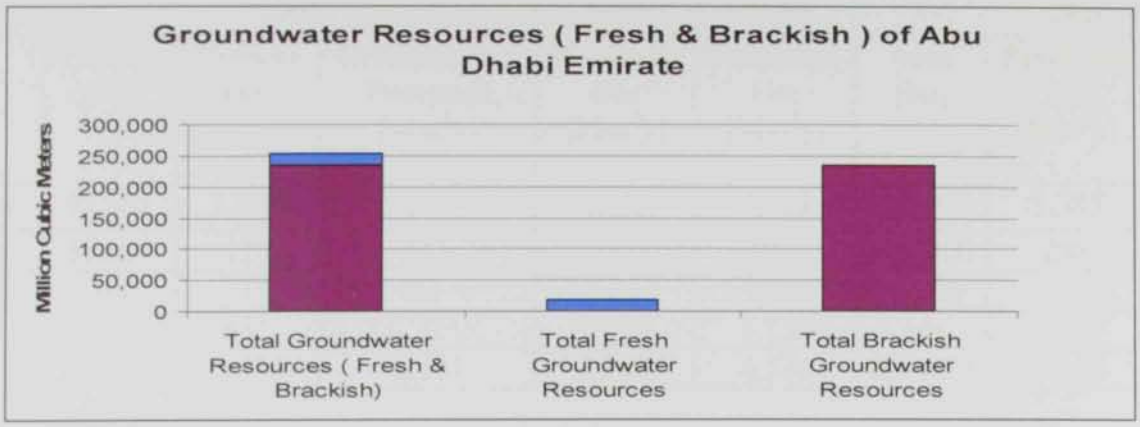

Figure (1.4): Groundwater Resources (Fresh & Brackish) of Abu Dhabi Emirate (EAD, 2003).

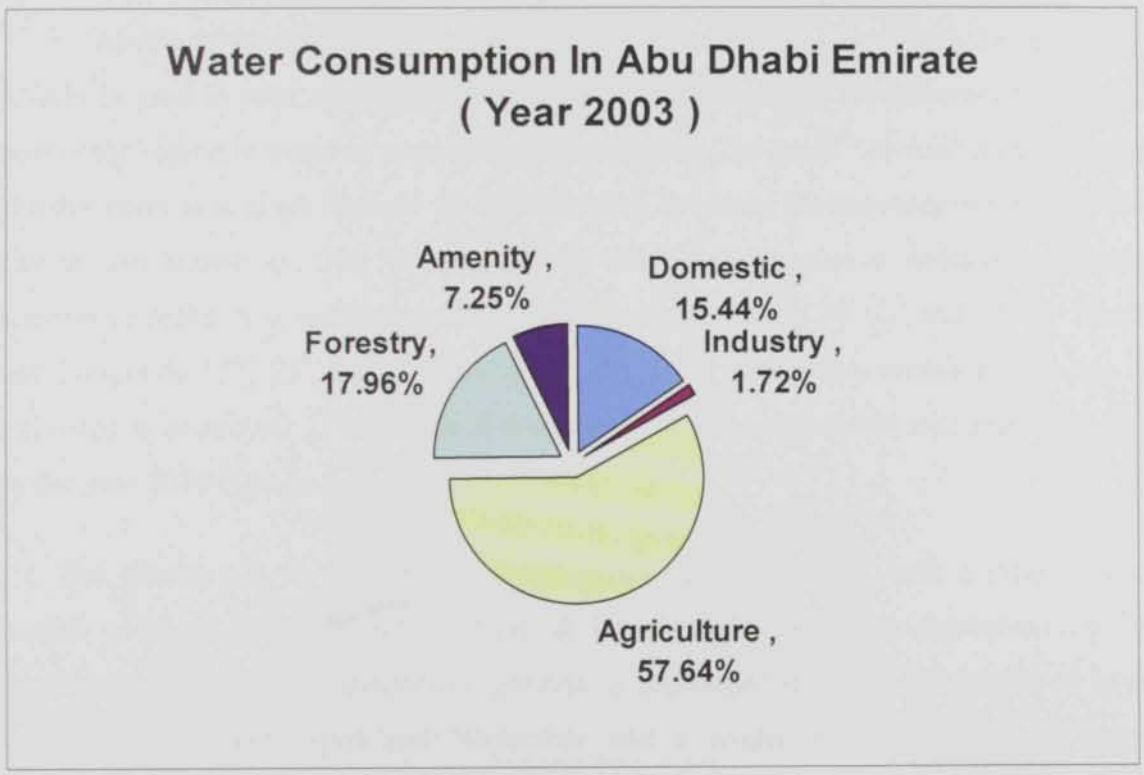

Figure (1.5): Water Consumption of Abu Dhabi Emirate in 2003 (EAD, 2003).

Table (1.4): Modeled Increase in Water Demand for the Eastern and Central Regions of Abu Dhabi Emirate by year 2020 (Dawoud et al, 2005).

Year	2002			2010	2015	2020		
Sector	Area [ha]	Present Water Demand [Mm^3y]	Groundwater Pumpage [Mm^3y]	Predicted Use [Mm^3y]	Predicted Use [Mm^3y]	Area [ha]	Predicted Use [Mm^3y]	Ground-water Pumpage [Mm^3y]
griculture:	59,807	1,692	1,430	2,453	2,728	130,050	3,385	1,310
Forestry:	59,000	124	115	211	250	112,000	288	139
Amenity	6,480	219	57	344	423	15,320	518	57
Domestic	n/a	451	22	772	1,135	n/a	1667	0
Totals	125,287	2,486	1,624	3,780	4,536	257,370	5,858	1,506

1.6 Water Resources in Al-Ain Region

1.6.1 Physical Settings and Climatic Conditions

Al-Ain is the largest city in the Eastern Region of the Abu Dhabi. In this study, Al-Ain is used to refer the eastern region as a whole, because it represents the central core of the region in terms of population and economy. The word "Al-Ain" means spring, and this name was given because the area contains abundant groundwater in the past. The city is also known as "The Garden City of the Gulf", because it contains numerous impressive parks. It is located approximately between latitude 24° 03′ and 24° 22′ North and Longitude 55° 28′ and 55° 53′ East. The 1995 population census for Al-Ain is estimated to be around 318,525 and it is expected that the population will reach 523,970 by the year 2010 (Qanim and Al-Qaydi, 2001).

The climate of Al-Ain is tropical and is deficient in rainfall, with a mean annual rainfall of about 96.4 millimeters (NDC & USGS, 1996). Climatic conditions can be characterized within two distinctive periods: a prolonged dry summer period of high temperature between April and November and a winter period of mild to warm temperature with slight rainfall between December and March. The average temperature during summer is about 35°C and during winter about 18°C.

Al-Ain is characterized by the vast arid desert of the Empty Quarter (Rub Al-Khali), a rugged mountainous region (Jabel Haft, Jabel Hajar), and fertile oases. Some of the

prominent geomorphological features include falajes, Jabel Haft, and the Piedmont Plain region. A brief discussion on the water resources in Al-Ain area is presented hereafter.

1.6.2 Conventional Water Resources

Conventional water resources in the Al-Ain include surface water, springs, falajes and groundwater .The following is brief discussion of each:

1.6.2.1 Surface Water

Due to it's location in an arid region, and because of the absence of permanent surface stream; Al-Ain is considered to be a better ephemeral surface water resource than the rest of the country, because of the occurrence of flash floods.

1.6.2.2 Springs

Ain Al-faydah (Ain Bu Sukhanah) is the only spring within Al-Ain. It is located 15 Km south of Al-Ain and 2 km west of Jabal Hafit. According to El-Shami (1990) the spring produces from Miocene gypsum and clay layers through thin Quarternary loose sediments. The spring represents the discharge area of a deep water source which finds its way up through one of several thrust faults dissecting the area.

The discharge of the spring was 2.5 Mm^3 of brackish water in 1999, which represents the highest discharge among the United Arab Emirates springs and ranks as second order according to Meinzer's (1923) classification. The high water temperature (39° C) and negative correlation between the spring discharge and local rain indicates that the spring receives most of its water from the northern Oman mountains further east (Rizk and El-Etr, 1994). Because of high temperature and high suphur content, Ain Al-Faidah was developed into a resort with some therapeutic capability. Additionally, the spring water is also used for growing palm trees which can tolerate relatively high salinity than traditional crops.

1.6.2.3 Falajes

Falajes are man-made constructions that intercept groundwater at footslopes of high mountains and bring it to the surface through tunnels having gentler slopes than the natural hydraulic gradient Figure (1.6) (Rizk, 1995).

There are a number of falajes in the Al-Ain area (Figure 1.7). In fact, due to declining water tables, there is now no totally naturally flowing falajes system left in Al-Ain, all those operating are either fully or partially supplemented from groundwater which is abstracted from nearby wells drilled within the oasis areas (Table 1.5). The total annual discharge from these falajes is 0.5 Mm^3/yr (EAD, 2003).

Table (1.5): The Aflaj systems in Al-Ain area (EAD, 2003)

Status of Falaj	Aflaj Name	No. of Aflaj
Partially supported by wells	Al Daoudi Falaj Al-Aini Falaj (Al-Ain City)	2
Supported entirely by wells	Al Mutared Falaj Al Mouaiji Falaj Al Jimi Falaj Al Qattara Falaj Al Hili Falaj Maziad Falaj	6
Not operating	Al Jahili Falaj Saa Falaj Al Mazimi Falaj Al Raki Falaj	4
Total Number of Falajes		12
Total Production Mm^3/yr		0.5

1.6.2.4 Groundwater

Al-Ain's aquifer is recharged by different sources. It is recharged by the infiltration of the precipitation in the interdune areas and gravel plains. It is also recharged from Jabal Hafit. Another source of recharge includes irrigation water, upward vertical recharge from deeper rocks and infiltration of water lost from the leaky water transmission lines, (NDC & USGS, 1993).

Previously, all of Al-Ain City's domestic water requirements were met from well fields (Table 1.6). However, massive increases in domestic demands, from an annual population growth rate of up to 8% (Brook, 2003), has meant that well fields have been placed under increasing stress, resulting in declining water levels, and increasing in groundwater salinity and a resultant decrease in total production (Figure 1.8).

The widening gap between groundwater supply and domestic demand has been met from an expansionist policy of desalination using all types of production process under an ever increasing responsibility of the private sector. In 2003, the total domestic wellfield production had reduced to only 26 Mm^3/yr, meeting only 17% of the total domestic requirements in the Eastern Region. Since 1998, production from the domestic wellfields has decreased by over 60%. Table (1.7) shows that a large proportion of abstracted groundwater no longer meets the Abu Dhabi drinking water standard (RSB, 2004) and this challenge has been met by blending indigenous, brackish groundwater with imported desalinated water from the Arabian Gulf and, more recently, from the Gulf of Oman at Qidfa, Al Fujairah.

Table (1.6): Classifications of the Eastern Region Domestic Supply Wellfields (Brook, 2003).

Wellfield Name	**Water Quality Classification**	**% Total 2002 Production**
Shuwaib South, Al Haiyer, Al Karaa, Ghashaba, Al Zaroub,Khashona, Um Ghafa.	Fresh	64%
Shuwaib North, Al Khadar, Bida bint Saud, Al Ashoosh, Jabal Oha, Al Wagan, Al Qua, Seih Al Raheel	Low Brackish	35%
Al Aslab	High Brackish	1%

Note: Fresh <1,000 mg/l TDS, Low Brackish 1,000 – 8,000 TDS, High Brackish 8,000-15,000 TDS

1.6.3 Non Conventional Water Resources in Al-Ain Region

Non conventional water resources in the Al-Ain area include desalinated water from Abu Dhabi Emirate; recently desalinated water has been introduced from Fujairah (Qidfa), and recycled wastewater from Al-Ain treatment plant in Zaker is also used. The total desalinated water use in the Al-Ain is about 125.73 Mm^3/y (EAD, 2003). Desalinated seawater is largely used for domestic supplies and its current use in farming is limited.

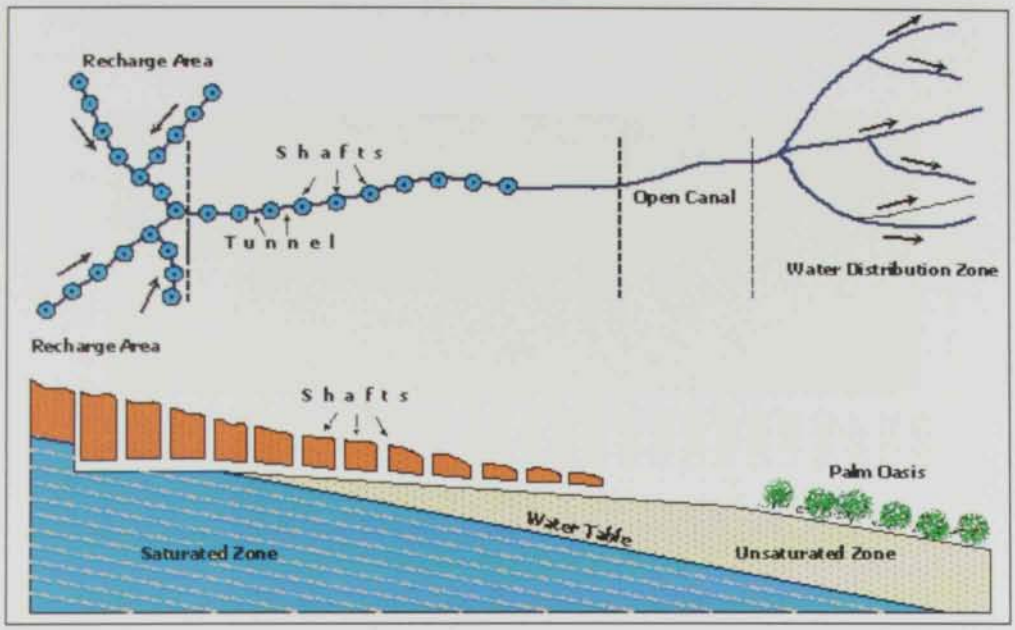

Figure (1.6): Map view and a vertical cross section of falaj (Modified from UAE National Atlas, 1993).

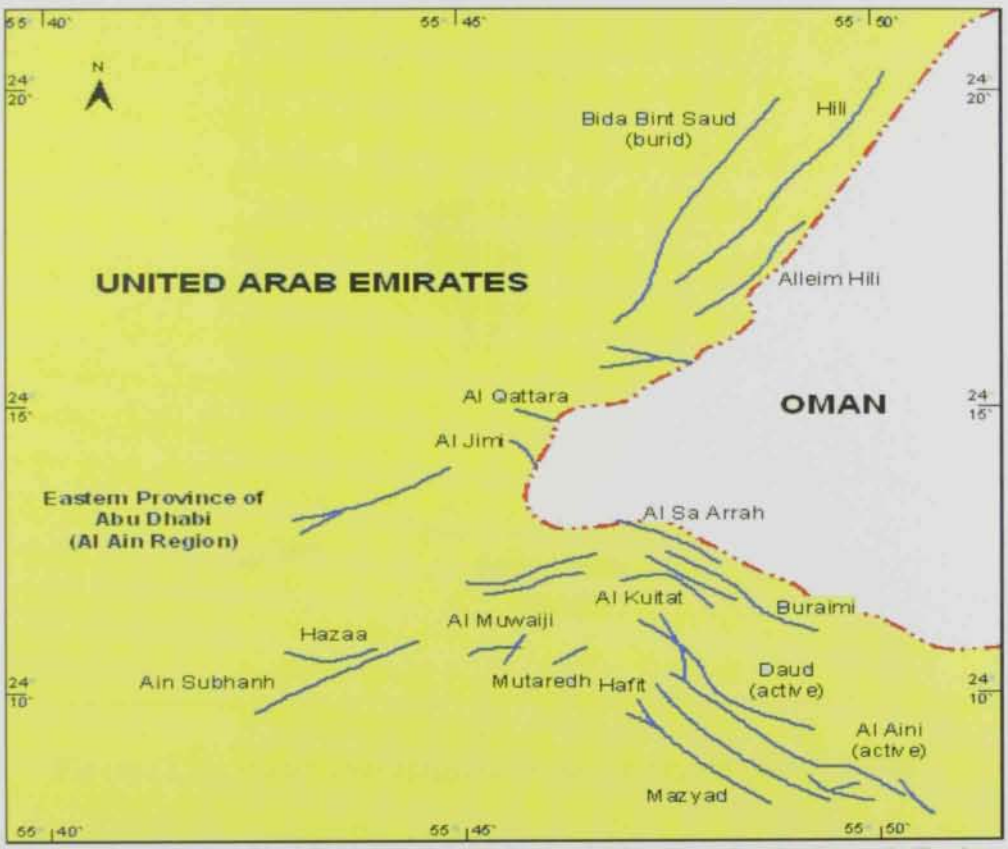

Figure (1.7): Location map of the falajes in the Al-Ain area, United Arab Emirates (After Rizk, 1998).

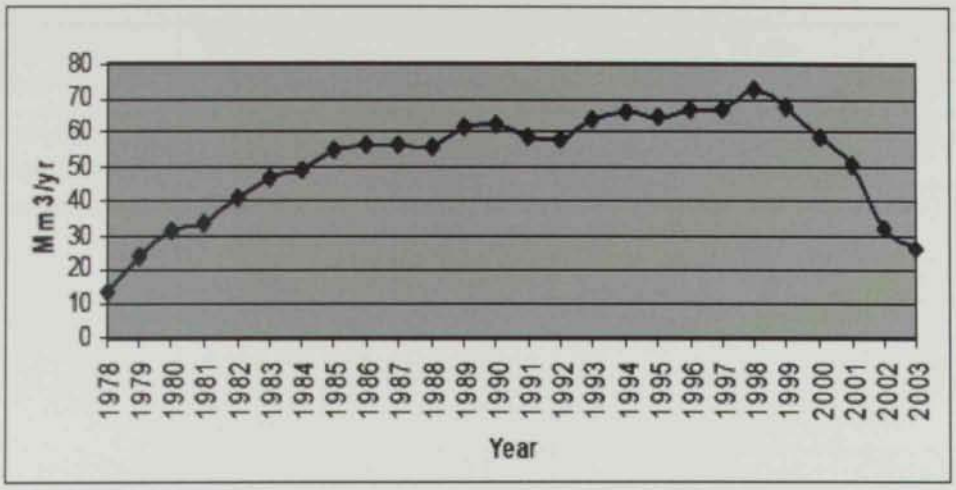

Figure (1.8): Al-Ain Well fields Total Production 1978 – 2003 (Brook,2003).

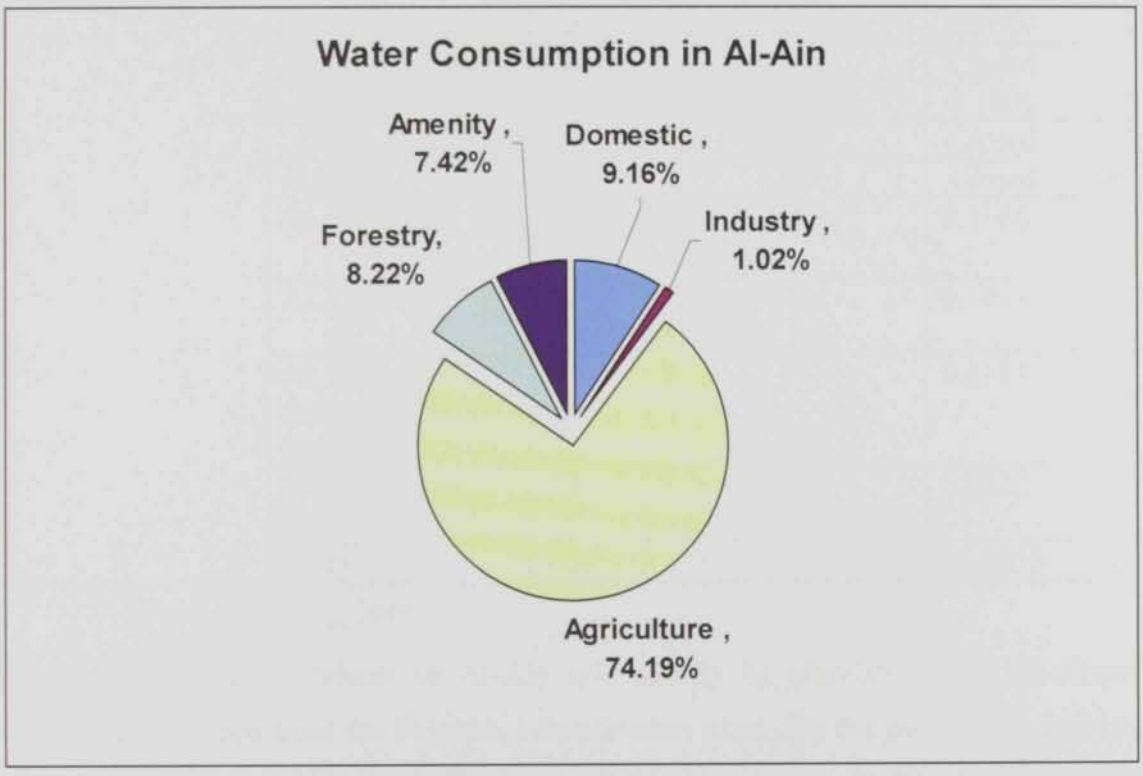

Figure (1.9): Water consumption in Al-Ain region (EAD, 2003).

Table (1.7): The Municipal well fields in Al-Ain, and their annual production in 2003 (Brook, 2003).

Eastern Region1	Well Field	Total Wells	Operating Wells	Production, Mm^3/yr
(potable supply and blended with desalinated water	SHUWAIB NORTH	74	49	2.8125
	SHUWAIB SOUTH	112	74	6.3163
	AL KHADAR	50	20	2.5040
	AL HAIYER	28	15	0.2067
	AL KARAA	62	45	4.4066
	BIDA BINT SAUD	62	38	2.7706
	GHASHABA	11	0	Closed
	AL ZAROUB	12	9	0.2944
	KASHONA	30	29	4.4319
	AL HAIYER N. VILLAGE	4	2	0.1951
	UM GHAFA	25	22	0.9069
	AL ASHOOSH	80	0	Closed
	JABAL OHA	3	3	0.1805
	AL SAA	2	0	Closed
	SABABA	1	0	Closed
	AL WAGAN	16	10 (Closed on 1/3/03)	0.1166
	AL QUAA	9	5 (Closed on 1/3/03)	0.1413
	AL ASLAB (based on 2002 production)	9	9	0.3187
	SEIH AL RAHEEL	10	3	0.1832
	Total	600	333	25.7853

Potable water supply deficits in Al-Ain will shortly be alleviated with desalinated supplies to be piped from the Fujairah I desalination plant .On the other hand, the total Treated waste water output from the TSE Plants in Al-Ain is 21.283 Mm^3/yr (EAD, 2003).

Table (1.9): Agricultural consumption in the Eastern Region (Al-Ain) (EAD, 2003).

Eastern Region (Al-Ain)	Water Use	Consumption, Mm^3/yr
Citizens Farms irrigated by 49894 wells (74% producing)	11,603 farms occupying 45,072 ha	913.55
Government Entities	State Fodder Farms – 16,792 ha	185.52
Traditional Date Gardens (Oases)	Al-Ain Date plantations	10

1.7.3 Forestry, Amenity Consumption

Irrigated forest plantations have expanded from less than 250 ha in 1969 to over 61,749 ha at present (Table 1.10), under a national policy of 'greening the desert'. The forests in Eastern Region are estimated to consume over 122.85 Mm^3/yr (EAD, 2003). Current consumption in amenity, parks, road verges, and gardens in Eastern Region is estimated at 111 Mm^3/yr (EAD, 2002).

1.7.4 Industrial/Commercial Consumption in the Eastern Region (Al-Ain)

In Al-Ain area, only two industries have been identified which have an independent water supply from pumped boreholes linked where appropriate, to desalination units on site; these are Al-Ain Mineral Water Company and Coca Cola Bottling plant. Current consumption in industrial and commercial sector is 15.21 Mm^3/yr Table (1.10) (EAD, 2003).

Table (1.10): Forestry, Amenity, Industrial and commercial consumption in the Eastern Region (Al-Ain) (EAD, 2003).

Eastern Region (Al-Ain)	Water Use	Consumption, Mm^3/yr
Plantations established since 1970- 61749 hectares, irrigated by over 2800 groundwater wells irrigating 12264320 trees	Forestry plantations	122.85
Amenity	Parks, Gardens etc	111
Industrial and Commercial Consumption		15.21

CHAPTER 2
Geology of Al-Ain Area

Geology of Al-Ain Area

The Study area is located south of Al-Ain, and comprises the Mubazarah , Ain Al-Faydah (Ain Bu Sukhanah) and Neima areas. The objectives of this chapter are to describe the general existing geological conditions within Al-Ain, with emphasis on the study area, and to investigate the lithological and structural controls of groundwater quality and flow. These geological elements comprise geomorphology, lithostratigraphy, geometry and distribution of geologic units along with the structural deformation affecting the hydrogeology of these units.

2.1 Geomorphology of Al-Ain

The geomorphology of Al-Ain area has been addressed by many researchers including, among others, Hunting (1979), Abou El-Enin (1993), Al-Shamsi (1993), UAE National Atlas (1993), Garmoon (1996), and Baghdady (1998). Al-Ain area can be divided into six geomorphic units. These units are; (1) mountain, (2) gravel plains, (3) drainage basins, (4) sand dunes, (5) interdune areas and (6) inland sabkhas. Figures (2.1 and 2.2). The following is a brief description of each of these geomorphic units.

2.1.1 Mountains

The mountains encountered in Al-Ain area include mainly Jabal Hafit, Jabal Malaget, Jabal Mundassah, Jabal Al-Oha and Jabal Huwayah. Based on the work of Hunting (1979) and Abou El-Enin (1993), Jabal Hafit is a Tertiary asymmetrical anticlinal structure plunging southeasterly in Oman and northwesterly in UAE (Figure 2.1). It is located southeast of Al-Ain City at latitudes 24° 02' – 24° 13' N and longitudes 55° 44' – 55° 49' E.

Jabal Hafit is considered as the most prominent feature of the Al-Ain area. It is approximately 29 km in length and some 5 km in width, and reaches an elevation of about 1160 m above sea level. The rocks forming the Hafit area composed of carbonates, clays and marls ranging in age from early Eocene to Miocene. The mountain has a whale-back form with beds dipping east and west off the fold axis. North of the core is composed of limestones and marls, which represents the lower and middle intervals of

the Dammam Formation (Middle or Late Eocene), the rocks are eroded forming a low-lying area of small hills enclosed between ridges of the Asmari Formation (Early to Middle Oligocene) . The eastern limb of Jabal Hafit is characterized by slumps because of high dip values in addition to the presence of rather incompetent marl beds alternation with the limestones (Hamdan and El-Deeb, 1990).

Jabal Malaget and Jabal Mundassah are considered as a part of the Oman Mountains and are located approximately 17 km east of Jabal Hafit.They form asymmetrical anticlinal structures (Warrak, 1987) with their eastern limbs forming the main part of the exposures. The rocks forming Jabal Malaget and Jabal Mundassah are composed of serpentinized peridotite (in cores of the anticlines) conglomerates, and carbonates of Late Cretaceous age overlain by marls and carbonates of Paleocene to Early-Middle Eocene age (Simsima, Muthymimah and Damam Formations) (Hamdan and El-Deeb, 1990) .

Jabal Al-Oha lies 8 km northeast of Al-Ain city. It consists of three NW-SE parallel hogback ridges averaging about 10 km in length. These ridges represent fault repetition of the western limb of the horseshoe-shaped southerly plunging anticline of Jabal Huwayyah exposed further east. Lithostratigraphically, Jabal Al-Oha and Jabal Huwayyah (Figure 2.1) are composed of a clastic sequence overlain by crystalline carbonate (Qahla and Simsima Formations) of late Cretaceous age the Jabal Al Oha succession attains a total thickness of about 85 m. It is divided into a lower unit composed of gray to khaki colored shale of the Qahlah Formation and a 3 m thick unit of red colored chert pebble conglomerate, which is overlain by white of the limestone Simsima Formation (Hamdan and El-Deeb, 1990).

2.1.2 Gravel Plains

Two gravel plains comprise the eastern part of the Al-Ain area, one which fringes the Oman Mountains and the second which fringes Jabal Hafit, the first reaches it's maximum development in the Al Jaww Plain Figure (2.2) between Jabal Hafit and Oman Mountains (Hunting,1979). It consists of a gentle westerly inclined gravel and sand plain built up of down alluvial fans deposited by drainage from the mountains.

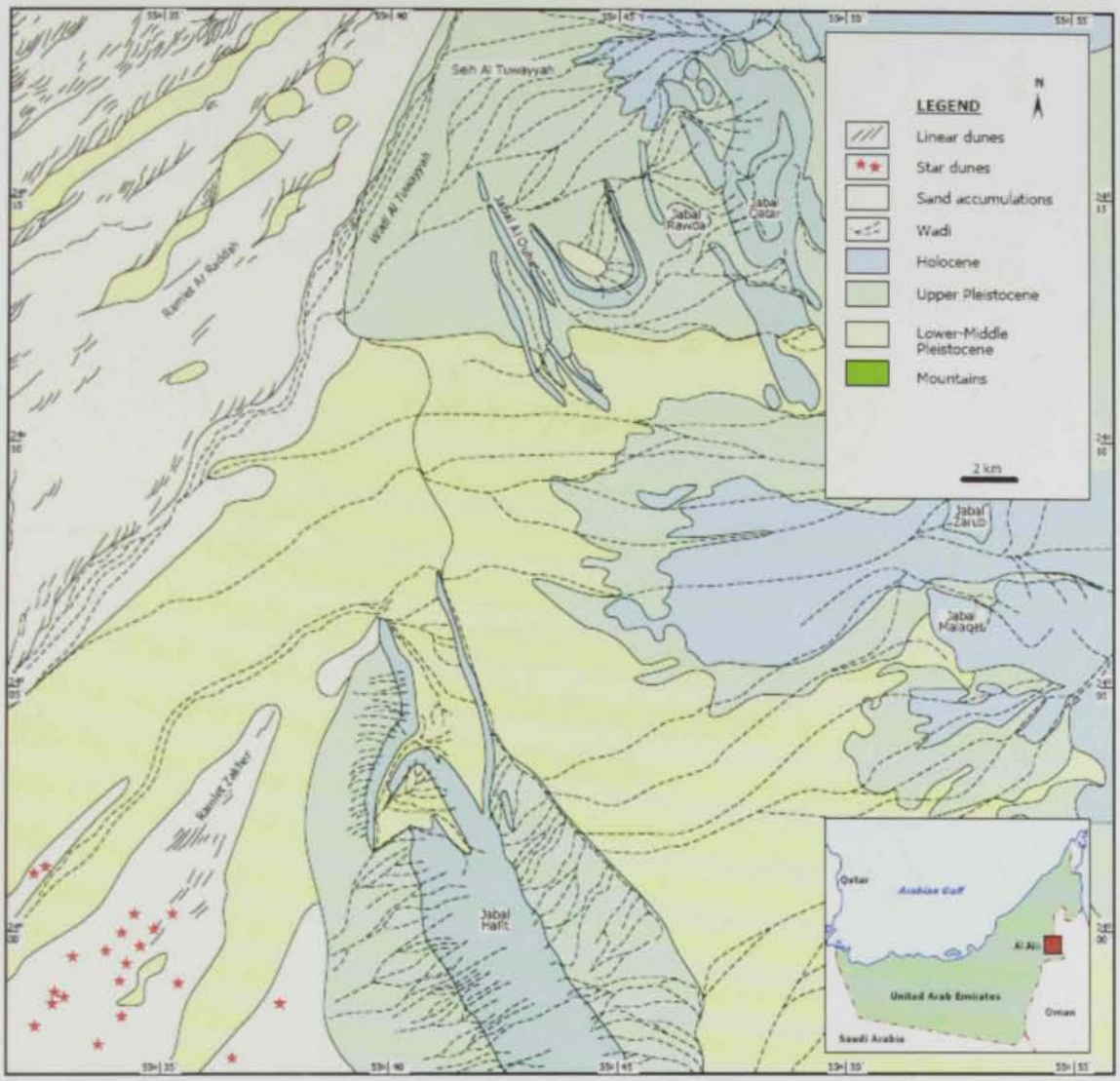

Figure (2.1): Geomorphology of Al-Ain Region, (Modified by Al-Nuaimi, 2003 after National Atlas of United Arab Emirates, 1993).

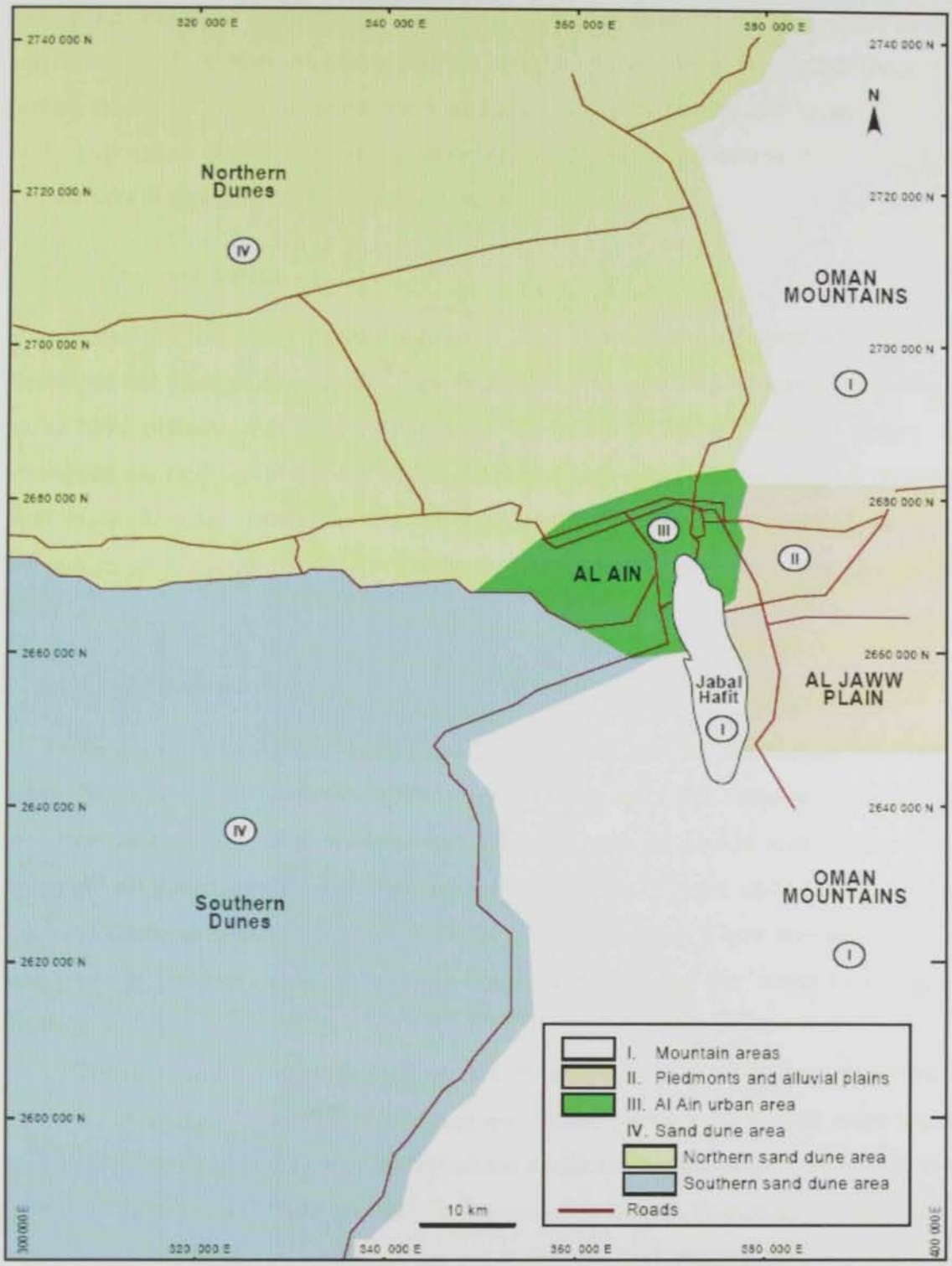

Figure (2.2) Physiographic subdivisions of eastern study area, (Modified from Al-Nuaimi, 2003)

The plain is crossed by numerous wadis, the most important of which are those of Al-Ain, Shik and Muraykhat. Al-Shamsi (1993) identfied three alluvial fans within the plain. Namely the Zarub fan in the north, the Mundassah fan in the middle and Arjan fan in the south. The second plain is that which occurs around Jabal Hafit. Because of its carbonate composition, it appears very light in color on satellite images.

2.1.3 Drainage basins

There are two systems of drainage in Al-Ain area, namely those of the Oman Mountains and those of Jabal Hafit (Figures 2.3 and 2.4). The Oman Mountains drainage basins have patterns that range from dendritic (characteristic of igneous rocks), to rectangular (in fault –controlled areas) and braided (in areas of gentle slopes) patterns. Jabal Hafit drainage basins have mainly subradial, dendritic and braided patterns. Parrallel or rectangular patterns occur in the structurally-controlled areas (Alshamsi, 1993).

2.1.4 Sand dunes

Sand Dunes in Al-Ain Area constitute the main part of the aeolian landforms system (Embabi and El Sharkawy, 1989; Embabi, 1991, and UAE National Atlas, 1993). They dominate the northern, western, and southern parts of Al-Ain area (Figure 2.2). Embabi (1991) attributed the regional and local variations in types and patterns of sand dunes to variations in wind regime, sand supply, and local relief. There are two dominant dune types in the study area; namely the branching linear and star dunes Figure (2.1) (Embabi, 1991).

The northern and western parts of Al-Ain area are occupied by branching linear dunes, which extend NE-SW. These dunes are darker (more reddish) and more dense towards the east. Star dunes occur mainly in the southeastern part of the study area, near Al Wagan Figure (2.1). Their occurrence is associated with E-W barchanoid and linear ridges. Embabi (1991) mentioned that star dunes develop their mature form in a low sand supply environment with suitable multidirectional wind regime and grow upward rather than outward.

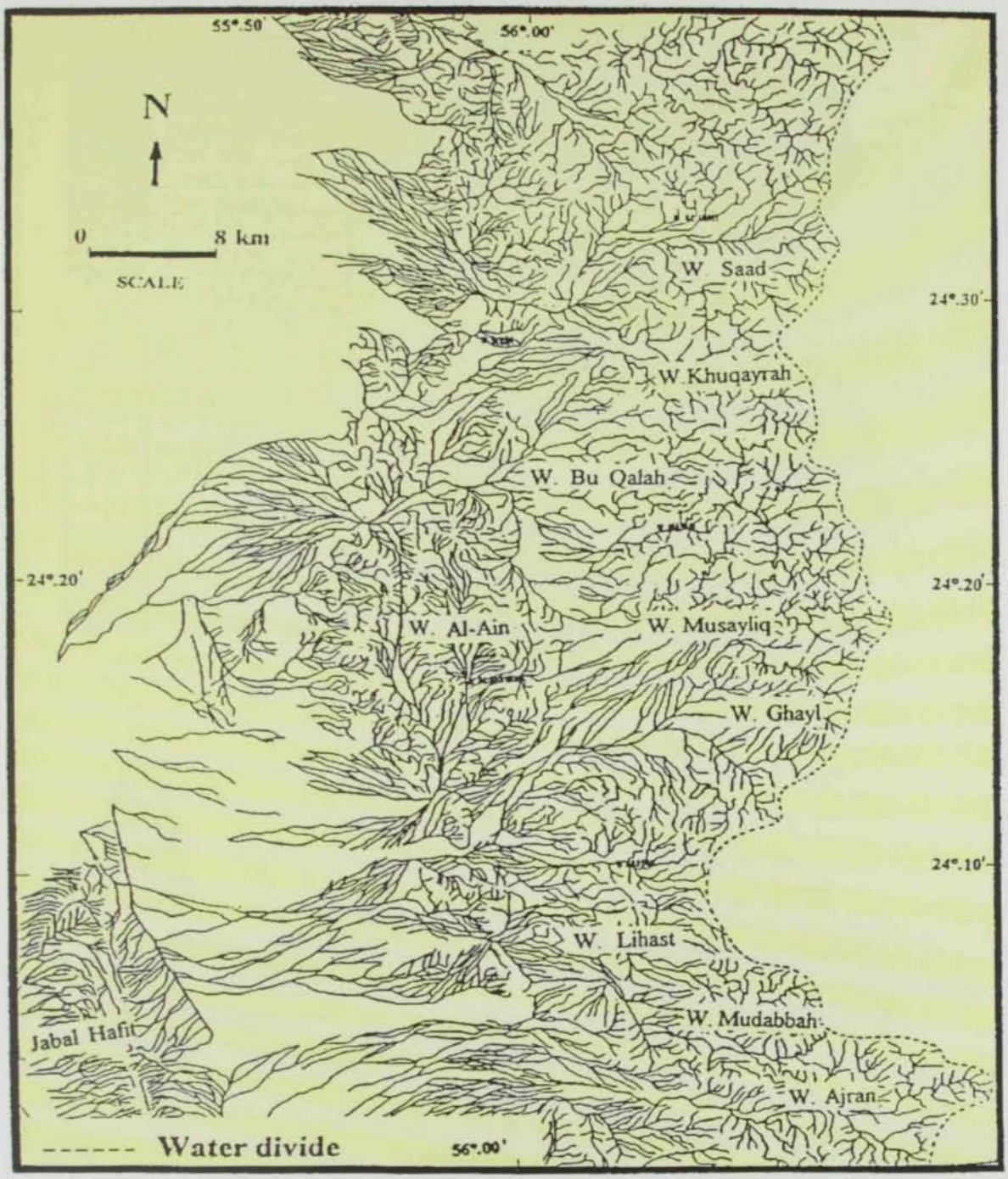

Figure (2.3): Drainage basins of Al-Ain area ; basins of northern Oman mountains and basins of Jabal Hafit (modified from Al-Shamsi, 1993).

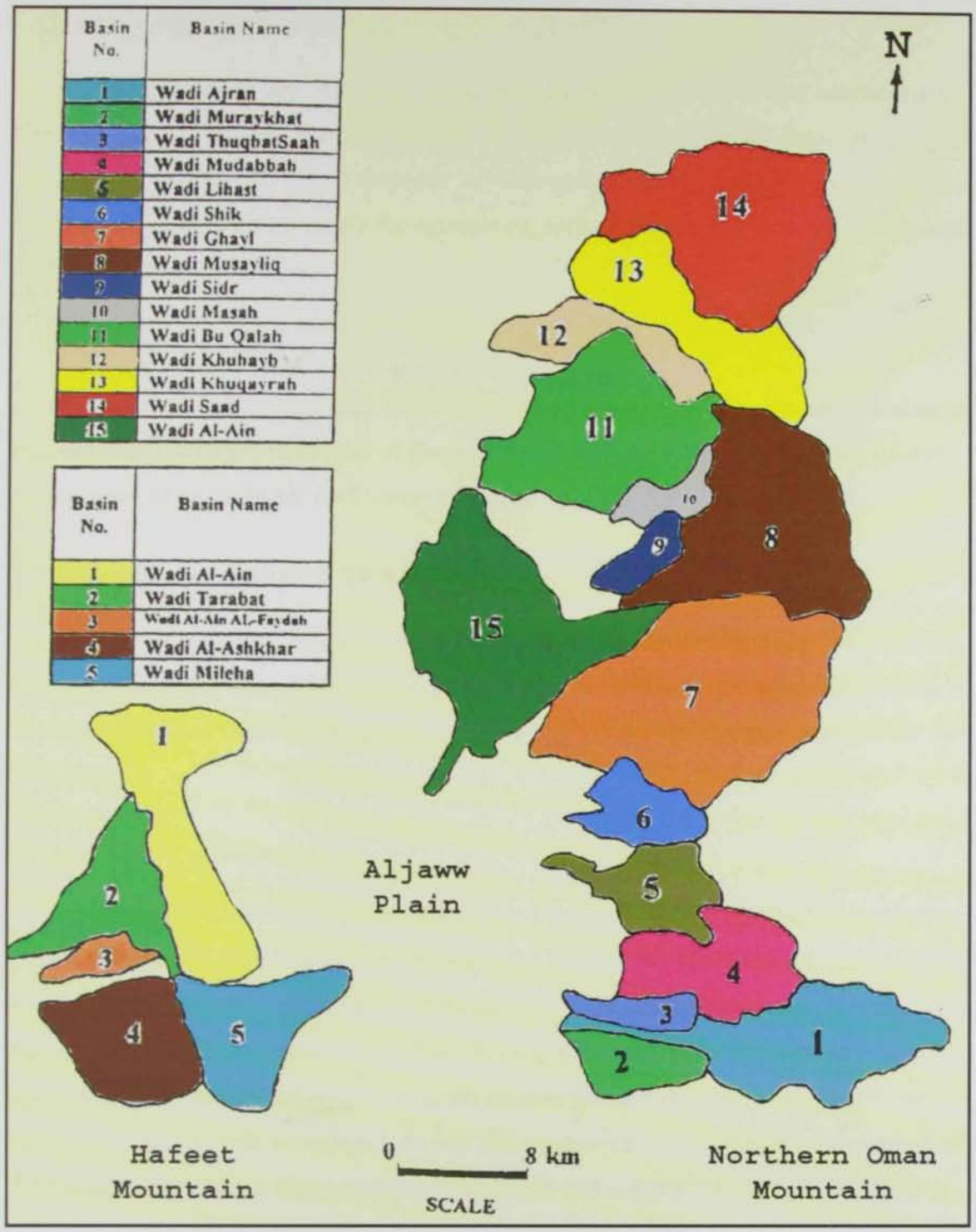

(Figure (2.4) Drainage areas of major basins in northern Oman mountains and Jabal Hafit, separated by Al-Jaww plain (modified from Al-Shamsi, 1993)

2.1.5 Interdune areas

Interdune areas are depressions occupied by ablation hollows and aeolian sands. They are described by Hunting (1979) as ablation hollows and flats. If shallow groundwater tables and high amounts of fine-grained sediments are available, the interdune areas become favorable for agriculture, such as that of Bu-Samara-Sweihan and Al-Ain –Misakin.

2.1.6 Inland sabkhas

Inland sabkhas are the low lands occupied by evaporitic sediments and are sites of groundwater discharge. Examples of these include sabkhat Al-Thwaymah along Al-Ain – Al Wagan road and sabkhat Al-Khatam along the Al-Ain – Abu Dhabi road.

2.2 Lithostratigraphy of Al-Ain

The stratigraphic sequence in Al-Ain area is composed of Upper Cretaceous, Paleocene, Eocene, Oligocene, Miocene, sequences as well as Quaternary sediments. A brief description of these geological formations is given hereafter (Baghdady, 1998; Al-Saiy, 2002).

2.2.1 Upper cretaceous

The Upper Cretaceous sequence includes (from base to top) the Semail ophiolites, Qahlah Formation, Simsima Formation and Fiqa Formation (Hamdan and Anan, 1993). Semail ophiolites are composed of Pre-Maastrichtian serpentinite and serpentinized periodotite. They represent the oldest exposed rocks in Al-Ain area, where they form the floor of Jabal Malaqet and Jabal Mundassah on their eastern sides. The Qahlah Formation consists of red to yellow unfossilliferous clast-supported conglomerates composed of rounded clasts of chert and serpentinised perodotite derived from the Semail ophioloites.

Hunting (1979) and Warrak (1987) believed that what is has been called the Qahlah Formation, is in fact the Hybi and Hawasina suite, which structurally underlies the Semail Ophiolites (Figure 2.5). The Simsima Formation is composed of medium to thick-bedded, shallow marine bioclastic limestone with rudists, corals and echinioids. It

disconformably overlies the Qahlah Formation (Hamdan and Anan, 1993). In the north and middle sections of Jabal Mundassah, however, the Simsima Formation unconformably overlies directly the Semail Ophiolites. This unit is also called Simsima Limestone (Hunting, 1979).

The Fiqa Formation is represented by tongues in Jabal Mundassah and consists of light grey to buff thinly bedded pelagic marls and calcareous shales with creamy to orange nodular to flaggy argillaceous limestone interbeds (Hunting, 1979).

2.2.2 Paleocene

The Paleocene unit is separated from the underlying Upper Cretaceous sequence by a regional unconformity with local conglomerate at its base. Hamdan and Anan (1989) and Hamdan and El-Deeb (1990) described this unit as the Pabdeh "equivalent" Formation. Nolan et al. (1990) formally named this unit the Muthaymimah Formation. Its age ranges from Late Paleocene to Early-Middle Eocene (Hamdan and El-Deeb, 1990). This unit is exposed in Jabal Malaqet and Jabal Mundassah. It consists of shale, marl and argillaceous limestone with conglomerate interbeds.

2.2.3 Eocene

Hunting (1979) was the first to subdivide the Paleogene succession in the Jabal Hafit area into different lithostratigraphic units. He gave the following names Tle_1, Tle_2, Tle_3, Tle_4, Tle_5, Tle_6 and Tle_7 to the limestone succession of Early-Middle Eocene ages. Moreover, Hunting (1979) gave the names; Tlo_2 and Tle_2 to the shale and Caralline Limestone of Early and Middle Oligocene ages.

Whittle and Alsharhan (1994) considered the Eocene sequence to include (from base to top): the Rus Formation and the Dammam Formation (Figure 2.5) . The Rus Formation (Early Eocene) is composed of fossiliferous dolomitized limestone with thin argillaceous limestone (equivalent to Tle_1) grading upward to well-bedded nodular limestone (equivalent to Tle_2). The formation forms the core of Jabal Hafit anticline where it has an unexposed base. The Dammam Formation (Middle to Late Eocene) unconformably overlies the Rus Formation (Hamdan and Bahr, 1992). It constitutes most

of the outcrops of Jabal Hafit and is made up of fossiliferous marl and limestone interbeds (equivalent to the intervals Tle_3 to Tle_6 of Hunting (1979).

2.2.4 Oligocene

The Asmari Formation ranges in age from Middle to Late Oligocene (Whittle and Alsharhan, 1994). It is composed upwardly of silty marl (equivalent to Tle_7), bioclastic nodular limestone (equivalent to Tlo_1), and interbedded bioclastic limestone and marl (equivalent to Tlo_2) (Figure 2.6). The formation constitutes the east and west cuestas of Jabal Hafit which extend north of Wadi Tarabat and the Al-Ain Cement Factory, respectively. At the western cuesta, the upper and lower contacts of the Asmari Formation are covered by alluvium.

2.2.5 Miocene

The Miocene succession unconformably overlies the Asmari Formation (Whittle and Alsharhan, 1994). It is low-lying and located at the eastern flank of Jabal Hafit (Figure 2.6) as interbeds of gypsum and clay and gypsiferous clay (Tm_2) (Hunting, 1979).

2.2.6 Quaternary

A large portion of the Al-Ain area is covered by Quaternary deposits. Five sediment types were recognized by Hunting (1979). They are broadly contemporaneous and represent different facies of deposits being formed by present-day processes.

(a) Deposits bedded containing discontinous lenses of cross-laminated sand. Around Jabal Hafit, the clasts are composed entirely of limestone. Toward Al-Ain City and further west, the gravel and conglomerate are replaced by interbedded sand, silt and calcrete. The sand and silt are cross laminated /calcareous and contain scattered pebbles and cobbles. The calcrete is typically white, lacks obvious bedding and contains scattered grains of chert fragments and altered igneous rocks with irregular fracture surfaces and vugs coated with manganese oxides.

(b) Desert plain deposits: Theses deposits occur between the dune ridges, mainly in the west and north of the study area. They are distinguished from fluvial

deposits by being unrelated to the present drainage pattern. These deposits are interlayered, laminated and loosely cemented by carbonate silt and sand. They represent dune sands which have been cemented by salts at times of higher water table, then re-exposed by ablation. (Hunting, 1979).

(c) Mixed deposits: These deposits are present in the northern part of Al-Ain. They include accreted, serpentinite granules and calcareous sandstone and are similar to the rocks of Miocene age. The lack of diagnostic fossils makes their age indeterminate (Hunting, 1979).

(d) Sabkhas: These deposits occur where the main wadi channels enter the sand dunes and at other locations within the Dunes liable to flooding by rising groundwater. Sabkhas are also developed on the lower parts of gravel and sand plains at and west of Ain Al-Fydah. The main rock type is loosely-cemented calcareous siltstone. (Hunting, 1979).

(e) Aeolian sand: The greatest part of Al-Ain area is covered by sand dunes. The sand varies from red and pink to white. Hunting (1979) emphasized that grains of these sand dunes are well-rounded carbonates and quartz with minor proportions of basic and ultrabasic igneous rock fragments. Sorting is poor and no pure silica sands were observed. (Hunting, 1979).

2.3 Geologic Structures

The Al-Ain area is located on a structural transition zone between the uplifted highly deformed rocks of the Oman Mountains to the east and the buried flat-lying to gently folded strata of western Abu Dhabi. The rocks exposed in the northern Oman Mountains east of Al-Ain City have undergone complex compressive deformation, primarly due to the Late Cretaceous obduction of the Semail ophiolites and associated rocks (Glennie et al, 1974; Coleman, 1981; and Lippard et al, 1986). A foreland basin which exists beneath Al-Ain area, was formed as a result of the obduction (Patton and O'Connor, 1988; and Warburton et al, 1990). Complex folding and faulting in the bedrock mountains of the

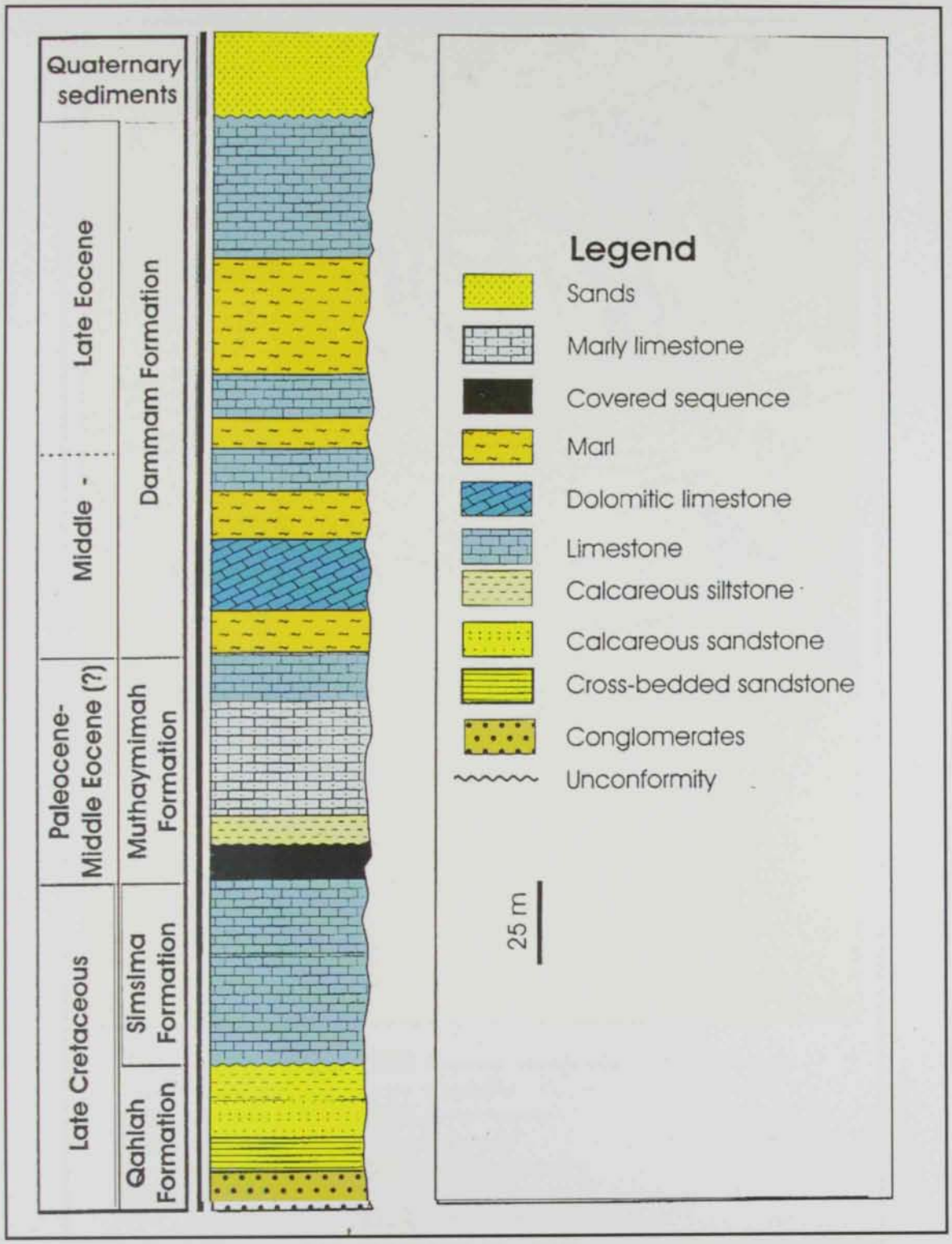

Figure (2.5): Stratigraphic description of the identified Creataceous/Tertiary rock units surrounding Al-Ain area (Abdelghany, in prep).

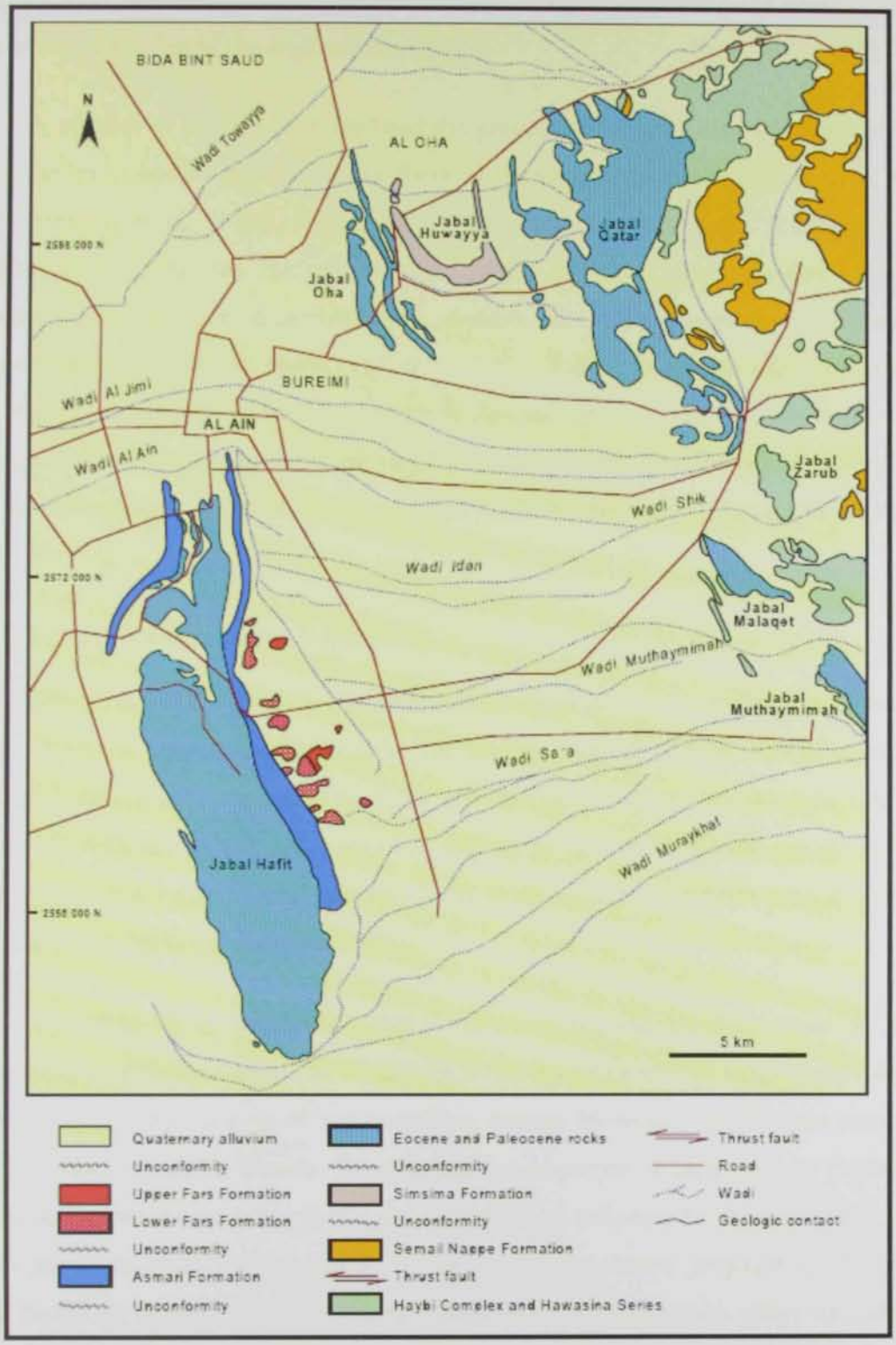

Figure (2.6): Geology of Al-Ain area (modified from Hunting Geology and Geophysics, Ltd., 1979; Warrak, 1987).

western Oman Mountains of the western Oman Mountains adjoining the eastern area of Al-Ain was identified in the regional mapping.

A number of studies have reported the presence of a large buried system of folds and thrust faults bordering the western flank of the Oman Mountain, (Boote et al, 1990; and Warburton et al; 1990). Woodward (1994) used 94 reprocessed seismic sections covering the Al-Ain area for outlining the major structural elements that affect the Quaternary aquifer. He described two distinct structural regimes dominated by compressional deformation; namely; (1) the tightly – folded, highly thrust-faulted regime north Al-Ain and (2) the less folded regime in Al-Jaww plain. The boundary between the two regimes trends ENE beneath the large Wadi Al-Ain system (Figure 2.7) presents a map for subsurface structures in the western flank of the Oman Mountains in Al-Ain area.

2.3.1 Northern Structural Regime

This structural regime is characterized by episodic and compressive tectonism. Starting from the western distal anticline, the folding consists of three sets of alternating anticline – syncline fold pairs. The folds are doubly plunging, the western folds are asymmetric with the axial surface dipping slightly to the west, and the estern folds are symmetric with a vertical axial surface. Most folds have been ruptured by a series of imbricate thrust faults (Woodward, 1994).

According to Woodward's (1994), there are six sub parallel zones of major eastward-dipping thrust faults. The F1 and F6 thrust zones consist of single faults: the F3, F4 and F5 zones are made up of two branching thrusts. However, the F2 zone comprises three discontinuous inline thrusts. The deformation sequence of the post-Late Cretaceous shallow sediments is one of an initial phase of folding followed by thrusting. The thrust system seems to be a leading imbricate fan with a westward propagating piggyback thrust. Based on seismic data, the northern anticline is thought to be either unfaulted or less faulted with little displacement along the thrust plain. In the central part of the anticline, the fold becomes more compressed, where the limbs begin to dip quite steeply, and a thrust fault develops near the central part of the fold and ruptures the fold west of

its crest. As compressional deformation increases the throw of the thrust increases and the anticline begins to be decapitated. At the southern end of the anticline, seismic sections show that the fold is broad and unfaulted and the limbs are dipping at low angles.

Warrak (1996) studied the origin of the Hafit anticline and analyzed its structural pattern. He concluded that the structure was formed as a result of one-sided compression acting from ENE and grew as a detachment fold. Also, the reversed verence and the fold superposed on the limbs of Hafit folds were formed due to simple shear as it moved up a listric,east-dipping thrust plane. Warrak (1986) emphasized that the Hafit anticline grew synchronously with the sedimentation from just before the Middle Eocene until the end of the Miocene.

2.3.2 Southern Structural Regime

The southern structural regime is dominated by Jabal Hafit , the distal fold, and includes the Al-Jaww plain . The mountain is a composite anticline with a sinuous doubly plunging fold axis. This large – amplitude fold is asymmetric in profile with a vertical to steeply overturned eastern limb.

The 440-km^2 Al-Jaww plain is a westward sloping, low-relief alluvial piedmont bounded on the east by Oman Mountains and the west by Jabal Hafit. Structurally, the plain is underlain by a series of southerly plunging folds that comprise a central anticline, flanked by a syncline, and easterly dipping thrust fault located near the eastern boundary of the plain.Despite striking dissimilarities , the two regimes share some common aspects: (1) the axial traces of folds generally trend NNW-SSE ;(2) all the major thrust faults dip to the east at moderate to steep angles ; (3) the distal structural elements of each domain are anticlinal (Jabal Hafit anticline, south of Al-Ain and a buried anticline to the north) ; and (4) west of the distal anticlines, the undisrupted layered bedrock dips gently to the west (Woodward, 1994).

Hunting (1979) emphasized that the structural settings suggest a main phase of deformation of Miocene age. However, stratigraphic evidence indicates, in addition, earth movements during the end of Cretaceous, Middle Eocene and Late Eocene.

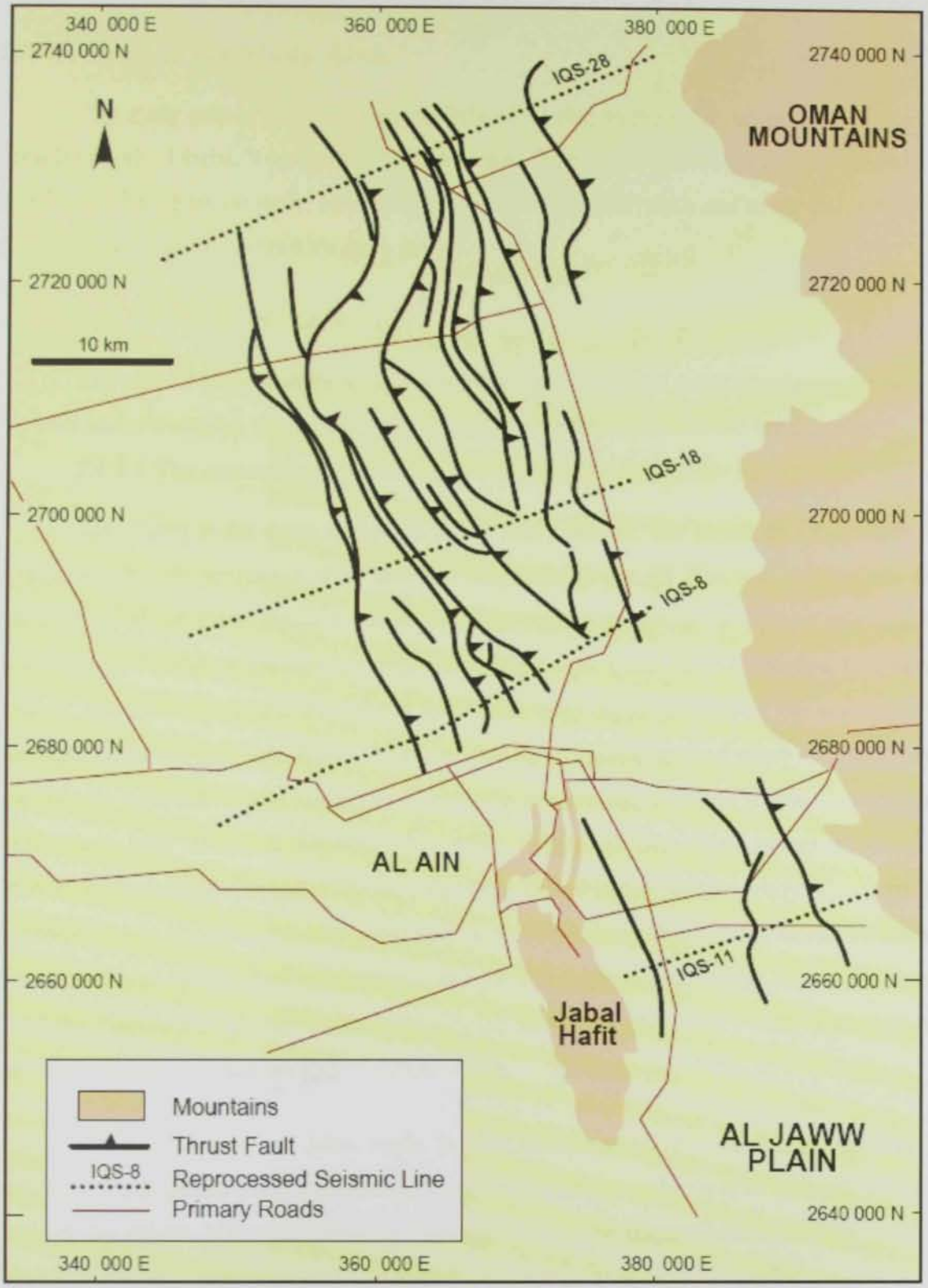

Figure (2.7): Subsurface structures in the western flank of Oman Moutains (after Woodward, 1994).

2.4 Geology of the Study Area

The study area is located south-easterly of Al-Ain in the most eastern part of the Emirate of Abu Dhabi. It comprises Neima area to the north, Mubazarah to the east and Ain Bu Sukhanah to the west. The study area is densely cultivated, and more than half of the cultivated area is covered by palm trees.

2.4.1 Geomorphology

The area of study can be simply distinguished into three main provinces, namely; the hills and mountains, the piedmont plain of Oman Mountains and the sand dunes.

2.4.1.1 The mountains province

Jabal Hafit is the main mountain in the study region. The shape of Jabal Hafit is determined by its anticlinal structure. Its length is about 29 Km and it reaches an elevation of about 1160 m above sea level. In its core to the south, where the succession is composed mostly of limestones and dolomites (Rus Formation) resistant to wadis erosion, the mountain has a whaleback form with beds dipping down to the east and to the west along the two fold limbs. North of the core, limestones and marls of the lower and middle intervals of the Dammam Formation are eroded, forming a low –lying area with small hills enclosed between the strike ridges of the more resistant Asmari Formation limestone. These two strike ridges are called in the present study the "eastern hogback" (it is not a cuesta, but is defined as mentioned in other works, as the beds are dipping 70° due east) which reaches in some parts an elevation of 320 m above sea level , and the "western hogback" (with beds dipping about 30° due west) with a maximum elevation of 460 m (Hamdan and El-Deeb, 1990).

The eastern limb of Jabal Hafit is also characterized by slumping due to the presence of competent rocks (limestones) and incompetent rocks (marls) and due also to the high dip values. It is represented by the repetition of the strata (Hunting, 1979).

2.4.1.2 The Piedmont Plain (Bahada) region

The term bahada refers to a depositional plain composed of coalescing series of alluvial fans formed at the foot slopes of mountain ranges. Normally when a wadi extends from a mountain area on to the adjacent plain, an alluvial fan is deposited. Deposition occurs due to the change in water flow energy. Water energy depends on, among other factors, velocity that is, in turn, a function of surface gradient. At the foot-slopes, water flow becomes slow and unconfined is divided into several braided channels. Therefore, the water energy becomes very weak and insufficient to transport its sediment, and this happens suddenly due to sudden change in slope-gradient. The result is the deposition of rock fragments. Fan number and size depend on wadi numbers and wadi size issuing from the mountain range. Consequently, the bahada surface relief extension depends on these factors and adjacent landforms systems (Hunting, 1979).

The bahada system in the investigated area fringes the mountain ranges. Therefore there are two bahadas, one on the west fringing the Oman mountains from the east, which can be referred in this study as the gravel plain), and the second, which fringes Jabal Hafit (can be referred as the carbonate plain).

The gravel plain reaches its maximum development in the Al-Jaww plain, between the Oman Mountains and the area east of Jabal Hafit. It consists of a gently inclined gravel and sand plain, built up of the sediment deposited by wadis from the eastern mountains. The plain is traversed by numerous wadis e.g. Al-Ain, Shik and Muraykhat. The continuation of the wadi courses to the north is marked by a string of patches of sabkhas, formed at the times of flood due to the rise of groundwater level. Most of the wadis are braided and run from east to west. Vegetation is sparse, comprising low trees and small shrubs. To the north of the Al-Jaww plain, a flat silty plain with extensive areas of low dunes is desely populated and sparsely vegetated (Al-Ain, Buraimi, Hili, etc) which represents the inter-dune piedmont plain (Hunting, 1979).

A carbonate debris plain occurs around Jabal Hafit and appears white in the Landsat image Figure (2.8). Vegetation tends to be most dense in this plain rather than in the gravel plain. The drainage is short and consequent on both flanks of Jabal Hafit.

2.4.1.3 The Sand Dunes

The western part of the investigation area is dominated by dune fields , composed of star dunes Figures (2.1 & 2.8), which are radially symmetrical, pyramidal sand accumulations with slip faces on arms that radiate from the high central part of the mound .Their occurrence is associated with W-E barchan and linear ridges. Star dunes start in an incomplete or immature fashion with one or two arms at the slip faces of barchan ridges. With progress eastwards, star dunes become mature with complete star form, and are organized as single rows or chains replacing the barchan or linear ridges. Further eastwards, the number of the star dunes increases and instead of star rows or chains, a random clustered pattern develops at the terminals of the linear ridges where sand supply increases significantly. Accompanied by this change, dune size increases, and compound forms develop. This change in dune development, organization, size and form eastward indicates that the star dune develops in a quite low sand supply environment with suitable multidirectional wind region (Hunting, 1979).

2.4.2 Stratigraphic Setting

2.4.2.1 Jabal Hafit

For description of the geologic succession in the prominent geomorphic units in the area is given on the geological map of Jabal Hafit (Figure 2.9). According to Hunting (1979) the succession in the Jabal Hafit anticline, which plunges northwards, is from oldest to youngest as follows:

A. The white to creamy limestone unit of the Paleocene to Middle Eocene age, forming the core of the anticline. The top of the creamy Limestone dips west at about 30°. It is overlain by a grey nodular limestone, chiefly exposed as a thin carapace on the dissected dip slope at the north end of the main mass of the

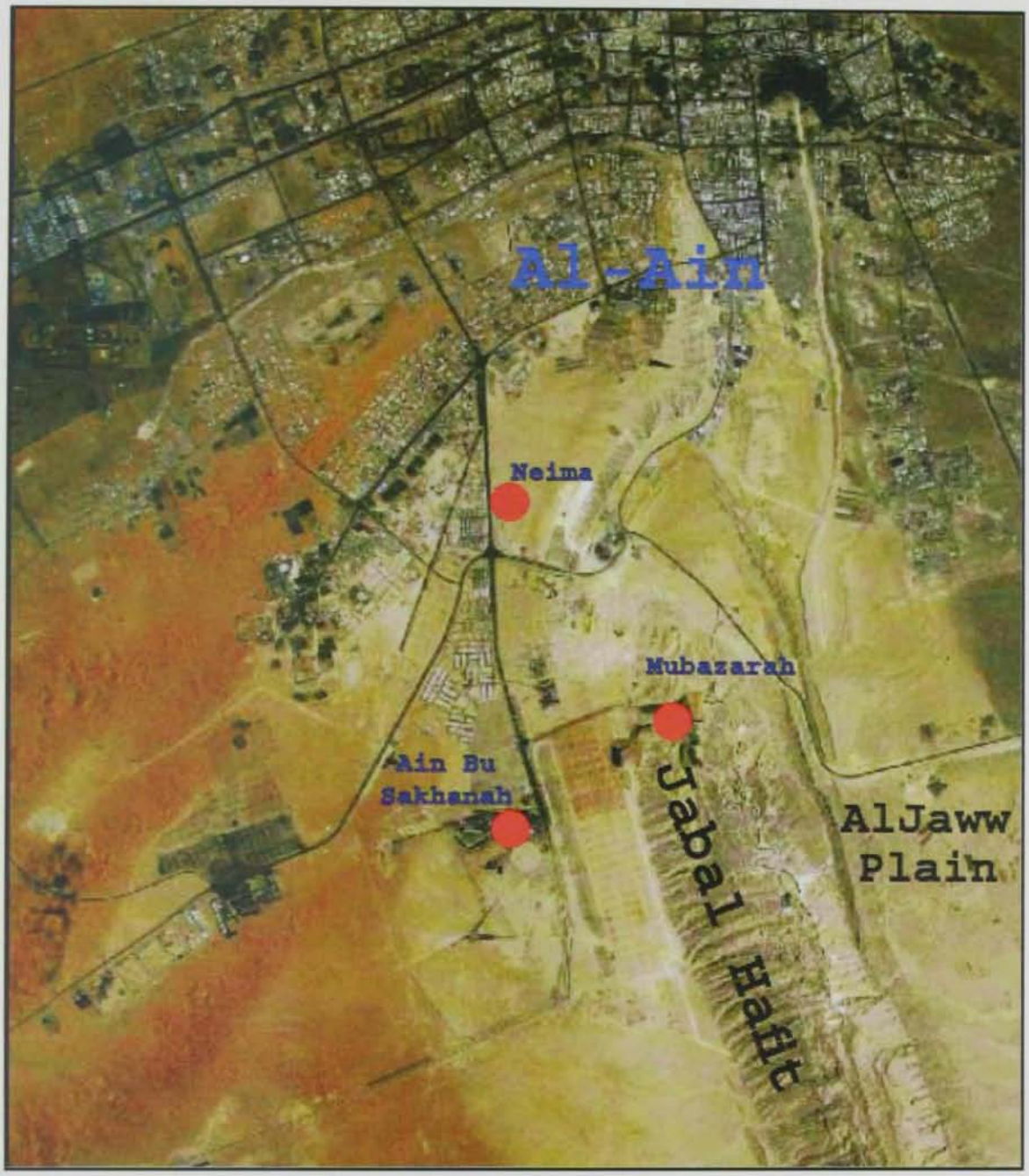

Figure (2.8): Landsat image showing the location of the study area.

mountain, besides nodular limestone , the unit contains bands of pebbles and boulder limestone conglomerate .

B. The marl and muddy limestone unit, which consists of a series of yellow marl, brownish limestone and muddy calcarenite. It ranges in age from Middle Eocene (lower yellow marl) to Upper Oligocene (muddy calcarenite).

C. The evaporites unit consisting of clay with gypsum and having an outcrop restricted to the Eastern flank of Jabal Hafit .Its base is marked by a band of bedded celestite of about 15 cm thick. This unit is of Miocene age. It is overlain by the youngest interval of the Jabal Hafit sequence which is also restricted in outcrop to the western Al Jaww Plain. This interval is of the Miocene age and is formed of mottled clay; it is distinguished from the underlying clay with gypsum by the absence of thick gypsum bands and the presence of thin layers of chalky carbonate.

Facies and thickness changes in the Jabal Hafit succession are shown in Figure (2.10) (Hunting, 1979) from which the following features are of interest:

- The thinning of the upper part of Midddle Eocene successions towards the south by an overlap onto the Paleocene –Middle Eocene creamy limestone.
- The change from shallow water limestone to mixed limestone and marl towards the north in the Middle and Upper Eocene.
- The dying out towards the south of the Oligocene limestone.

2.4.2.2 The Quaternary

Most of the area is covered by Quaternary deposits. Four types have been recognized and are described below.

I. Fluvial Deposits

Alluvial deposits occur beneath the piedmont plains fringing Jabal Hafit. They range from boulder gravel and conglomerate where wadis debouch from the Oman Mountains to fine sand and silt where the main wadis become lost in the dunes further

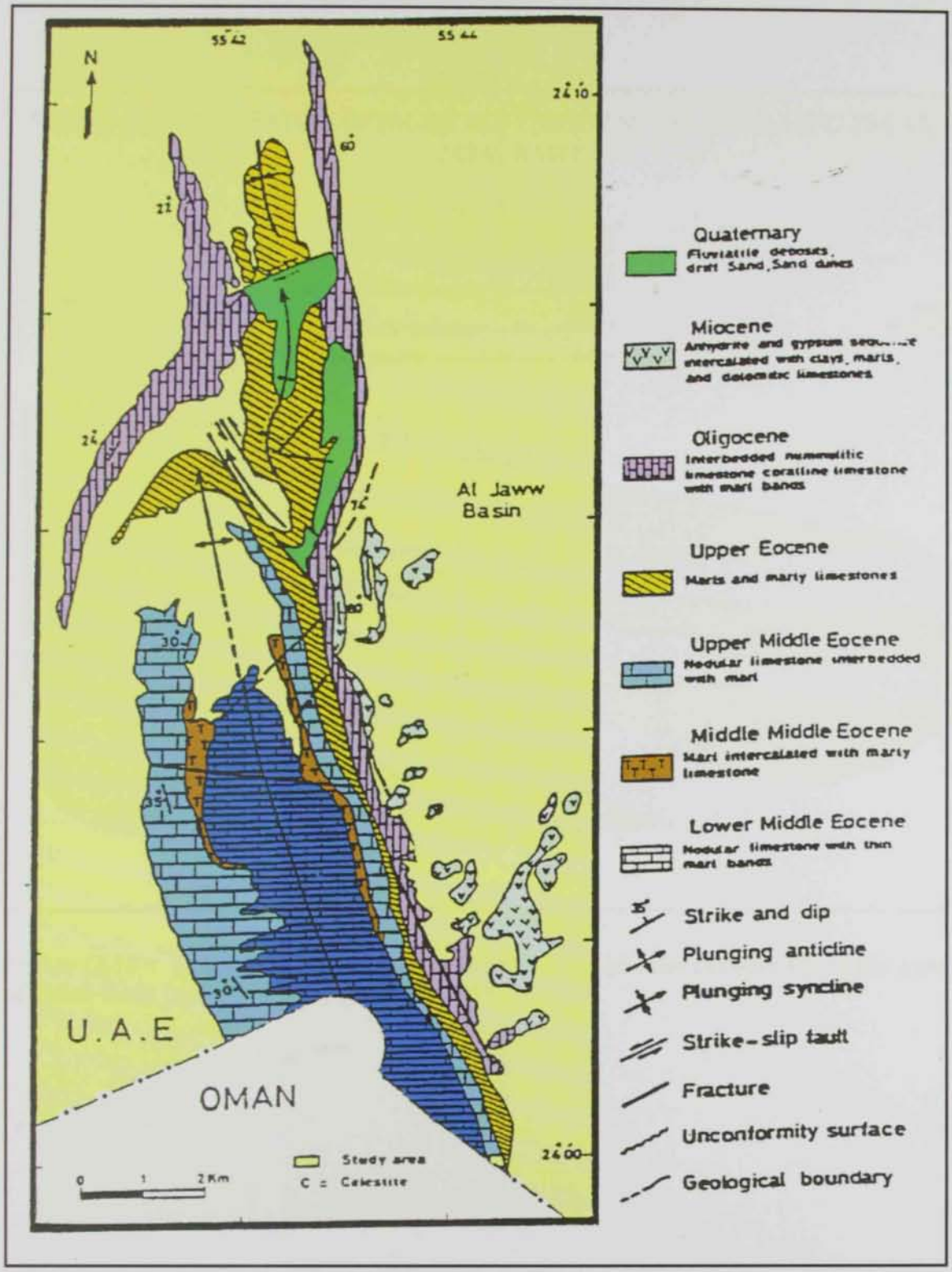

Figure (2.9): Geological map of Jabal Hafit (modified from Cherif and El-Deeb, 1984).

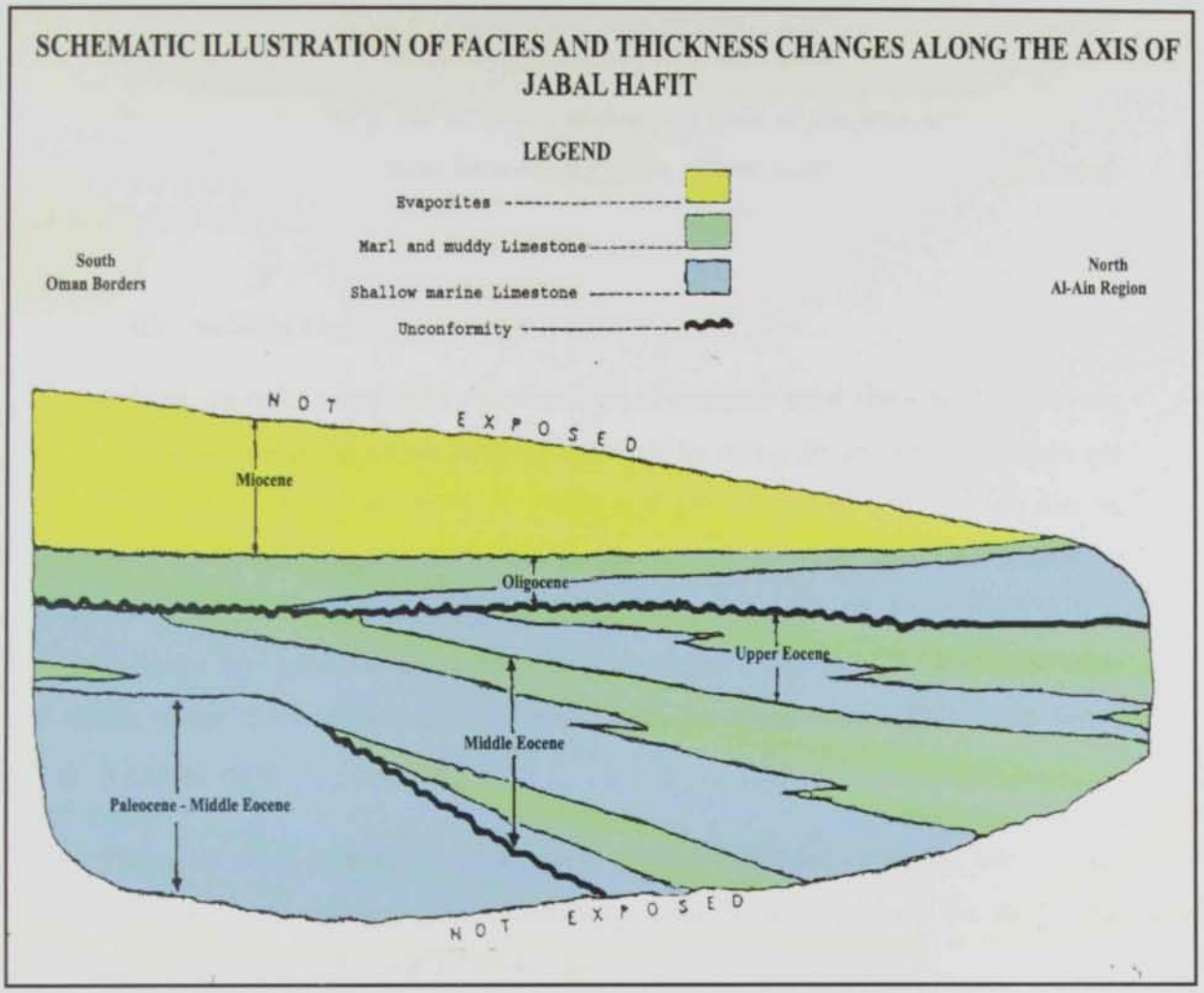

Figure (2.10): Schematic Illustration of facies and thickness changes along the axis of Jabal Hafit (modified from Hunting, 1979).

to the west. Towards the west where the alluvium becomes sufficiently fine-grained, it is subjected to wind action and the area partly covered by low sand dunes (Hunting, 1979).

II. Desert Plain Deposits

Most of the remaining flat or gently undulating parts of the area are underlain by desert plain deposits. They occur between the dune ridges mainly in the west and north of the studied area (Hunting, 1979).

III. Sabkha Deposits

Sabkha deposits occur where the main wadi channels enter the sand dunes at the other locations within the dunes liable to flooding by rising groundwater. Sabkhas are also developed on the lower parts of gravel and sand plains at and west of Ain bu Sukhanah. They are distinguished on the air photographs by their light tone caused by surface layers of calcareous silt deposited from the pools of flood water. Such light – toned patches are common along the margins of the distal parts of the main wadi channels where the alluvium is interspersed with low sand dunes. This setup forms traps for flood water.

The main rock type is a buff to gray, loosely cemented calcerous silt. Visible gypsum, which is common in the Sabkhas near the coast, is rare in the study area except around Ain bu Sukhanah (Hunting, 1979).

IV. Aeolian Sand

The western part of the area is covered by sand dunes. The sand varies in color from red and pink to white and tends to be lighter in tone where involved in active transport as at the crests of dunes. The clastics are of well-rounded grains of carbonate and quartz with minor proportions of basic and ultra basic rock types. Sorting is generally poor and no pure silica sands have been observed (Hunting, 1979).

2.4.3 Geologic Structure

The main structure in the study area is Jabal Hafit anticline, which is a periclinal fold plunging southwards in Oman and northwards in the U.A.E. It overturned and partly overthrust to the East. Northeast of the cement factory, the axis of the fold is offset towards the East by a zone of complex structure. In the north the hinge zone is located in the Middle and Upper Eocene rocks. The overlying Oligocene limestone is steeply dipping in the west limb, indicating overturning towards the east. The rocks are cut by numerous normal and nearly vertical faults and other fractures as well as by reverse faults (Hunting, 1979).

CHAPTER 3
Hydrogeology of Al-Ain Area

Hydrogeology of Al-Ain

Al-Ain area lies in an arid belt characterized by low rainfall and high evapotranspiration. The main objectives of this chapter are to describe the main hydrogeological conditions in Al-Ain, quantify available water resources in Al-Ain area and study the hydrogeological conditions in the study area.

3.1 Hydrogeology of Al-Ain

The area of Al-Ain is considered as a collecting basin; it receives water from the main catchment areas of the Oman Mountains and Jabal Hafit, which comprises high mountains and hills of basic igneous and limestones. A number of wadis running East-West form an active drainage pattern for surface run-off to the plains; the most important wadis being Al-Ain, Shik and Muraykhat . Moreover, groundwater flows into Al-Ain area through three main intermountain " gaps ": the Mahdah gap north of Al-Ain , The Zarub gap at the northern part of Al-Jaww plain and the Ajran gap at the southern part of Al-Jaww plain (Gibb and Partners, 1970).

3.1.1 Groundwater Bearing Formation

The main existing aquifers in Al-Ain are the Quaternary aquifer flanking the Northern Oman Mountains, the Jabal Hafit Limestone aquifer in the south and the Sand dune aquifers in the north and south. A discussion of these aquifers with more emphasis on the aquifers existing on the study area (Quaternary aquifer and Jabal Hafit limestone aquifer) is provided hereafter. For more detail about the different types of aquifer in the UAE, reference is made to Garmoon, (1996); Bakhit, (1998); Rizk, (1999) and Alsharhan et al, (2001).

3.1.1.1 The Quaternary Alluvial Aquifer

The Quaternary alluvial aquifer represents the most important aquifer in Al-Ain area, because it contains the largest reserve of fresh groundwater. It consists of fine to coarse sands and gravels and is recharged from the Oman Mountains in the east through several buried channels. When the alluvial material was initially deposited by streams

that discharged from Oman Mountains, the layers of gravel, sand, silt, and clay contained a large percentage of void space that could store and transmit a considerable volume of groundwater. Over long periods of time, however, minerals precipitating from groundwater and clay formed by weathering have filled the original pores and cemented the deposits. The cemented parts of the alluvial deposits yield only small volumes of water to wells. Major wadis emerging from the Oman Mountains have eroded channels through the cemented parts of flood plain deposits. Sand and gravel deposited in the eroded channels can be prolific sources of groundwater, where the water table is above the bottom of the unconsolidated deposits (Hydroconsult, 1978).

The Quaternary aquifer is characterized by high porosity, high permeability and low salinity (Hydroconsult, 1978). Several groundwater fields around Al-Ain city tap this aquifer and produce considerable amounts of water from it (Table 3.1).

Table 3.1 Properties of groundwater fields around Al-Ain area, (Hydroconsult, 1978).

Name	Location	No. of wells	Well Depth (m)	Water Depth (m)	T (m^2/d)	Salinity (mg/l)
Al-Khudr	70 km North of Al-Ain	90	45-75	18-25	25-60	<1,000
Kashunah	SE of Al-Khudr	120	80-90	20-30	400	500-800
Khaznah		150	30-75	15-20	30-100	4,000-6,000
Gabiah-Shubak		150	5-25		80-250	900-9,000

The Quaternary units are composed by gravel and conglomerate outwash fans deposited by flood flows from the Oman Mountains. These outwash fans cover older geologic units and infill shallow depressions resulting in a relatively featureless plain sloping from east to west. The quaternary sediments thicken toward the west and as much as 400 m of sediments were encountered in a borehole in the western side of Jabal Hafit, (Gibb and Partners, 1970).

The Quaternary deposits become fine-grained toward the west away from the mountain source, in the plain lying to the west of Jabal Hafit, the thickness of the Quaternary deposits has a very wide range; it gets thicker towards the west. The thickness reaches about 500 m at the extreme west of that plain. The absolute water level is in the order of 230 m above sea level (Gibb and Partners, 1970).

3.1.1.2 Jabal Hafit Limestone aquifer

Limestone formations can be prolific sources of groundwater where fractures, fissure, or solution cavities have developed in the otherwise impermeable rock. Fractures and fissures develop where the rocks have been folded and faulted by tectonic forces such as those that uplifted the Oman Mountains and produced the jabals, and limestone outcrops near the mountain front. Solution cavities develop when slightly acidic groundwater dissolves soluble minerals from the limestone. Fractures and fissures in deeply buried limestones are typically filled with mineral deposits or constricted by the weight of overburden (Hutchinson, 1996).

Jabal Hafit is composed of 1500 thick limestone and marl interbeds with gypsum and dolomite and evaporite formations of Lower Eocene to Miocene age. Limestone of the Middle Eocene Dammam Formation constitutes an aquifer in Jabal Hafit. The aquifer is characterized by extensive dolomitization and is affected by numerous faults and fractures. Porosity is virtually null except for infrequent unfilled fractures, vugs and heterogeneous secondary porosity (Whittle and Alsharhan, 1994).

According to Stringfield and Le Grand (1966), if thick deposits of low permeability overly a carbonate terrain, and if the carbonate was never elevated into a groundwater circulation system, then little secondary porosity will be developed. On the other hand, early elevation of the carbonate into a groundwater circulation system will lead to development of secondary porosity and permeability and to partial or complete removal of the carbonate. The emergence of mature carbonate terrain relative to sea level lowers the base level for groundwater discharge permits meteorically derived fluids to penetrate the "elevated" terrain more deeply, which thereby contributing to secondary porosity and the formation of deep-seated karst.

White (1977) proposed three conceptual models for carbonate aquifers:

1. Diffuse-flow carbonate aquifers; have had little solutional activity directed toward opening large channels, and these are to some extent homogeneous.

2. Free-flow aquifers; receive diffuse recharge, but have well-developed solution channels along which most flow occurs. Groundwater flow in free-flow aquifers is controlled by the orientation of the bedding planes and fractures that determine the location of solutional conduits, but not by confining beds.

3. Confined-flow carbonate aquifers; have solution openings in the carbonate units, but low permeability non-carbonate beds exert control over the direction of groundwater movement. This category is similar to the aquifer system in the Jabal Hafit area where the marl unit capping the Eocene limestone rocks acts as the confining layer of the aquifer.

(Figure 3.1) shows a conceptual model of the three water bearing zones in Jabal Hafit area. These are: a fresh water zone replenished by meteoric water, a mixing zone where fresh water mixes with brackish water and a deep saline water zone (White, 1977). The model supports a mixture of two different sources, fresh water from rain falling on the Jabal and saline water moving upward from 2,000 m deep by gas or temperature drive. Brackish water is formed due to the mixing of the two types of water. Then, the aquifer water cools and becomes more dilute.

3.1.1.3 Sand Dune Aquifer

The sand dunes that cover much of the land surface of Al-Ain contain considerable void space between the individual grains of sand. Although the vast volume of void space could store considerable volume of groundwater, most of the void space is unsaturated. Even in areas where the lowest sections of sand dunes are saturated, the steep topographic relief and high permeability of the dunes allows groundwater to flow rapidly from beneath the dunes into low-lying interdunal areas where it evaporates, (Imes et al., 1994).

Consequently, where groundwater exists in dunes, it generally is found in relatively thin layers and is difficult to extract using conventional drilled wells. Shallow hand-dug wells that yield small volumes of relatively fresh water can be found within dunes in Al-Ain, but the source is limited (NDC & USGS, 1993)

Generally sand dunes are the least studied aquifer type in Al-Ain. The Groundwater Research Project of the National Drilling Company (NDC) and the United States Geological Survey (USGS) confirmed the presence of a fresh water aquifer in the Quaternary sand dunes between Liwa and Madinat Zayed. Preliminary hydrogeological investigations of sand dunes in the Bu-Hasa oil field indicate the presence of a similar fresh water mound. Exploration of the sand dunes between Al-Wagan and Liwa lead to the discovery of similar fresh water lenses

3.1.2 Groundwater Recharge

Rainfall is the original source of natural recharge to the groundwater system but several avenues are available for the rainfall to enter the system. Direct infiltration of rain falling on the land surface overlying an aquifer is an obvious recharge mechanism. Rain can also infiltrate into surrounding areas migrate through permeable material, and enter the groundwater system as underflow. In addition, the bed rock that forms the mountains bordering the eastern boundary of Al-Ain transmits groundwater into the aquifers underlying Al-Ain. Streams flow across the permeable flood-plain surface, seepage from the streambed contributes water to the underlying groundwater system. Although runoff events are sporadic, they constitute a significant source of recharge for brief periods of time (Maddy, 1993).

Studies suggest that only a small percentage of rain falling directly on the land surface infiltrates into the underlying groundwater system. Based on studies completed in similar environments, investigators concluded that infiltration of rainfall through sand dunes is relatively minor (Maddy, 1993). On the coarse grained surfaces of the gravel plains and on bedrock outcrops, investigators estimated that 5 percent of the rainfall infiltrates and enters the underlying groundwater system. Because the total area of the permeable land surface is large, this small percentage of infiltration may constitute a

major source of natural recharge. The long-term average rate of infiltration of precipitation in Al-Ain area was estimated to be 18 million Mm^3/Year, (Maddy, 1993).

Although sporadic wadi flow can be dramatic, the infrequent and short lived phenomenon contributes only small volumes of water to the groundwater system. The long term average recharge from runoff events in Al-Ain area was estimated to be about 0.3 million cubic meters per year, (Maddy, 1993). Because the recharge occurs during brief periods, groundwater levels in shallow aquifers near the wadis can rise dramatically during a runoff event but usually fall to pre-flood levels within a short period of time.

A model constructed by Maddy (1993) was used to verify estimates of long-term average rates of subsurface inflow through wadi gaps in Al-Ain area. Observations of water table gradients along the mountain front suggested that the rate of subsurface flow through bedrock areas is comparable to the flow through the sand and gravel deposits which fill the wadi gaps. The combined total of subsurface inflow from wadi gaps and bedrock was estimated to be about 9.5 million cubic meters per year.

Man-induced recharge occurs from irrigation return flow, leakage from pipelines and runoff from waste-water disposal facilities. The volume of recharge from these sources is difficult to quantify, but it may be substantial in some areas. Where the source of irrigation water is from wells, the return flow is merely unused groundwater that returns to the underlying aquifer. Where irrigation water is derived from reclaimed waste water or from desalinated sea water, the irrigation return flow is supplemental water that adds to the groundwater supply. Leakage from pipelines may constitute a major source of recharge in densely populated service areas.

3.1.3 Groundwater Storage

In 1986, Shankland and Cox estimated total storage of fresh water in the Quaternary aquifer in Al-Ain area to be 2,600 million m^3 and the total storage of brackish water to be 18,000 million m^3. Therefore, the estimated total storage of fresh and brackish water in Al-Ain area is 20,600 million m^3.

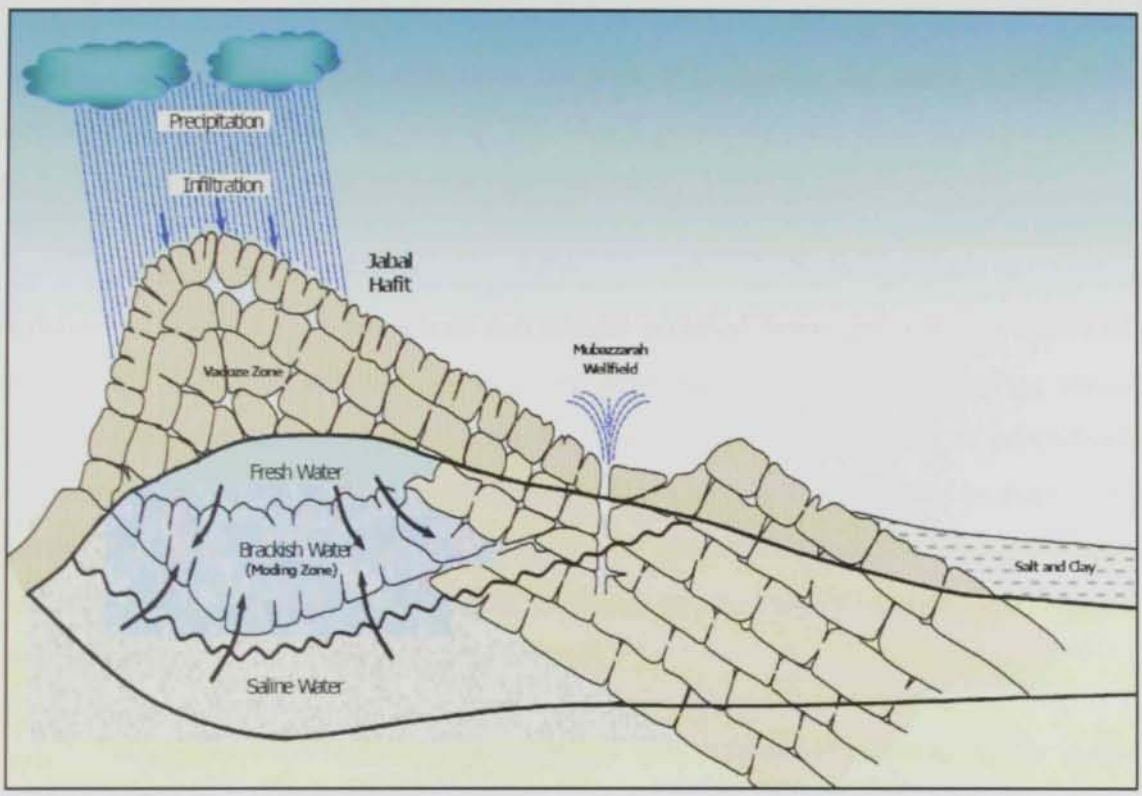

Figure (3.1): Conceptual model of recharge and discharge of the Tertiary limestone aquifer at Jabal Hafit, (Al-Nuaimi,2003 after Khalifa, 1997).

3.1.4 Groundwater Discharge

Groundwater flows through aquifers to points of discharge where it leaves the groundwater system. Natural points of discharge include low lying areas where groundwater flows to the surface as springs or seeps, sabkhas and salt flats, where it is evaporites directly from the soil, and vegetated areas where deep rooted plants extract water directly from the water table. Groundwater flow from one region or area to another can also be considered discharge from the area even though the water is still in the aquifer. Groundwater that is pumped from wells or widthdrawn from falaj networks is part of the overall discharge from the aquifer (Maddy, 1993).

Under natural conditions, most of the groundwater discharge from the Emirate occurred as evaporation from inland and coastal sabkhas. Some groundwater also flows beneath the coastline and discharges to the Arabian Gulf in offshore springs. Before groundwater development altered conditions, an estimated 17 million m^3 of groundwater evaporated annually from shallow aquifers in Al-Ain area or was removed by deep rooted plants. The rate of flow to the Arabian Gulf under natural conditions was estimated to be 11 Mm^3/yr. The 28 million m^3 of natural discharge approximately balanced the long-term average rate of natural recharge (Maddy, 1993).

Pumpage from the groundwater system has dramatically altered the long-term balance between natural recharge and natural discharge. For Al-Ain area, Hutchinson (1996) estimated that the 1994 flow from falaj networks was about 7 Mm^3/Year, pumpage of fresh water from wells was about 95 Mm^3/Year, and pumpage of brackish water was about 310 Mm^3/yr.

Pumpage from the groundwater system greatly exceeds the natural rate of recharge. Although part of the deficit is derived from reduced rates of natural discharge (primarily reduced evaporation from inland sabkhas and vegetated areas), most of the deficit is obtained by depleting aquifer storage.

3.1.5 Occurrence and Movement of Groundwater

Groundwater moves under the influence of gravity or pressure differentials from areas of recharge to points of discharge. Under water table conditions, gravity moves water down the hydraulic gradient in a fashion similar to overland flow of water down sloped surfaces. Under confined conditions, pressure differential is the driving force. In general, groundwater moves laterally but differences in pressure between aquifers can cause vertical movement to occur through confining layers. Vertical flow most commonly occurs in areas of recharge or discharge where underlying aquifers receive or yield water to or from overlying aquifers. In recharge areas, water levels in deep wells are lower than water levels in shallower wells and downward flow of groundwater occurs. In discharge areas, deeper wells have higher water levels than shallower wells and upward flow of groundwater occurs (Hutchinson, 1996).

Rates of groundwater flow were calculated from aquifer characteristics and the slope of the water table or pressure gradient. Typical rates of flow in the unconsolidated alluvial aquifer near the mountain front are a few tens of meters per day. In sand aquifers, the rate of flow is somewhat slower and may be on the order of a few meters per day. High rates of flow may occur near pumping wells where water table gradients are steep and in some very permeable aquifers such as limestone with open fractures and solution cavities. Under theses circumstances, rates of flow may be on the order of several hundred meters per day. In general, however, flow rates rarely exceed 10 to 100 meters per day (Hutchinson, 1996).

Aquifers may have preferential groundwater flow paths (bedding planes or fracture zones, for example) that allow water to move more easily in certain directions; the general direction of groundwater movement is perpendicular to the lines of equal water level elevation. According to Hutchinson (1996); the groundwater flows from the recharge areas near the Oman Mountains toward the discharge areas along the Arabian Gulf. As groundwater development occurred, extraction of groundwater from wells has altered the natural pattern of groundwater movement. Groundwater that would have

flowed to discharge areas under natural conditions is now captured in depression in the water table surface produced by groundwater pumpage.

The levels of the pre-development water table in Al-Ain aquifer ranged from 350 m above mean sea level near the Oman Mountains to 60 m at the northwest limit of the eastern investigated area. A large mound of groundwater exists near Jabal Hafit . This conclusion was based on water-levels from seismic uphole-survey data collected between 1981 and 1982 (Woodward and Menges, 1991). The steeper hydraulic gradient was established due to the difference in altitude of about 80 m between Al Jaww plain east of Jabal Hafit and gravel plains west of Jabal Hafit. The groundwater mound indicates the following:

- Infiltration of the rainfall through the permeable units of Jabal Hafit.
- Upward movement of groundwater through fractures of Jabal Hafit, derived by gas pressure or thermal gradient.

The depth to the groundwater table decreases with distance from the Oman Mountain from 30 m in the eastern part of Al-Ain to about 3 m in the western part. The regional water level in Al-Ain aquifer is shown (Figure 3.2). There were depressions in water levels in some areas due to groundwater withdrawls during 1990-1991. The largest water level depression was about 790 km^2 and extent west from Al-Ain to Abu Samara and south from Al zaala to She Sabra (Al Maqam depression). Al Maqam depression started as disconnected groups of smaller depression in Jahar, Saad, Zaala, Meya and Maqam well fields. The maximum drawdown in Meya, Jahar and Saad together were 80, 50, and 40 m respectively (NDC & USGS, 1993).

The decline in the water-level resulted in the following:

- Raise the water costs due to drilling of new wells and lifting the water with higher electricity costs.
- Disrupting the regional groundwater flow patterns when large quantities of groundwater are intercepted.
- Degradation of the water quality due to the flow of saline water vertically (upcoming of low quality water) (NDC & USGS, 1993).

The thickness of fresh water in Al-Ain aquifer is shown in Figure (3.3). The aquifer is composed of interbedded permeable and slightly-permeable layers. The thickness of the permeable material is not uniform. As a result, neither the aquifer thickness map nor the fresh water thickness map represents the total thickness of permeable material. (NDC & USGS, 1993)

The boundary between brackish water and saline water exists above the bottom of the deep boreholes in the basal confining system (Figure 3.4). The brackish water has a thickness of about 200 m near Zarub Gap. This Thickness becomes slightly more than 500 m along the east side of Jabal Hafit while it ranges between 100 to 200 m in the northern dune area. The areas in the northeast and south have larger thickness, (NDC & USGS, 1993)

3.2 Hydrogeology of the Study Area

The study area is generally located southeastern of Al-Ain , between longitudes 37° and 37° 50′ E and latitudes 26° 61′ and 26° 73′. However, special emphasis was given to the triangular area bounded by Al-Neima in the north, Mubazzarah in the east and Ain Al-Fayda (Ain Bu Sukhanah) in the west. (See Figure 2.8 in chapter 2)

Jabal Hafit is considered as the most prominent feature of the study area, and its geological nature significantly affects the hydrogeology of the area. The following is a brief description of the hydrogeological conditions in Mubazzarah, Neima and Ain Bu Sukhanah respectively.

3.2.1 Hydrogeology of Mubazarah

The Mubazarah area (Figure 3.6) is in a valley about 2 kilometers long by 0.5 kilometer wide at the north end of Jabal Hafit near Al-Ain. Fifteen large diameter wells have been drilled in the wellfield, with about 10 wells capable of producing large quantities of water. Well depths range from 90 to 200 meters and yields of as much as 4,600 cubic meters per day (m^3/d), or 850 gallons per minute (gal/min), are attributed to fracture permeability and dissolution. A substantial drop in yields is probable if secondary

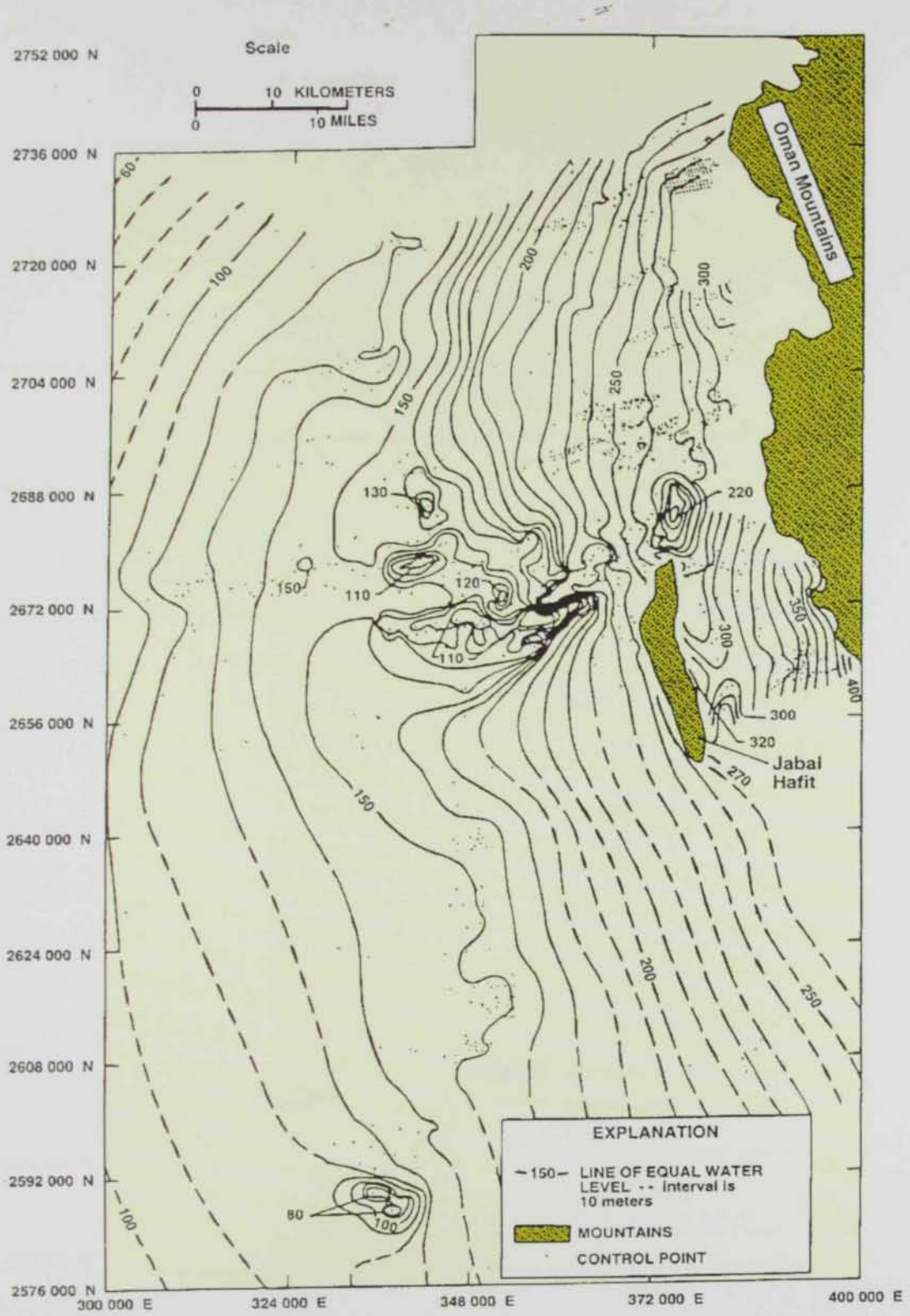

Figure (3.2): Regional water level in Al-Ain aquifer in 1991 (modified from NDC and USGS, 1993).

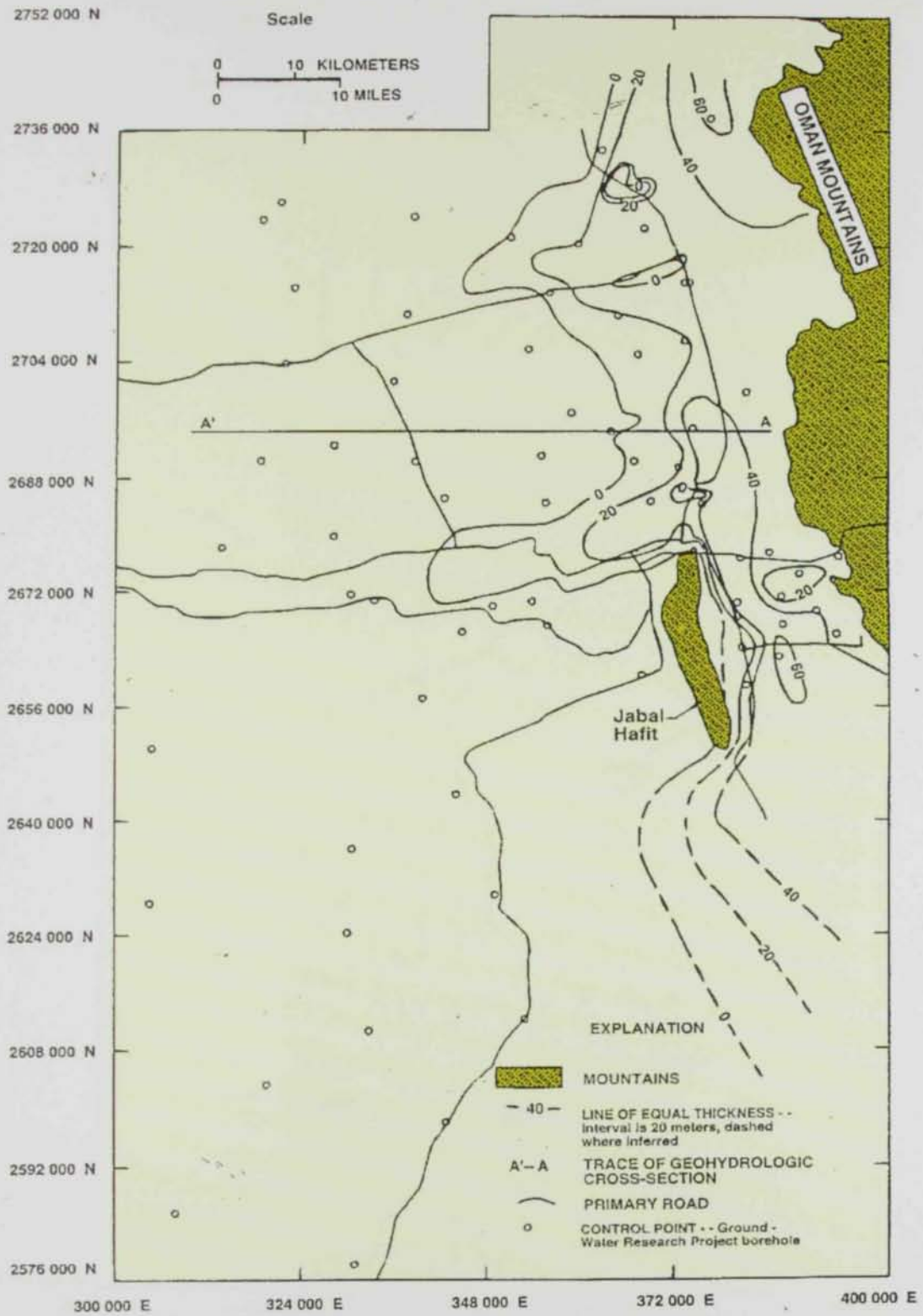

Figure (3.3): Thickness of freshwater in Al-Ain aquifer (modified from NDC and USGS, 1993)

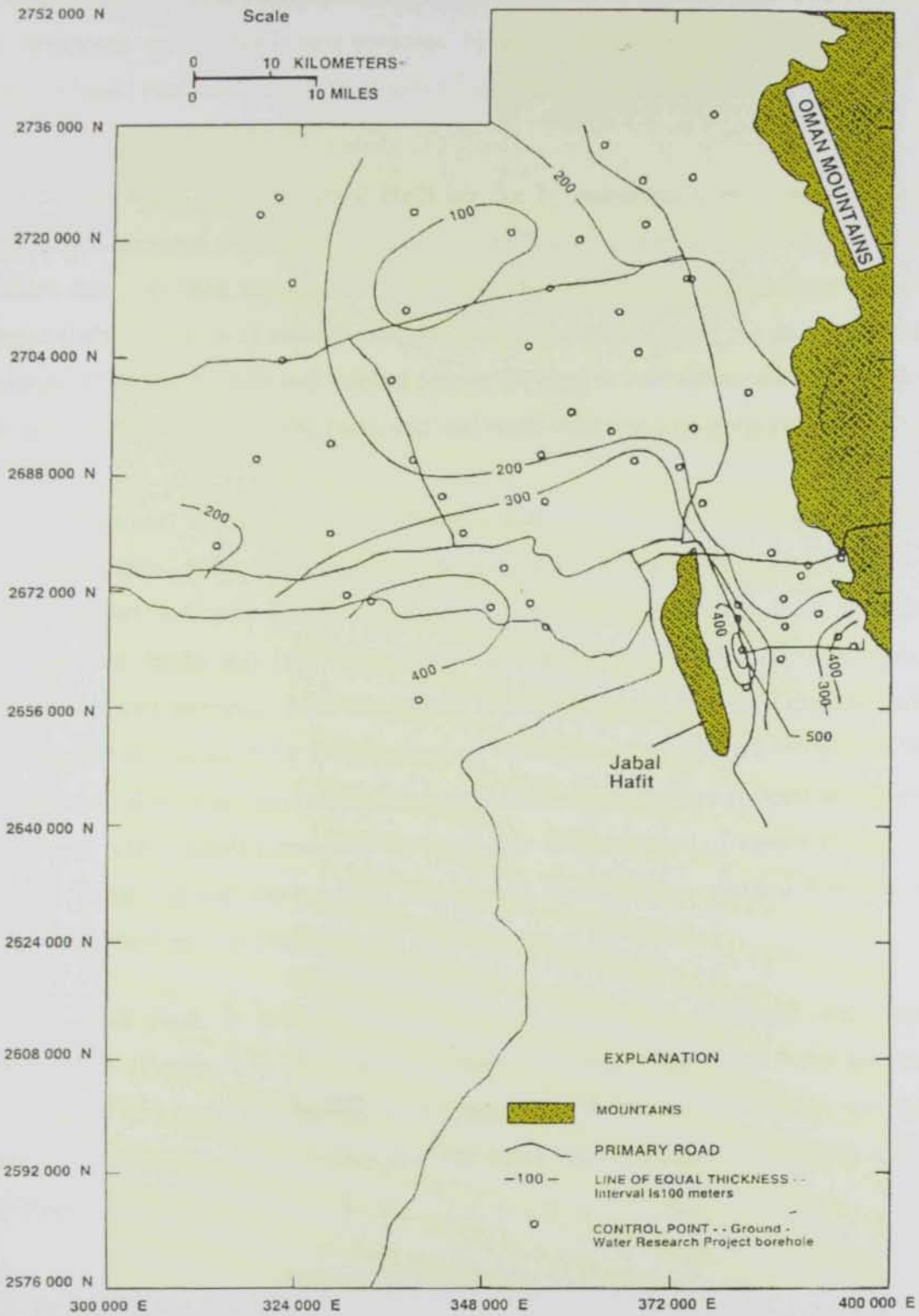

Figure (3.4): Thickness of the brackish water in the basal confining system (modified from NDC and USGS, 1993).

porosity features are not interconnected. Water produced by the well field is being used for a therapeutic spa and for leisure purposes. Measured discharge to a holding pond west of the well field has been as high as 21,000 m^3/d (4,000 gal/min) (Khalifa, 1997).

The rocks that form Jabal Hafit are cut by numerous normal and near vertical faults and fractures. Faults are considered to be fracture planes or fracture surfaces along which there has been appreciable movement. The normal-fault displacement of rocks at Jabal Hafit is a result of collective or differential movement along the numerous fracture planes. The normal faults and fracture pattern exposed at the outcrop strike perpendicular to the axis of the fold or form north-east and north-west trending conjugate sets, (Khalifa, 1997).

Because of their nearly planar nature, faults and fractures provide an inhomogeneous secondary porosity in carbonate aquifers. Kastning (1977) has demonstrated that with respect to their influence on groundwater flow and conduit enlargement, faults may have a positive, negative, or neutral effect. If the presence of faults increases permeability of the aquifer or otherwise enhances flow characteristics of the aquifer, the effect of the fault is positive. Examples of the positive influence of faults on groundwater movement include characteristically open fracture systems resulting from tensional (extensional) forces and increased rate of breakdown of cavern roofs in areas where faults intersect the caverns. Extensional, open-fracture systems typically occur parallel to the crest and perpendicular to the plunge of the anticline.

Jabal Hafit is primarily composed of interbedded carbonate and evaporite formations (Figure 3.5) of Lower Eocene to Miocene age. The rocks are mainly limestones and marls interbedded with gypsum and dolomite. The average thickness is about 1,500 meters, but the thickness of the water-bearing formation is significantly less, (Khalifa, 1997).

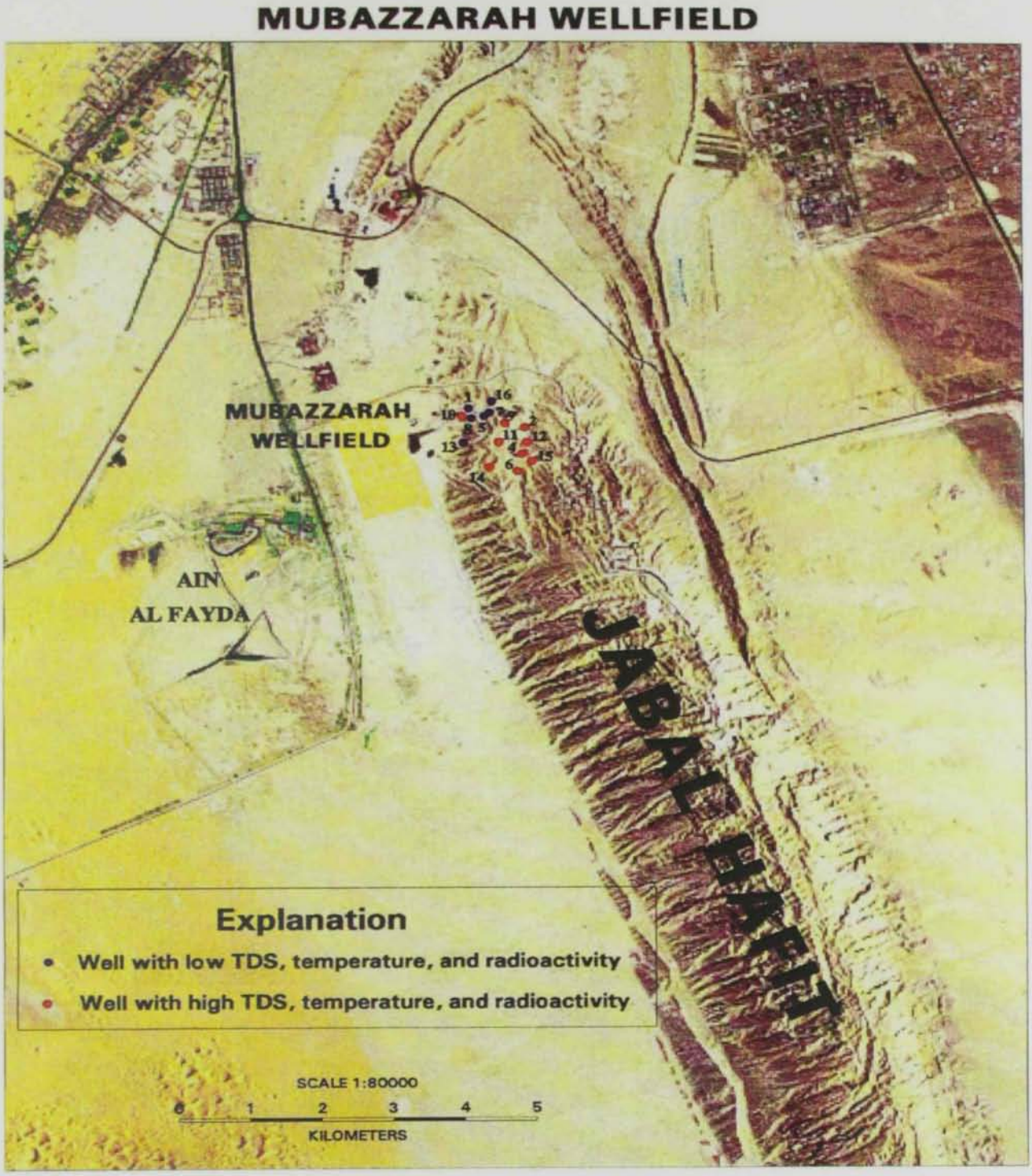

Figure (3.5): Location map of Mubazzarah well field and Jabal Hafit, (Khalifa, 1997).

During the geological time, relatively large amount of rain have fallen on the limestone of Jabal Hafit anticline. As the water dissolved, the carbonate rocks of the jabal, it increased the pore space and permeability. The rocks of the jabal are relatively permeable owing to the fissures, faults, and joints. Consequently, infiltration is relatively high and evaporation and runoff are limited. In areas of folded carbonate rocks, like the Jabal Hafit anticline, zones of fracture and solution enlargement are commonly located along the crest of the anticline and to a lesser extent in synclinal troughs, (Khalifa, 1997)

Dissolution of limestone forms a karst aquifer system, characterized by solution channels and caves. Figure (3.6) shows a conceptual model of the three water-bearing zones in the Jabal Hafit area:

- Fresh water zone, recharged by meteoric water.
- Mixing zone where fresh water mixes with brackish water .
- Deep saline-water zone.

Wells that produce water with relatively high temperature and specific conductance are located close to the fold axis of the jabal as compared to wells that produce cooler and fresher water which are located further from the axis. Deep fractures may act as conduits to bring thermal and saline water close to the surface before it cools or become diluted (Khalifa, 1997).

According to Khalifa (1997), the source of the water may be either meteoric water that rises by hydraulic pressure after having descended to a great depth or saline water that ascends due to gas pressure or thermal gradient. The conceptual model of the Jabal Hafit karst, supports a mixture of the two different sources. The flux of fresh recharge water through the jabal may be greater than the lateral or upward flow of saline water into the conduits. Therefore, the result is a water in the mixing zone that is brackish. The water in the conduits is heated by normal geothermal gradient at a depth of approximately 2,000 meters below the surrounding land (3,000 meters below the jabal). The conduits bring the mixed water to the base of the clastic aquifer where it enters the shallow

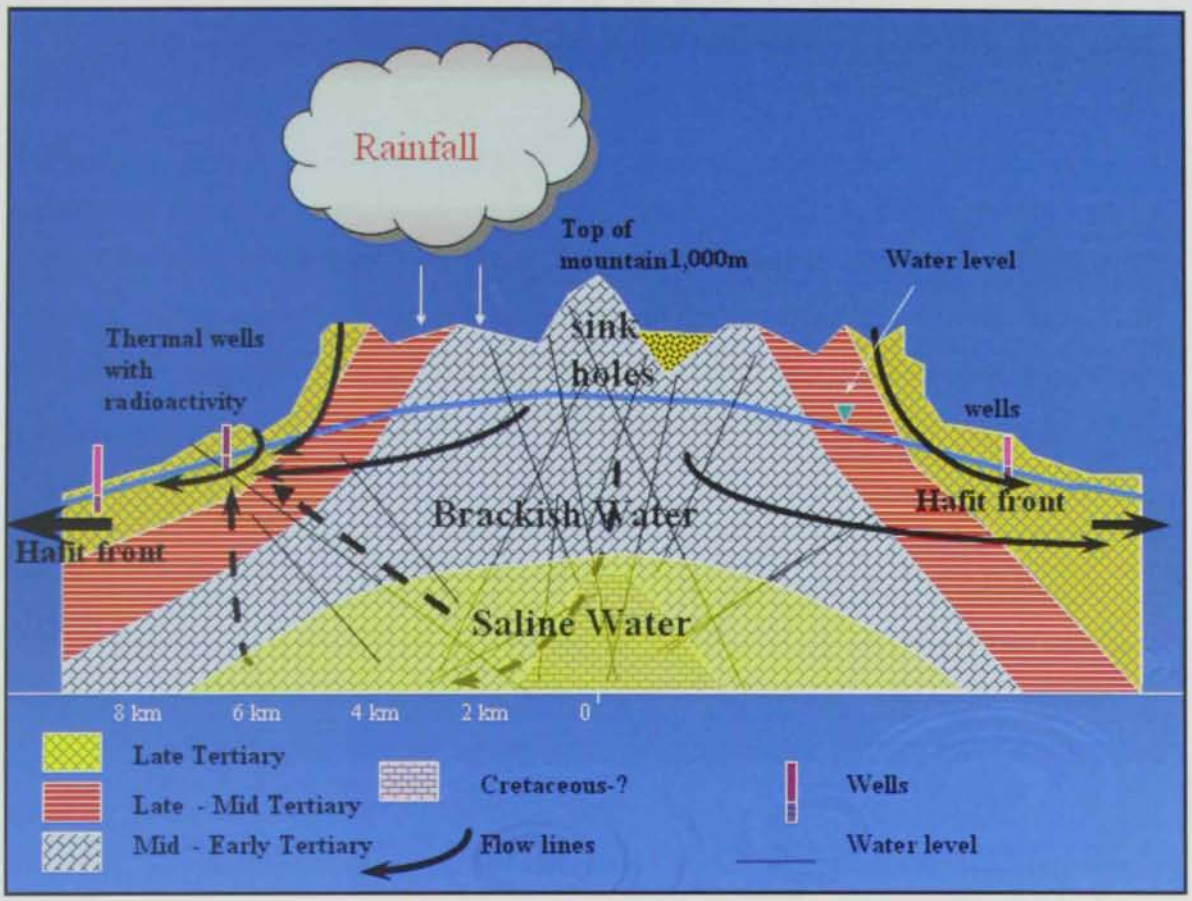

Figure (3.6): Conceptual model of the three water-bearing zones in the Jabal Hafit area, (Khalifa, 1997).

regional flow system. The aquifer water cools to near the ambient aquifer temperature, and becomes even more dilute.

Water levels range from 5.71 meters below land surface in well JH-16 to 60.94 meters below land surface in well JH-15 (June 1996). Water levels generally are declining in those wells that are frequently pumped or are adjacent to pumped wells. An example of declining water levels is the hydroraph for well JH-4 shown in Figure (3.7). The water from the pumped wells flows downstream where it enters unlined pools and channels. Water levels in wells in the downstream areas generally are rising, perhaps in response to recharge water percolating downward from the channels and ponds. An example of rising water levels is the hydrograph for well JH-7 shown Figure (3.8), (Khalifa, 1997).

3.2.2 Hydrogeology of Neima

Neima area is located about 2 kilometers north of the northern peak of the Jabal Hafit anticline. The Jabal outcrop located about 1 km to the east, represents an exposed limestone outcrop on the limb of an anticline. In early February 2003, an old municipal well began flowing after reportedly being abandoned about 10 years ago because it had dried up. The well is located about 6 kilometers south of Al-Ain city, and is about 2 kilometers north of the road at the base of Jabal Hafit (Figure 3.9). The well was supposedly drilled some 15 years ago to a depth of 550 ft (Khalifa, 2003).

From the available interpretations of the hydrogeology of the Jabal Hafit area located south of the flowing well and seismic line interpretations in the area, Khalifa (2003) provided the following description of the hydrogeologic setting in the area of the flowing well:

- Fresh and brackish water of limited areal extent is found within limestones in the Jabal Hafit area. These sources are only found in exposed outcrops in the limbs and crest of anticlines. The Jabal, rock outcrop, located about 1 km to the east of the flowing well represents an exposed limestone outcrop on the limb of an anticline.

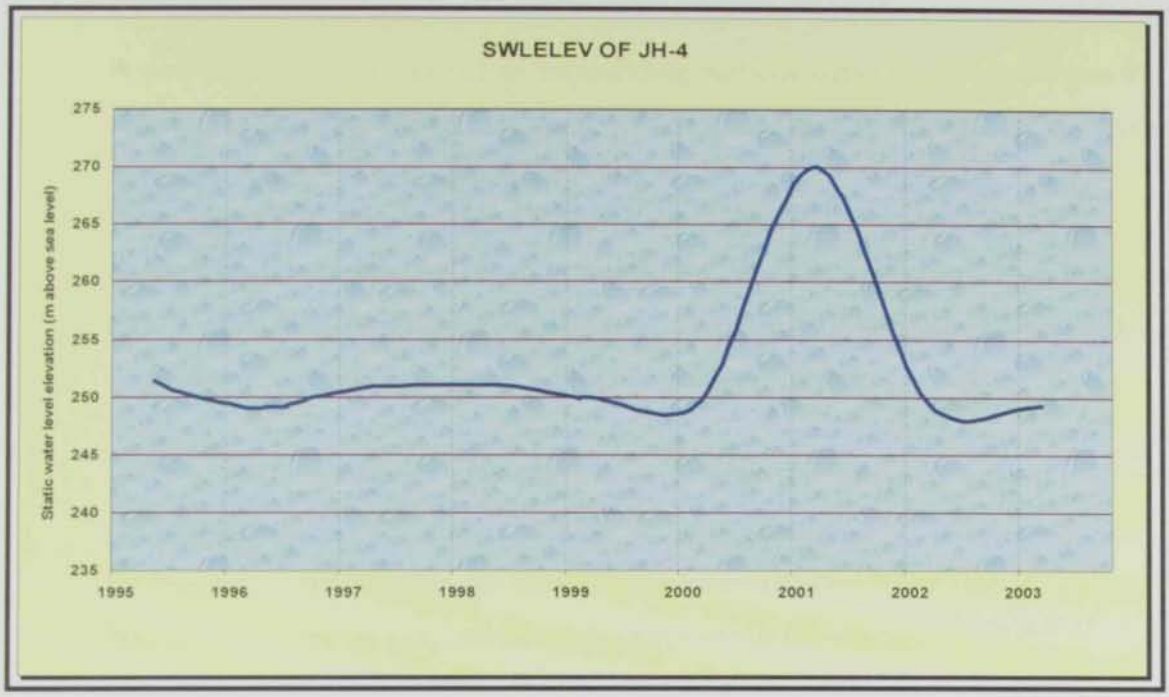

Figure (3.7): Static water level for well JH-4, (Khalifa, 1997)

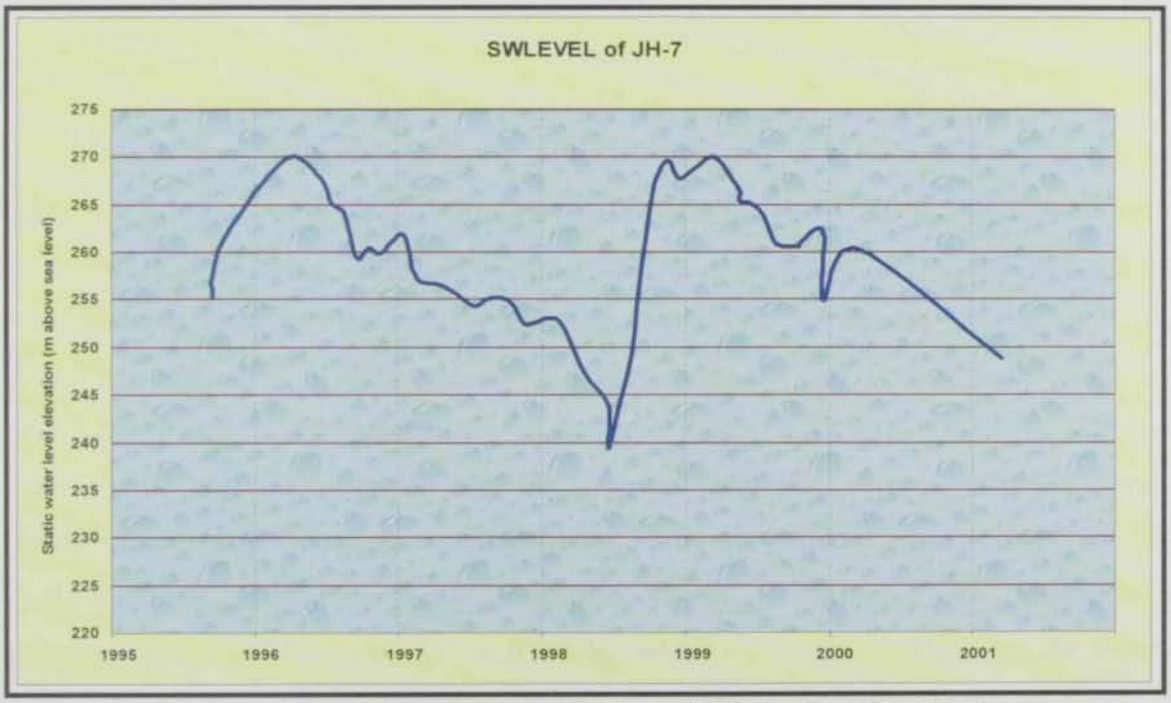

Figure (3.8): Static water level for well JH-7, (Khalifa, 1997).

- The source of fresh and brackish water in the vicinity of these limestone outcrops is rainfall on the rock outcrop or surrounding surficial deposits. In some cases the recharge is from the recent past (0 to 10's of years) and in other cases it is from the distant past (100's to 1,000's of years).

- In the vicinity of the rock outcrop, the limestone aquifer is unconfined. Further (down dip) away from the rock outcrop, the limestone aquifer is either semi-confined or confined by underlying and overlying rock units.

- The principal avenue by which water flows through the limestone aquifer is either through naturally occurring pores in the intergranular matrix (chalky limestones), by interconnected solution cavities created when the limestone matrix has been dissolved, or through interconnected fractures in the limestone.

The geohydrologic setting in the surrounding area of the flowing well based on this information is demonstrated in a conceptual geohydrologic cross section from the Jabal located approximately 1 km east of the flowing well to a location west of the flowing well (Figure 3.10).

On March 2003, the Agriculture Department of Al-Ain Municipality, ran a TV camera down the flowing well to document flow in the well (Figure 3.12). The video showed that PVC casing extended to a depth of 32 ft, PVC screen was found from 32 ft to 53 ft depth, there was a 1 foot gap between 53 to 54 ft, and stainless steel screen was found from 54 to 194 ft (all depths are in ft below land surface). Although the well was reportedly drilled to 550 ft, gravel was observed obstructing the well at the 194 ft depth. Upward flow was observed in the well casing in the depth range of 155 to 157 ft and was determined by observing pieces of material tied to the camera housing. Below 155 to 157 ft, the absence of cloth movement indicated that the water in the casing was stagnant. It is not clear if the water entering the well casing between 155 to 157 ft is from the water bearing formation occurring at this depth. The possibility exists that the water is from a

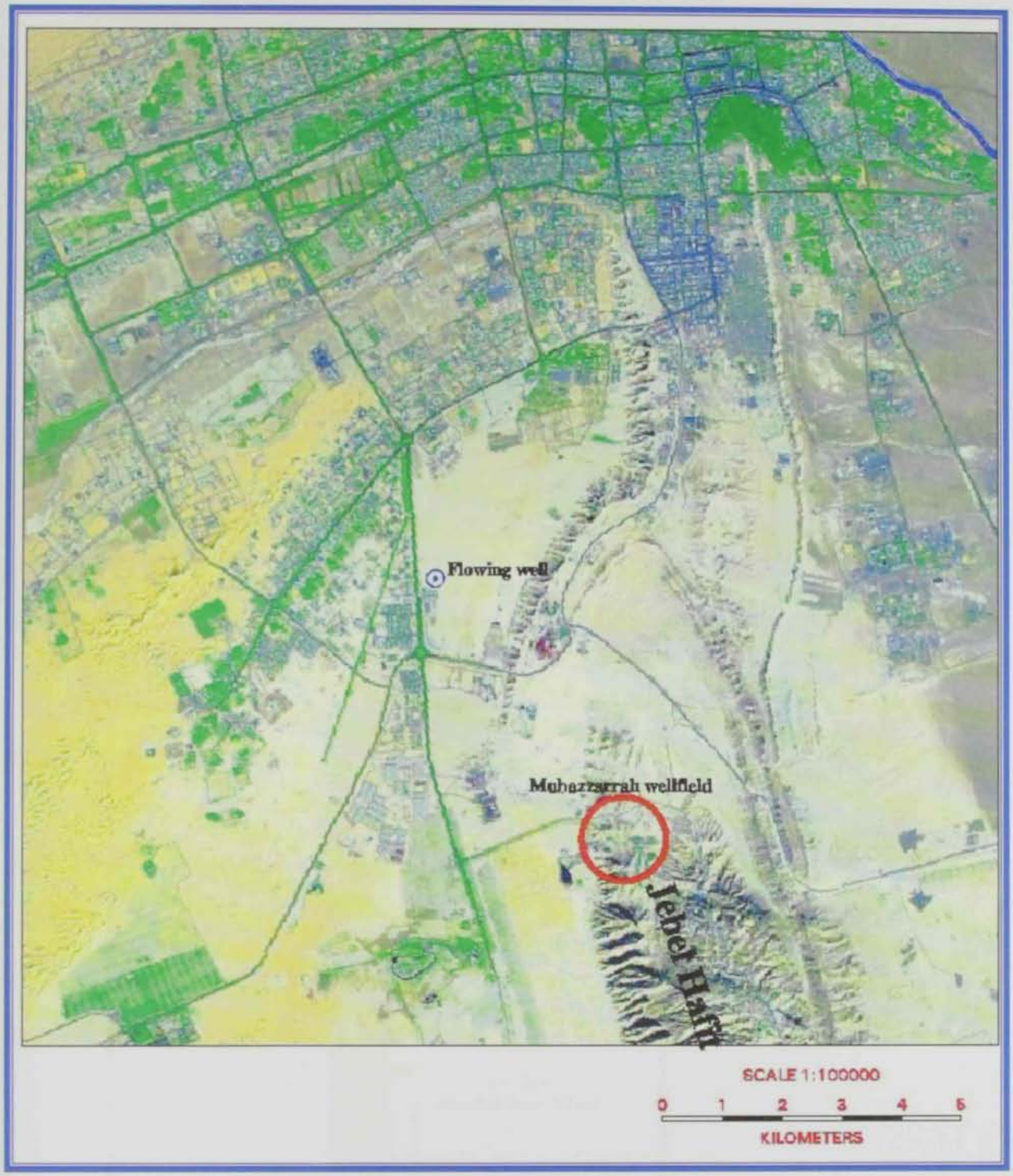

Figure (3.9): Location map of the flowing well in Neima area, (Khalifa, 2003).

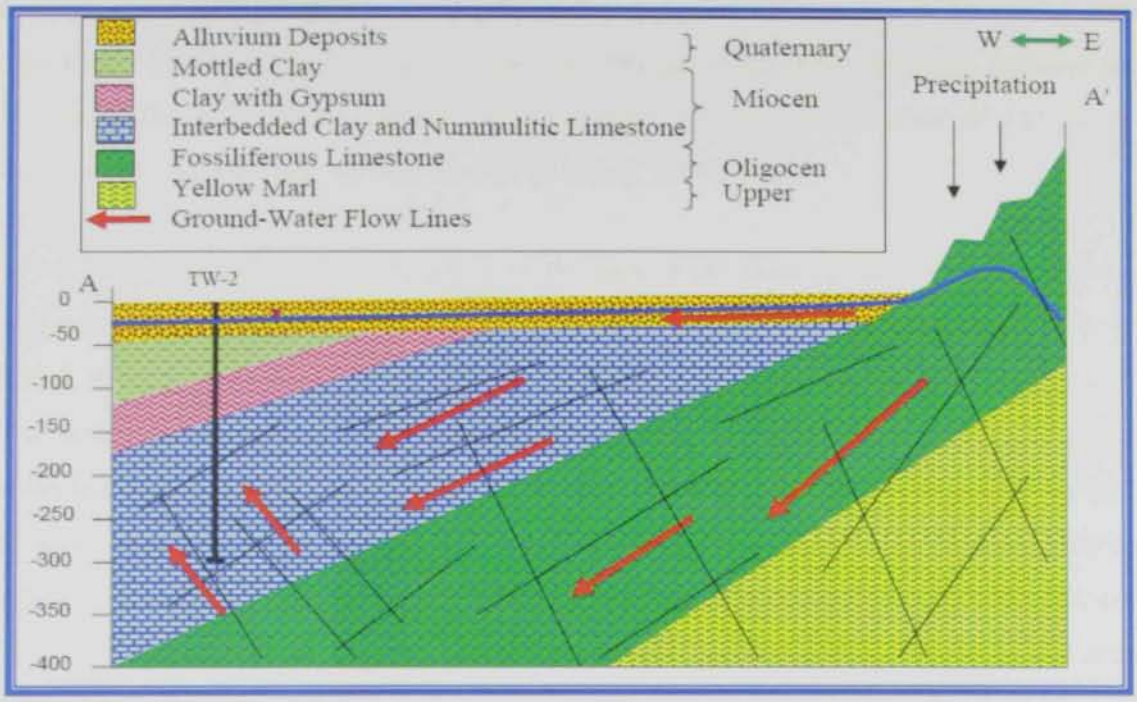

Figure (3.10): Conceptual geohydrologic cross section in Neima area, (Khalifa, 2003).

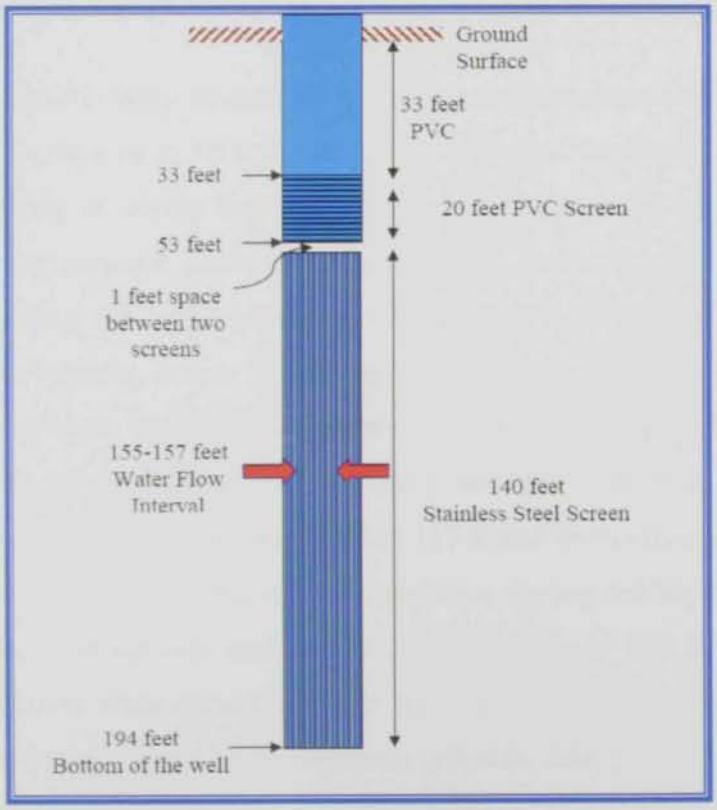

Figure (3.11): Down hole survey using TV camera of the flowing well, (Khalifa, 2003).

deeper water bearing source in the depth interval between 194 and 550 ft. The water from this deeper source could be migrating up the annulus of the well, the space between the outside of the well casing and the well bore wall, to the depth interval of 155 to 157 where it begins entering the well casing, (Khalifa, 2003).

The lithology in the subsurface in the area of the flowing well (Figure 3.12) was determined based on observations of the cuttings collected from two test holes, TW-1 and TW-2, drilled by the Agriculture Department about 100 meters east of the flowing well. The description was also based on the interpretation of borehole geophysical log data collected by the GWRP in the second of the two test holes. The site is underlain by 40 ft of sand, 100 ft of clay that varies from calcareous to gypsiferous, 70 ft of varying lithology including nummulitic limestone, gypsiferous mudstone, gypsum, and marl, and 290 ft of gypsiferous mudstone. Based on available geologic descriptions in the area, these lithologic units are believed to represent the following geologic units: Quaternary Alluvium, Upper Fars Formation, Lower Fars of Miocene age, respectively. The limestone outcrop in the Jabal 1 km east of the flowing well is the Asmari Limestone of Oligocene age, (Khalifa, 2003).

A preliminary assessment of the lithologies encountered indicates the 40 ft of sand at land surface (0 to 40 ft depth) and the 70 ft of limestone, mudstone, gypsum, and marl occurring at depths between 140 to 210 ft, are believed to be aquifers that are water bearing geologic formations that readily yield water to wells. The 100 ft of clays separating the two aquifers, depth of 40 to 140 ft; and the mudstone underlying the deeper aquifer, below 210 ft depth, are believed to be confining units. Confining units may be water bearing geologic formations but they don't readily yield water to wells. The source of water in the flowing well is believed to be from the deeper aquifer as flow in the well was observed at a depth of 157 ft and within this unit. Ancillary evidence for the deeper aquifer was the loss of circulation during drilling of TW-1, at a depth of 165 ft below land surface, and in TW-2, at a depth of 160 ft below land surface. Loss of circulation often occurs in highly permeable zones (aquifers), when solution opening or large fracture zones are encountered (Khalifa, 2003).

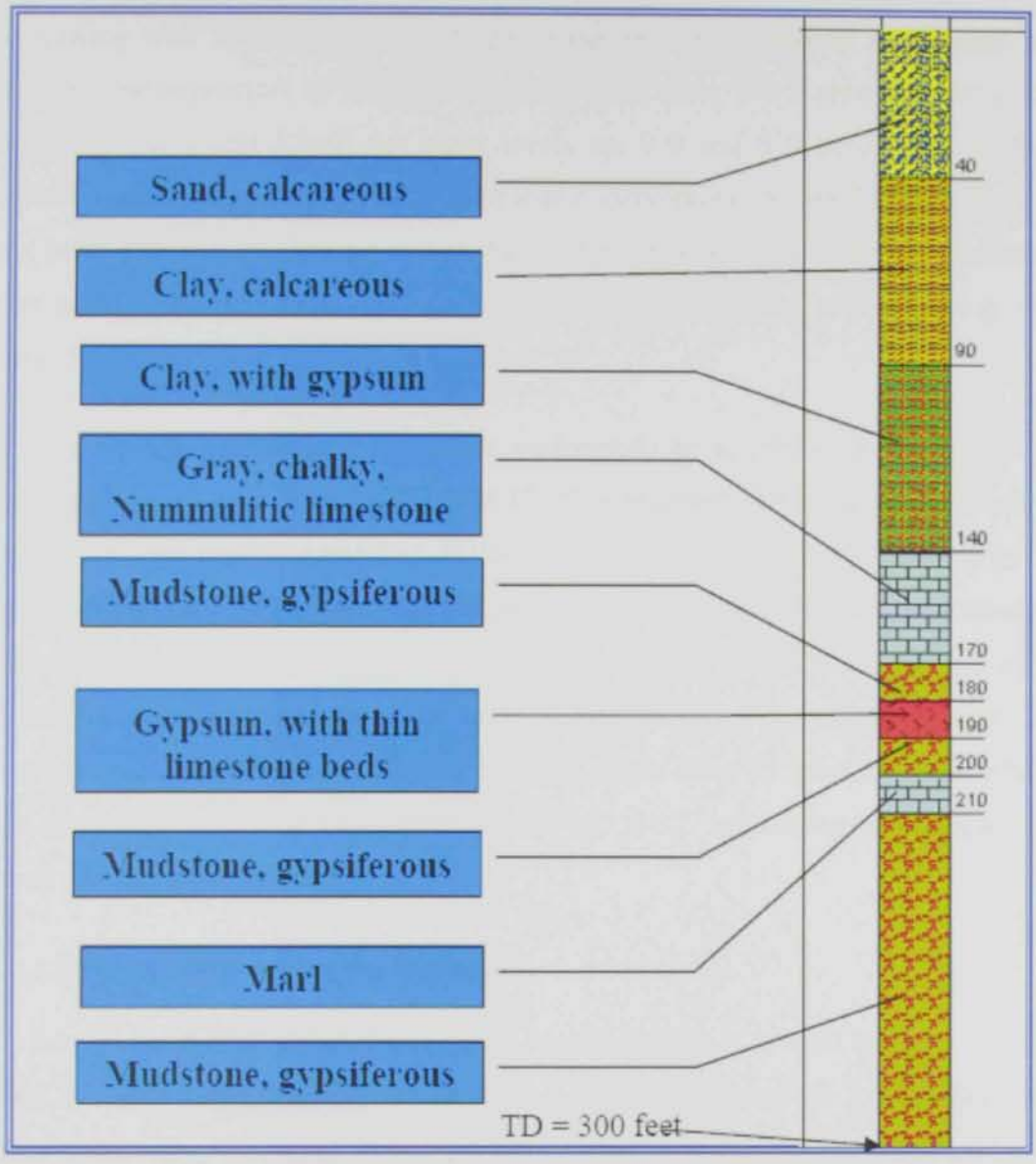

Figure (3.12): Lithologic Description of Borehole TW-2, (Khalifa, 2003).

While the two test wells, TW-1 and TW-2, are not flowing wells, they are similar to the flowing well showing that the deeper water bearing formation is confined and under considerable pressure as indicated by water level some 140 ft above the top of the formation. In TW-1 and TW-2, the water levels are 9 ft and 8 ft below land surface, respectively; indicating the previously mentioned assumption. An explanation for why the test holes may not be flowing is that they did not intersect the same interconnected solution cavities or interconnected fractures that were encountered in the flowing well, (Khalifa, 2003).

The Al-Ain Agriculture Department performed two aquifer tests on the flowing well by installing a 3-inch pump at depth of 175 ft below land surface. In the first test on March 22, 2003 the pumping rate was 44.26 m^3/hour and the water level declined by 5.4 meters in 150 minutes of the test. The water level recovered and the well was naturally flowing again after 13 minutes. The second test on March 23, 2003 was pumped at the same rate, 44.26 m^3/hour and the water level declined 6.17 meters in 240 minutes. The water level recovered and the well was flowing again after 25 minutes. The relative specific capacities from these short duration tests 197 to 177 m^3/min/day are indicative of high well yields, (Khalifa, 2003)

3.2.3 Hydrogeology of Ain Bu Sukhanah

Ain Bu Sukhanah or sometimes called Ain Al-Faydah is located less than 2 Km to the west of Jabal Hafit Figure (3.6). It has an annual discharge of 2.5 million cubic meters. It apparently discharges from a gypsum aquifer, probably well karstified adjacent to the western side of Jabal Hafit. The discharge of Ain Bu Sukhanah spring reflects no direct relation to groundwater levels, because in 1991, the groundwater level in Al-Ain declined compared to 1990. The groundwater level at the nearby observation well declined from 34.1 m (below ground surface) in 1990 to 42.2 m (below ground surface) in 1991. Whereas the spring discharge increased from 1.58 x 10^6 m^3/yr in 1990 to 2.5 x 10^6 m^3/yr in 1991 Table (3.2) (Ministry of Agriculture and Fisheries, 1993).

Table (3.2) The 1984 – 1991 records of the annual discharge (million m^3) of Bu Sukhanah spring, (Ministry of Agriculture and Fisheries,1993).

Year	Discharge
1984	0.96
1985	1.10
1986	1.42
1987	1.58
1988	1.51
1989	1.45
1990	1.58
1991	2.5

Geology of this area is not well known because of the quantities of water involved and the anticlinal structure of the Jebel Hafit intervening and isolating the gypsum aquifer from the shallow aquifer of Al-Jaww plain, it may be deduce that the Jabal Hafit forms the catchment area of this spring, (Hydroconsult, 1978)

In the report of Hydroconsult (1978) it was stated that the quantities of recharge that could occur in Jabal Hafit related to the annual yield of the spring makes this deduction reasonable as can be seen from following analysis, the mean annual rainfall for Jabal Hafit which is assumed to be equal to that of Al-Ain (100 mm/yr) . Part of this rainfall is expected to infiltrate and flow towards towards the east and west, the remainder to evaporate. The catchment area of this massif is about 90 Km^2 and if 15% is taken as runoff as for the lower mountain outcrops of the Oman Mountain range, then a total of 1.4 million m^3 may be considered as runoff. The bulk of the rest is expected to infiltrate since much ponding is not expected to occur and the loss of water by direct evaporation must be rather small. If it is assumed that 60 mm (out of 100 mm) infiltrates then some 2.5 million m^3 is estimated as entering the limestone mass. This quantity corresponds quite closely to the annual yield of the spring, suggesting that the Jabal Hafit is the feeding area for the spring. Besides, no other clearly recognizable source for maintaining the yield of the spring is available.

This deduction is quite important since it indicates that a Tertiary limestone (Karastic System) exists in the Hafit structure which may be interconnected with the

gypsum aquifer. A possible explanation for the brackish water at Bu Sukhanah spring is that fresh water of the Jebel Hafit becomes brackish on its way through the gypsum (Figure 3.12).

3.2.4 Geohydrologic setting in the study area

Water-level measurements have been taken by NDC & USGS in more than 20 wells and springs in the study area. This information was combined with water level data from GWRP wells in the surrounding area and used to determine the direction of ground-water flow. The water-level data were used to compute water-level elevations which were then used to prepare a contour map (Figure 3.13) (Khalifa, 2003). The results indicated that ground-water flow is from east to west direction in the study area.

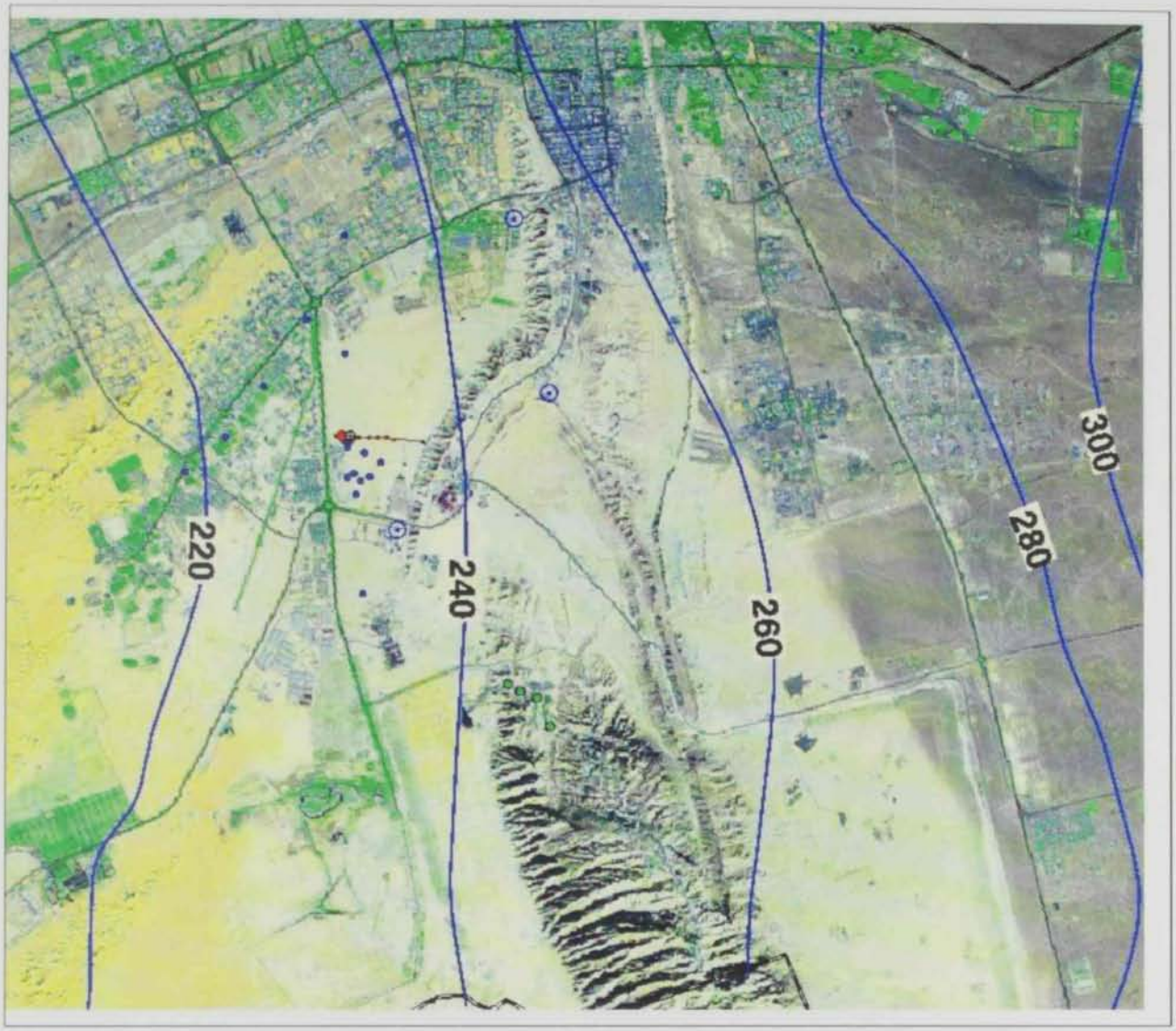

Figure (3.13): Water level contour map of the study area.

CHAPTER 4
Geophysical Aspects

PART ONE

Theory of the Electrical Resistivity Imaging

4.1.1 Introduction

Electrical Imaging (EI) is a geophysical method developed over the past several years that provides a two or three dimensional resistivity model of the subsurface. EI can provide information about distinct subsurface boundaries and conditions, which can indicate soil or bedrock lithology variations. In particular, the purpose of electrical surveys is to determine the subsurface resistivity distribution by driving a direct current (DC) signal into the ground and measuring the resulting potentials (voltages) created in the earth. From that data the electrical properties of the earth can be derived and thereby the geologic properties inferred. The ground resistivity is related to various geological parameters such as the mineral and fluid content, porosity and degree of water saturation in the rock.

Traditional resistivity measurements are carried out on the earth's surface with a specified array in order to obtain apparent-resistivity sounding curves, apparent resistivity profiling data or apparent resistivity pseudosections, all of which qualitatively reflect the vertical or horizontal variations in subsurface resistivity. This technique is widely used in groundwater, civil engineering and environmental investigations.

In the last decade, there have been great improvements in computerized data acquisition systems, 2D and 3D inversion software, so that electrical imaging or resistivity tomography has become an increasingly attractive exploration technique. Many geophysicists have shown that it is possible to reconstruct an accurate resistivity image of the subsurface using a large number of measured data (with enough spatial samples and coverage) and employing 2D or 3D imaging or inversion schemes (Daily and Owen 1991; Park and Van 1991; Shima 1992; Li and Oldenburg 1992; Sasaki 1994; Loke and Barker 1995, 1996; LaBrecque et al. 1996).

New advances in EI have allowed for three-dimensional surveys and cross-borehole surveys which will make this technique even more successful for sinkhole and fracture characterization in complex systems.

4.1.2 Theory

Fundamental to all resistivity methods is the concept that current (**I**) can be impressed into the ground through two current electrodes (**A** and **B**) and the effects of this current within the ground can be measured at two potential electrodes (**M** and **N**) Figure (4.1). The effect of potential (**V**) is the commonly measured effect of the impressed current. In a homogeneous earth, current flows radially outward from the source to define a hemispherical surface. The current distribution is equal everywhere on this surface which is also called an equipotential surface. Starting with Ohm's law (**V = IR**) and defining the resistance **R** in terms of the resistivity ρ and the area of the shell (equipotential surface), the potential difference across the shell is

$$dV = i(R) = I\left(\rho \frac{L}{A}\right) = I\left(\rho \frac{dr}{2\pi r^2}\right) \qquad (4.1)$$

where **V** is the voltage (or electrical potential), **I** is the current, ρ is the resistivity, and **r** is the radius of the equipotential surface. Integrating the above equation and setting the potential at infinity to zero, the electric potential at a distance R from the source is given by:

$$V = \frac{\rho I}{2\pi R} \qquad (4.2)$$

Resistivity has units of ohm.m and is not to be confused with resistance which has units of ohms. The resistivity of a material is defined as $\rho = RA/L$, where **R** is the resistance of the material, **A** is the cross-sectional area through which current flows and **L** is the length on the material.

The potential has been derived due to a single current source. The goal in resistivity surveying is to measure the potential different between two points due to the current from two current electrodes. The potential at each electrode is determined due to the current sources:

$$V_{P1} = \frac{I\rho}{2\pi r_1} - \frac{I\rho}{2\pi r_2}$$
$$V_{P2} = \frac{I\rho}{2\pi r_3} - \frac{I\rho}{2\pi r_4} \qquad (4.3)$$

Where the $r_{1,2,3,4}$ are shown in Figure (4.2). The potential difference $\Delta V = V_{P1} - V_{P2}$ which simplifies to

$$\Delta V = \frac{I\rho}{2\pi}\left(\frac{1}{r_1} - \frac{1}{r_2} - \frac{1}{r_3} + \frac{1}{r_4}\right) \qquad (4.4)$$

The above equation can then be solved for the resistivity ρ. In a nonhomogeneous earth, the resistivity which is measured is not actually the true resistivity of the subsurface. For an earth with more than one layer, the apparent resistivity measured will be an average of the resistivities of the additional layers. The apparent resistivity data needs to be interpreted in terms of a subsurface model in order to determine the actual resistivities of the layers. The apparent resistivity (ρ_a) value is calculated.

$$\rho_a = k\,V/I \qquad (4.5)$$

Where **k** is the geometric factor which depends on the arrangement of the four electrodes.

Resistivity meters normally give a resistance value, **R = V/I**, so in practice the apparent resistivity value is calculated by :-

$$\rho_a = k\,R \qquad (4.6)$$

The calculated resistivity value is not the true resistivity of the subsurface, but an "apparent" value which is the resistivity of a homogeneous ground which will give the same resistance value for the same electrode arrangement. The relationship between the "apparent" resistivity and the "true" resistivity is a complex relationship and in order to determine the true subsurface resistivity, a computer program can be used to calculate the inversion of the measured apparent resistivity values .

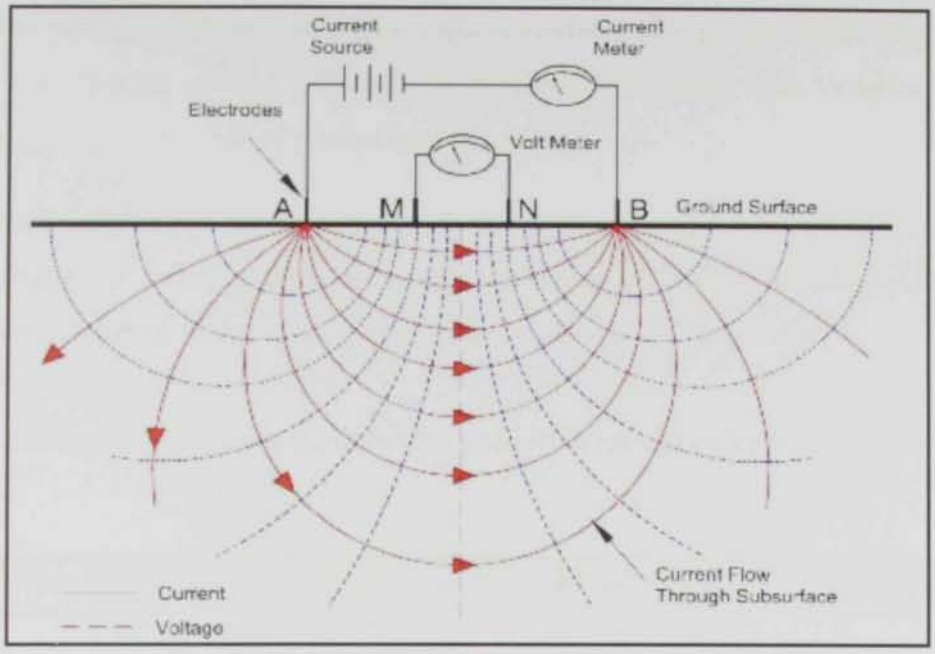

Figure (4.1) Schematic diagram showing the basic principle of DC resistivity measurements.

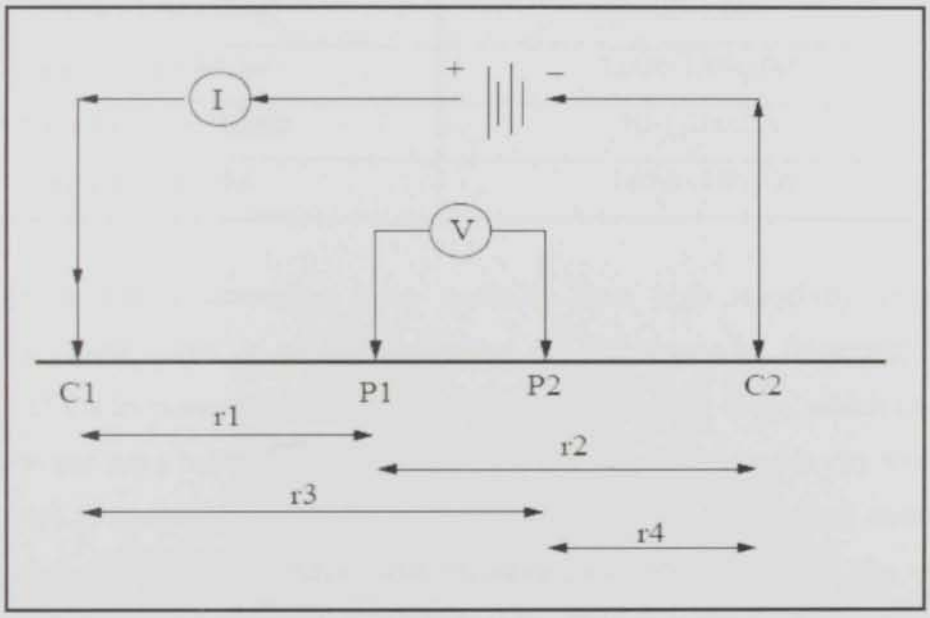

Figure (4.2) Schematic diagram showing the resistivities formed between current electrodes and potential electrodes

The principal differences among various methods of electrical resistivity lie in the number and spacing of the current and potential electrodes, the variable quantity determined, and the manner of presenting the results.

Resistivity values are found for earth materials to cover a wide range. This variety of resistivities is what makes resistivity surveying a viable technique for many applications. Table (4.1) describes typical resistivities of earth materials.

Table (4.1): Typical Electrical Resistivities of Earth Materials, (Keller and Frischknecht, 1966).

Material	Resistivity (ohm.meter)
Clay	1-60
Sand, Wet to Moist	20-200
Shale	1-500
Sandstone	150-450
Porous Limestone	100-1,000
Dense Limestone	1,000-1,000,000
Metamorphic Rocks	50-1,000,000
Igneous Rocks	100-1,000,000

Igneous and metamorphic rocks typically have high resistivity values. The resistivity of these rocks is greatly dependent on the degree of fracturing, and the percentage of the fractures filled with groundwater. Sedimentary rocks, which usually are more porous and have higher water content, normally have lower resistivity values. Wet soils and fresh groundwater have even lower resistivity values. Clayey soil normally has a lower resistivity value than sandy soil. However, note the overlap in the resistivity values of the different classes of rocks and soils. This is because the resistivity of a particular rock or soil sample depends on a number of factors such as the porosity, the degree of water saturation and the concentration of dissolved salts, (Keller and Frischknecht, 1966)

4.1.3 Types of Electrical Imaging

- **2-D Electrical Imaging**

One of the new developments in recent years is the use of 2-D electrical imaging/tomography surveys to map areas with moderately complex geology (Griffiths and Barker 1993). Such surveys are usually carried out using a large number of electrodes, 25 or more, connected to a multi-core cable. A laptop microcomputer together with an electronic switching unit is used to automatically select the relevant four electrodes for each measurement (Fig 4.3). At the present study, field techniques and equipments to perform 2-D resistivity surveys are described in the following section.

- **3-D Electrical Imaging**

Since all geological structures are 3-D in nature, a fully 3-D resistivity survey using a 3-D interpretation model (Fig 4.3) should in theory give the most accurate results. At the present time, 3-D surveys are subject of active research. However this method has not reached the level where, like 2-D surveys, it is routinely used. The main reason is that the survey cost is comparatively higher for a 3-D survey of an area which is sufficiently large. There are two current developments that should make 3-D surveys a more cost-effective option in the near future. One is the development of multi-channel resistivity meters which enables more than one reading to be taken at a single time. This is important to reduce the survey time. The second development is faster microcomputers to enable the inversion of very large data sets (with more than 8,000 data points and survey grids of greater than 30 by 30 to be completed within a reasonable time, (Loke and Barker, 1996). Figure (4.4) shows one possible arrangement of the electrodes for a 3-D survey using a 25 electrodes system. For convenience, the electrodes are usually arranged in a square grid with the same unit electrode spacing in the x and y directions. To map slightly elongated bodies, a rectangular grid with different numbers of electrodes and spacing in the x and y directions could be used. The pole-pole electrode configuration is commonly used for 3-D surveys, such as the E-SCAN method (Li and Oldenburg 1992).

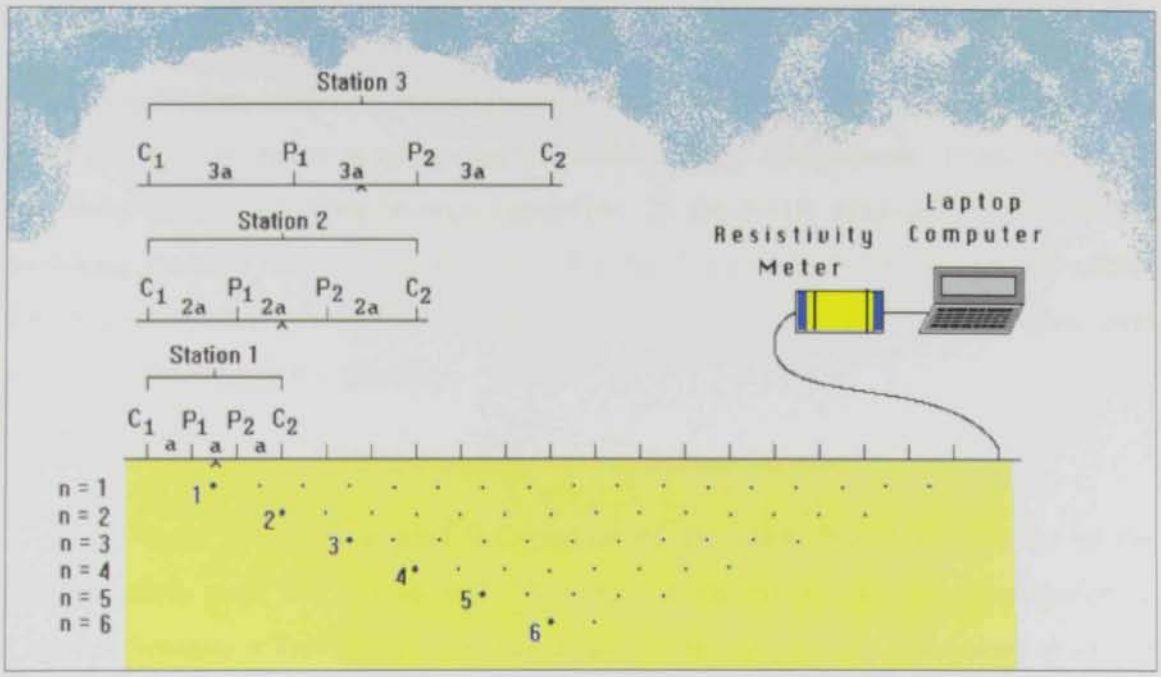

Figure (4.3): Example of data measurement locations for 2D surveys (modified from Loke, 1997).

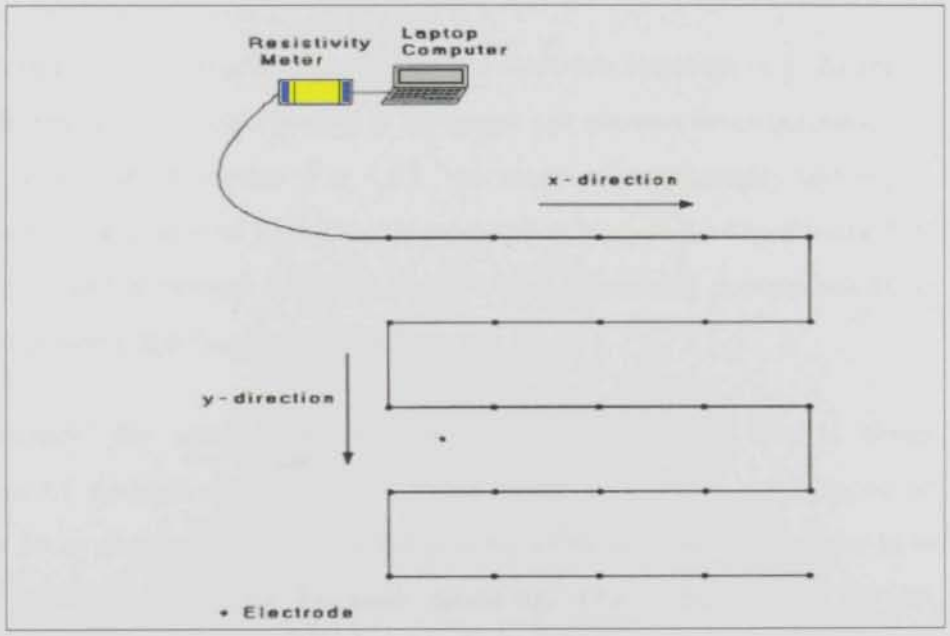

Figure (4.4): Schematic diagram for one possible layout for a 3D survey (modified from Loke, 1997)

4.1.4 EI Data Collections

For EI data collection, a Sting/Swift multielectrode system is commonly used (Fig 4.5). The EI equipment is composed of three primary components: 1) the Sting R1 resistivity meter with data storage capability; 2) the Swift automatic multielectrode switching system, which is an accessory for the Sting; and 3) the Sting/Swift cables which contain fixed cylindrical stainless steel switches that attach to stainless steel electrodes placed into the ground.

4.1.5 Field survey method and measurement procedures

In order to obtain a good 2-D picture of the subsurface, the coverage of the measurements must be 2-D as well. A simple electrical method of investigation is Constant Separation Traversing, where an array of four electrodes is maintained at a fixed spacing and moved along the ground to provide information on resistivity at a single sounding depth. Using a Wenner array, the increment for such a traverse is typically equal to the electrode spacing (a).

Repeating the traverse using increased electrode spacings (e.g. $2a$ then $3a$, etc.), adds additional layers of information to the graph and permits investigation of the vertical variation in ground properties (Fig 4.6). The electrical tomography technique requires collection of data at several multiples of a (commonly up to 12) to provide information at a range of depths, termed n levels . Each n level effectively corresponds to a constant separation traverse at a fixed multiple of a.

Because the same electrode positions are occupied several times during acquisition of multiple traverses it is much faster to lay out an array of electrodes (typically 64 or more) connected by a multicore cable and use a computer to switch on the four electrodes required for each sounding. The computer can be set to run automatically through the required number of levels, performing noise checks and reacquiring bad data points to the operator's satisfaction.

The instrument front panel

Long manual cable set

Battery pack

Battery charger

Stainless steel electrode

Sting communication cable

Test resistor

Figure (4.4): Super Sting R1 IP earth resistivity and IP meter and its accessories.

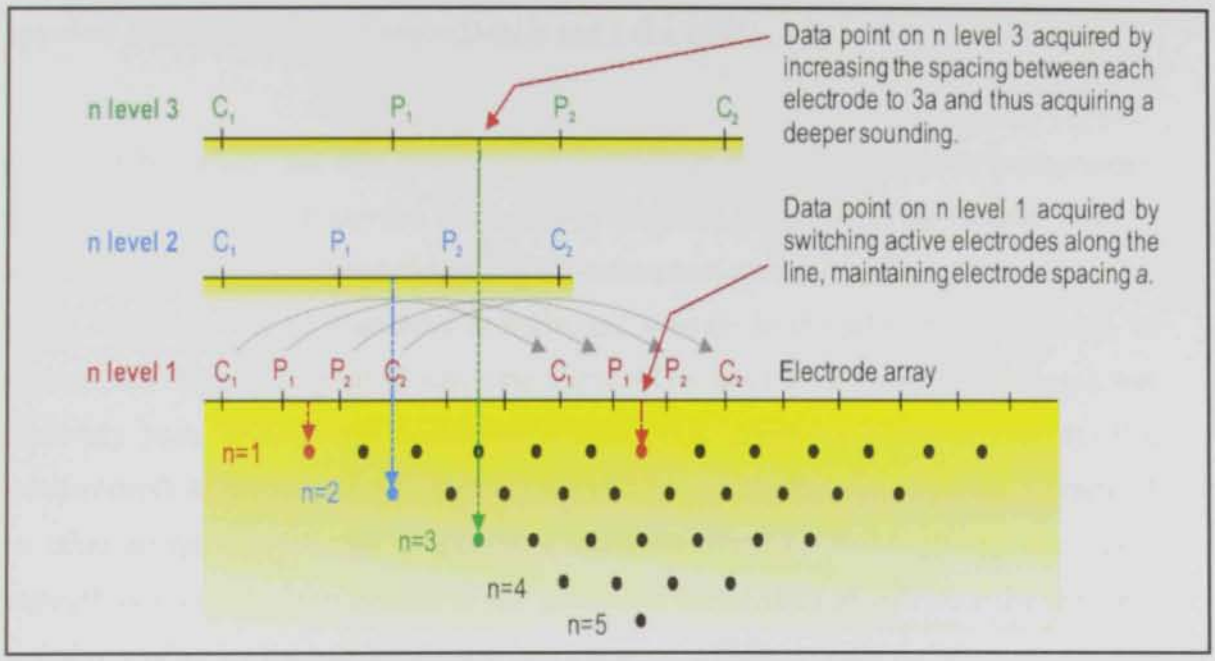

Figure (4.6): Example of data acquisition geometry during a 2D electrical tomographic survey, showing how increasing electrode spacing facilitates study of deeper ground materials.

To get the best results, the measurements in a field survey should be carried out in a systematic manner so that, as far as possible, all the possible measurements are made. This will affect the quality of the interpretation model obtained from the inversion of the apparent resistivity measurements (Dahlin and Loke 1998).

In this study, the data are collected typically in a Wenner electrode arrangement. Many of the early 2-D surveys were carried out with this array. The Wenner array is relatively sensitive to vertical changes in the subsurface resistivity below the centre of the array. However, it is less sensitive to horizontal changes in the subsurface resistivity. In general, the Wenner is good in resolving vertical changes (i.e. horizontal structures), but relatively poor in detecting horizontal changes (i.e. narrow vertical structures). The median depth of investigation is approximately 0.5 times the "a" spacing used. Compared to other arrays, the Wenner array has a moderate depth of investigation. The signal strength is inversely proportional to the geometric factor used to calculate the apparent resistivity value for the array (Griffiths and Turnbull, 1985) .

For the Wenner array, the geometric factor is $2\Pi a$, which is smaller than the geometric factor for other arrays. Among the common arrays, the Wenner array has the strongest signal strength. This can be an important factor if the survey is carried in areas with high background noise. One disadvantage of this array for 2-D surveys is the relatively poor horizontal coverage as the electrode spacing is increased. This could be a problem if a system with a relatively small number of electrodes has been used, (Griffiths et al; 1990).

4.1.6 Data Modeling and Interpretation

The apparent resistivity **ρa**, as measured by the EI system, is the product of a large area of the subsurface responding to the impressed current. Interpretation of apparent resistivity data collected in the field without reduction provides a qualitative product. Since the earth is inhomogeneous, it is useful to model the resistivities at discrete locations in order to make the interpretation more quantified. Inverse modeling of the data is performed using RES2DINV/RES3DINV (Loke, 1997) to produce two-

dimensional or three-dimensional resistivity models based on the apparent resistivity data.

Final data processing involves the generation of color-enhanced contour maps of the data using a two-dimensional mapping program. EI resistivity models are presented in cross-section or 3D model blocks, with inline distance shown along the horizontal axis, depths, or elevation along the vertical axis. The geoelectrical model presents the electrical stratigraphy (electrostratigraphy) of the subsurface.

PART TWO

2-D Electrical Imaging Field Survey and Interpretation

4.2.1 (2-D) Electrical Imaging Resistivity Survey in the Study Area

The present 2-D electrical imaging survey was planned to study the fractured limestone (karst aquifer system) and the quaternary alluvial aquifer in the study area. It also includes delineation of the layer succession and the distribution of resistivity in the subsurface layers. In addition, it is concerned with determining the vertical and lateral extent of the resistivity anomalies.

4.2.2 Field Work

The 2-D resistivity imaging survey was conducted in selected locations in the study area. Nine profiles were carried out parallel to the strike of the limestone exposure at Jabal Hafit (Figure 4.7). These profiles were distributed along three parallel lines directed North-South. The 2-D resistivity imaging was carried out for mapping the fractured limestone (karst aquifer system) in Mubazarah and Neima areas and to map the Quaternary aquifer west to Jabal Hafit.

Wenner electrode array was applied, which is very sensitive to vertical changes in resistivity at moderate depths. The maximum length of the measured profiles was 600 m with unit electrode spacing of 20 m (Resistivity section 1-1' 600m length, resistivity section 2-2' 600m length, resistivity section 3-3' 540m length , resistivity section 4-4' 540m length, resistivity section 5-5' 600 m length, resistivity section 6-6' 420 m length, resistivity section 7-7' 540 m, resistivity section 8-8' 600m length and resistivity section 9-9' of 600 m length).The total number of the measured points along each profile is varying from 70 to 145 with (n) factor ranging from 7 to 10 .

All the resistivity measurements have been carried out using a single channel memory Sting R1 resistivity meter manufactured by Advanced Geosciences, Inc. (AGI) of Austin, Texas (available at Geology Department , United Arab Emirates University), that enables measuring the potential difference, which multiplies by the geometric factor to give the resistivity values in ohm.m.

The measurements were run manually using four wheels of electric wires and the distances between the current electrodes and the potential electrodes were controlled manually as well by striding along the profile line.

4.2.3 Interpretation of 2-D Inversion Data

Pseudo-section resistivity data gives a pictorial representation of resistivity in the subsurface. An accurate image of the subsurface can be obtained through the inversion of the pseudo-section (Inman et al., 1973, Barker, 1981, Smith and Vozoff, 1984, Griffiths and Barker, 1993, and Loke and Barker, 1996 a & b).

In this study, the 2-D resistivity inversion aims to construct an image of the obtained true subsurface resistivity distribution, and to map the fractured limestone and quaternary aquifers within the selected profiles. The measured resistivity pseudosections were inverted using RESD2INV inversion software, version 3.54. The RES2DINV program uses the smoothness constrained least-squares method inversion to produce a 2-D model of the subsurface from the apparent resistivity data (Sasaki, 1992). The 2-D model divides the subsurface into a number of rectangular blocks and the resistivity of the blocks are adjusted in an iterative manner to reduce the difference between the measured pseudo-section and the calculated model.

The sequence of processing of each profile shows the inversion results after iterations ranging from (4-15 iterations) with RMS errors (2.5-24.2 %) which are considered the optimum model for interpretation. The illustration of the nine profiles is given below

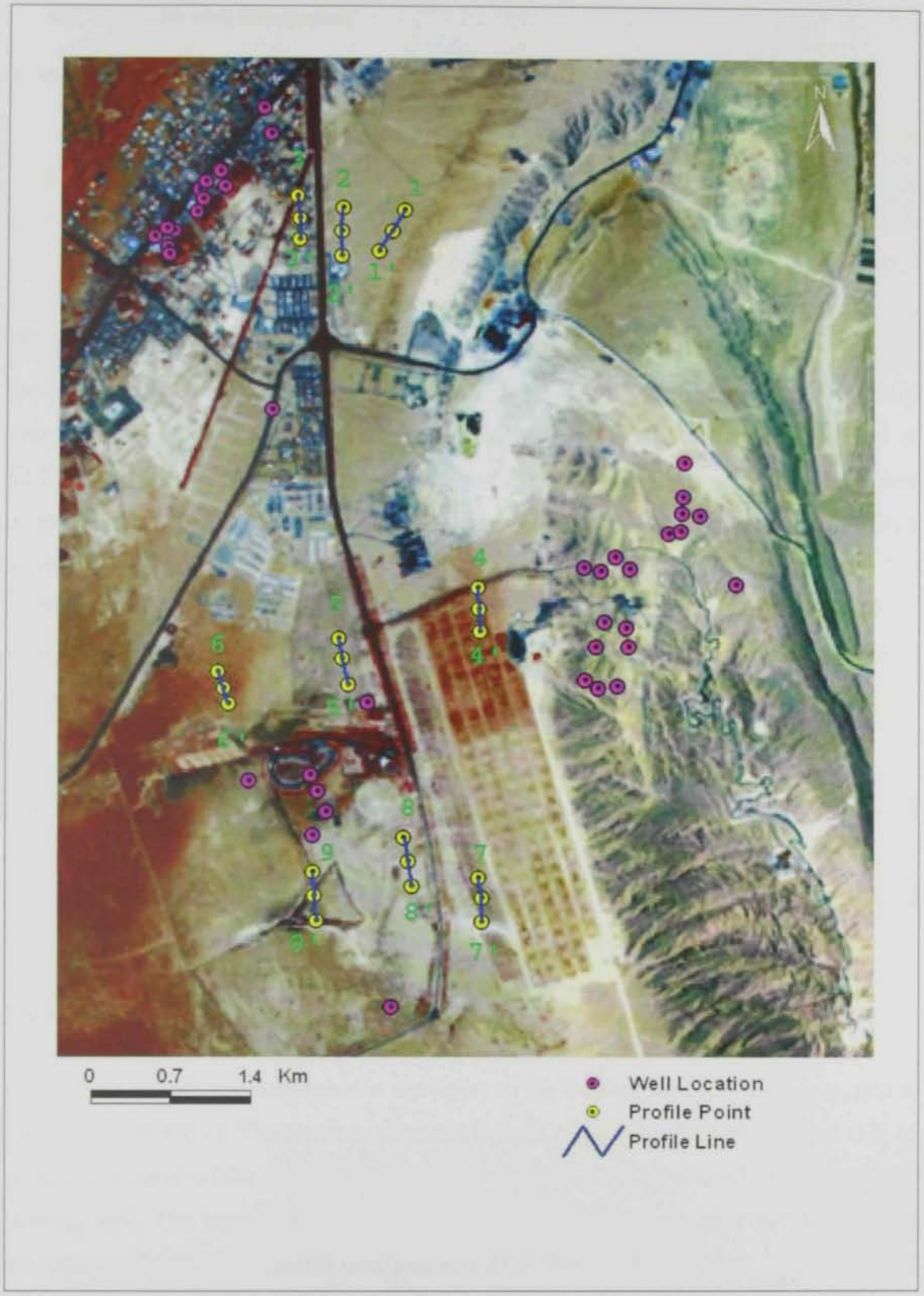

Figure (4.7): Location map of the selected 2-D resistivity profiles in the study area.

4.2.4 Results and Discussion

Line- 1

This profile was conducted to the east of the flowing well in Neima area. The Jabal Hafit outcrop located less than one kilometer to the east of this profile represents an exposed Asmari limestone outcrop on the limb of an anticline (Photo 4.1). The profile was oriented along the strike direction of Jabal Hafit to intersect the maximum possible geological features in this area. The length of this profile is 600 m. The resulting 2-D inversion model was obtained after 15 iterations with 16.2 % error, which is considered the optimum model for interpretation. The model (Figure 4.8) shows a zone with very low resistivity values ranging between 2.5 – 12.0 ohm.m. This zone located at a depth of 62.7 m on the center of the inline distance and reached the ground surface at the inline distances from 0 - 200 m. On the right this zone separates two anomalies of high resistivity values and reached the ground surface at the inline distances from 340 – 500 m. This zone of low resistivity may be attributed to the fractured limestone of Jabal Hafit. However, these areas may also be interpreted as clay or soil cover, where low resistivities occur near the ground surface.

Finally two anomalies of high resistivity values ranging between 33 – 93 ohm.m. One of theses anomalies is below the inline distances from 200 – 320 m and reached were detected a depth of 50 m. The second anomaly is below the inline distance of 400 m, at depth of 86.8 m. Theses two anomalies may be interpreted as clay pockets and mudstone layer respectively.

Line-2

This profile was conducted in proximity to the flowing well in Neima area, and to the west of profile -1. The line was oriented in such a way that the flowing well will be close to the center of the profile. This will help to delineate the fractured limestone of the flowing well. The length of this profile is 600 m, and the depth obtained by the 2-D inversion model is 117 m after 9 iterations and 24.2 % error (Figure 4.9).

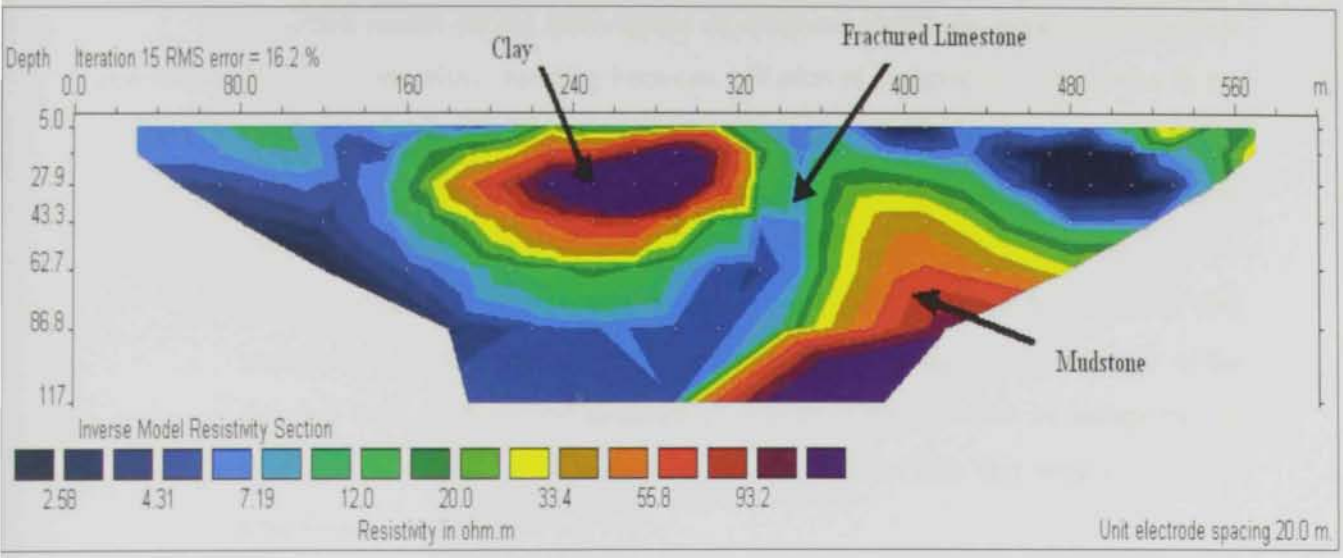

Figure (4.8): Tomographic Image of Line-1.

(Photo 4.1) Limestone outcrop about 1 Km east to the location of Line -1.

The resulted model shows three zones of different resistivity ranges. A very low resistivity zone with resistivity ranging between 1-9 ohm.m, located at many areas in the model:-

- Between the inline distance of 100 – 220 m and to a depth of 17 m, this area may be interpreted as clay layer near the ground surface.
- At the inline distance of 160 m and to a depth of about 80 m , this low resistivity area moves up and reached the ground surface at the location of the flowing well at the inline distance of 300 m. This area can be interpreted as fractured limestone. Whereas, near the ground surface this area could be a clay layer.

The second zone has a resistivity ranging between 9 – 72 ohm.m, occurred as pocket below the inline distance of 340 m between depths 17 m to 80 m, and to the east of the profile, from the inline distances of 100 – 240 m. This moderate resistivity zone can be interpreted as clay layer. Finally a high resitivity zone, with resistivity values above 130 ohm.m to the extreme east of the profile to depth of 43 m. This zone may represent a dry aeolian sand deposits.

Line-3

This profile was measured to the west of the flowing well in Neima area. The resulting model after 10 iterations and 14.9 % error shows three zones of resistivity (Figure 4.10). A high resistivity zone near the ground surface with resistivity above 17 ohm.m, which can be interpreted as sandy soil in that area. A moderate resistivity zone to the east below 55 m and diminishes toward the west. This zone may be representing a clay layer in the subsurface. Lastly a very low resistivity zone with resistivity ranging between 1 – 5 ohm.m. The depth for this zone extended between 5 – 60 m in the east of the profile, while at the west of the profile it is between 17 – 80 m. This low resistivity zone can be interpreted as saturated quaternary alluvial sediments, which represents the aquifer in this particular area.

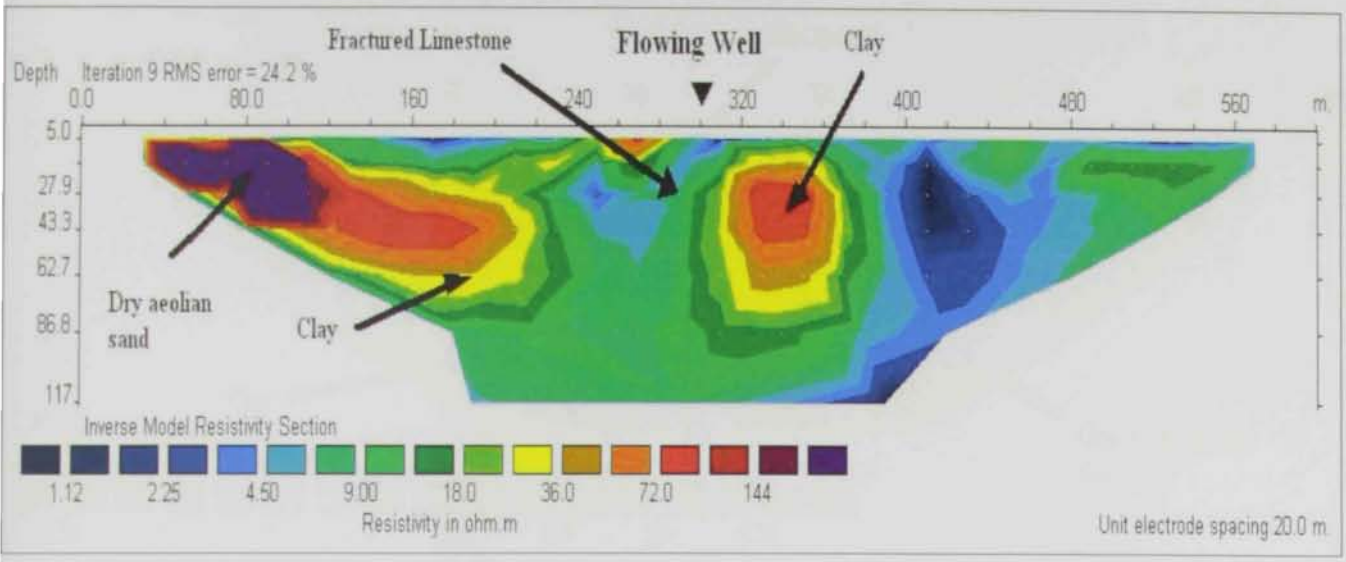

Figure (4.9): Tomographic Image of Line-2.

(Photo 4.2) Field measurements on Line – 2.

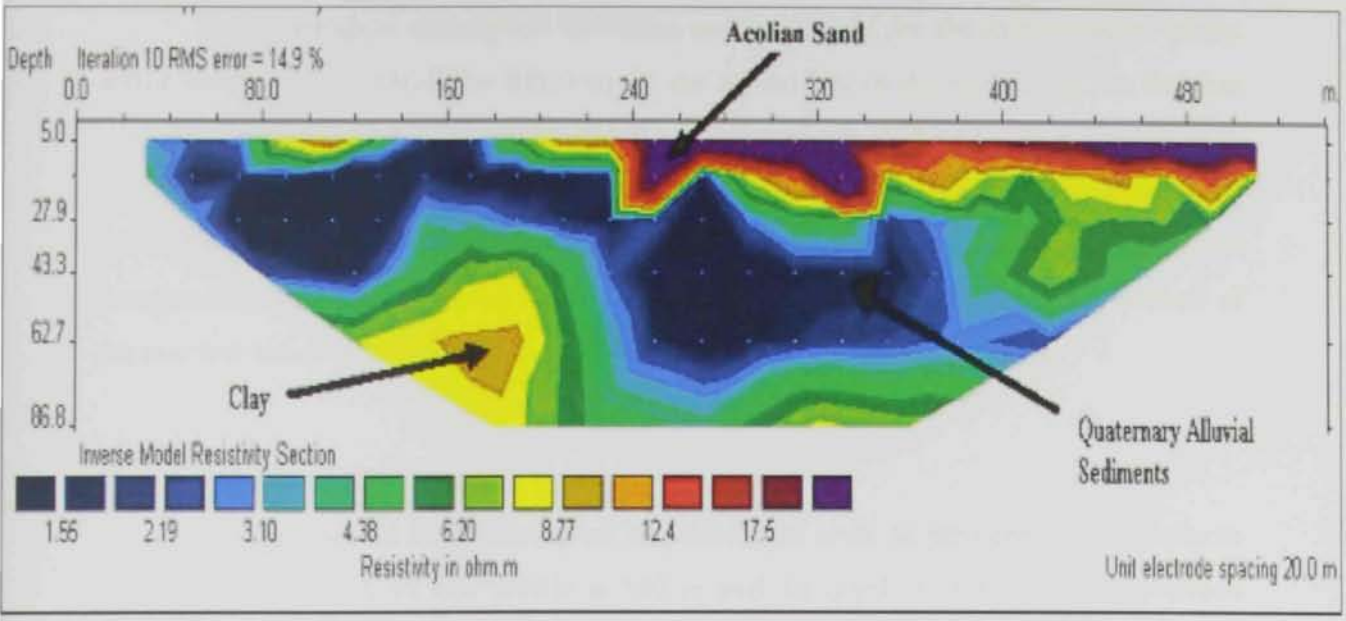

Figure (4.11): Tomographic Image of Line-3.

The lithological description in Neima area was used for the interpretation of the above mentioned profiles. The lithology in the subsurface in the vicinity of the flowing well was determined by NDC/USGS based on observations of the cuttings collected from two test holes, TW-1 and TW-2 (Figure 3.13), drilled by the Agriculture Department about 100 meters east of the flowing well. The description was also based on the interpretation of borehole geophysical log data collected by the GWRP in the second of the two test holes. (Khalifa, 2003)

Line-4

This profile has been conducted in Mubazarah area, in proximity to Mubazarah well field. The length of this profile is 540 m and the depth acquired by the inversion model is 86.8 m. The results obtained from traverse Line-4 (Figure 4.11) after 5 iterations and percentage error of 4.5 % shows that there are two distinctive features of resistivity. One with resitivities less than 13 ohm.m, which may be attributed to the fractured limestone of Jabal Hafit at depth below 27.9 m from the surface and in some locations, reached depth of 17 m at inline distances 120, 200 and 400 m. The second feature with resistivity ranged between 17 and 69 ohm.m, which characterized the surficial layer of the aeolian sand. The water table according to this profile is about 16-26 m from the ground surface.

Line -5

This profile was placed to the west of Mubazarah area and profile-4. The length of this profile is 600 m and the maximum depth obtained by this profile is 117 m. The electrostratigraphy model from processing line 5 is presented (Figure 4.12). This model obtained after 5 iterations with error 4 %. The model shows zone with low resistivity (2.78-5.5 ohm.m) between depths 5-44 m. This zone was interpreted as areas of quaternary alluvium sediments saturated by brackish water due to the low resistvity values. However, these areas may also be interpreted as soil where low resistivities occur near the ground surface.

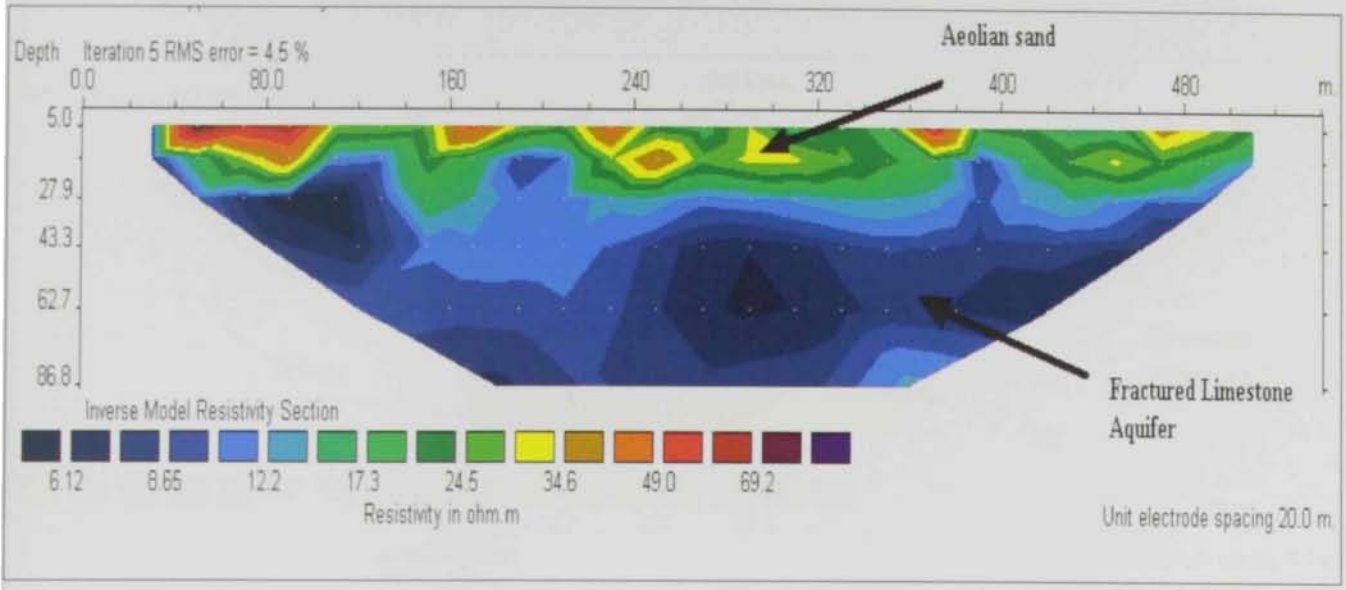

Figure (4.11): Tomographic Image of Line-4.

(Photo 4.3) Field measurements on Line – 4.

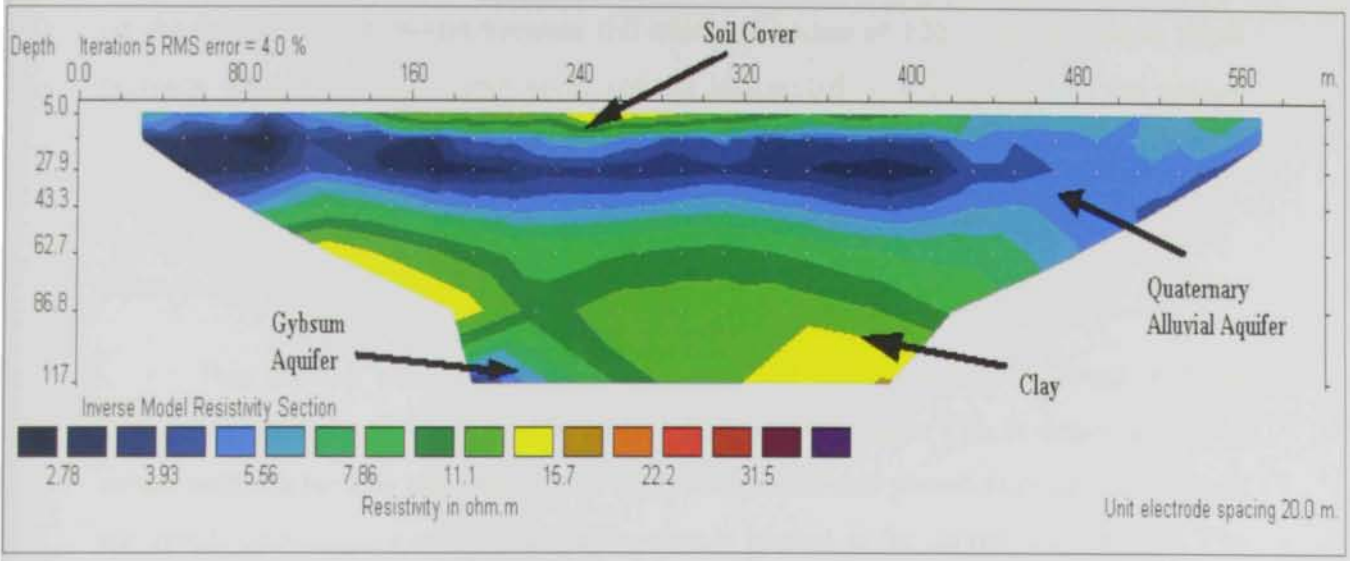

Figure (4.12): Tomographic Image of Line-5.

(Photo 4.4) Field measurement on Line – 5.

Finally areas with resistvity ranging between 7-15.7 ohm.m ,which can be found on the surface of the model between the inline distances of 120 – 420 m and at depth between 48 and 117 m. These areas can be interpreted as clayey soil on the ground surface and clay layer in the subsurface. The water table in this area is about 15 m from the ground surface.

Line -6

This profile was conducted to the west of line-5 and North-West Ain Bu Sukhanah. This area characterized by a very shallow water table. This is demonstrated by trench well available in this area (photo 4.5). The profile was placed in close proximity to the trench well and in such a way that the well is located at the center of the profile. The length of this profile is 420 m and the maximum depth acquired by the model is 63.7 m.

Interpretation of the inversion model (Figure 4.13) after 9 iterations and 11.3 % error percent shows a very low resistivity zone (1- 4.5 ohm.m) along the center of the profile between depth 25 to 50 m and reached to depth of 5 m at the center of the profile where the trench well is located. This zone may be attributed to the Quaternary alluvial sediments. The very low resistivity values are due to the high salinity of water. The field measurement of TDS for a water sample collected from the trench well was 11,500 ppm.

The second zone has a resistivity values between 8-12 ohm.m which located at depth below 50 m and at the surface between depths 5-15 m. This zone may be represented a clay layer at the subsurface and a surficial layer of clay covered by aeolian sand at the surface.

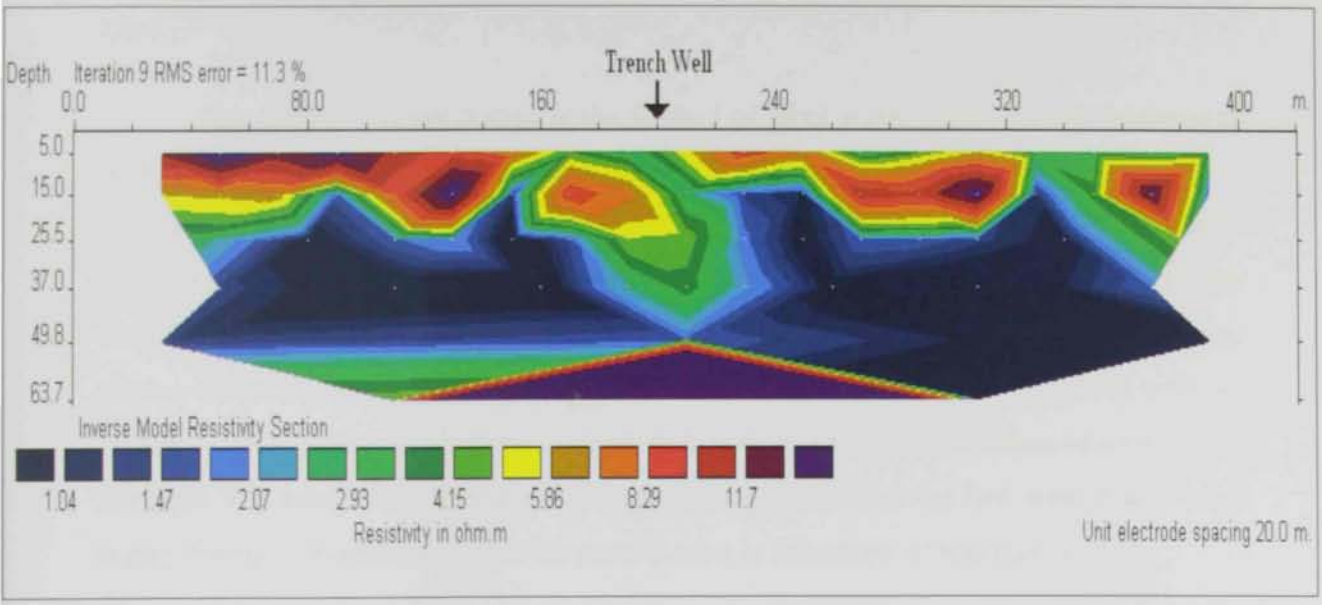

Figure (4.13): Tomographic Image of Line-6.

(Photo 4.5) Trench well at location of Line – 6.

Line -7

This profile was conducted at the foothill of Jabal Hafit, South-East of Mubazarah well field. The length of this profile is 540 m and the maximum depth achieved by the 2-D inversion model is 86.8 m. The result of the 2-D inversion model (Figure 4.14) after 4 iterations and 2.5 % percent error shows two resistivity zones. One with resistivity ranges from 3.58 to 9.0 ohm.m. This zone is situated from the surface to the depth of 40 m and getting deeper as we moved to the right. The second zone has a resistivity values between 10 and 14 ohm.m and it is located at depth below 40 m and it is diminishes as we move to the right. The interpretation of these two zones is assumed that the first zone is an area of highly fractured limestone, while the second zone is limestone of less fracture.

Line -8

The profile was carried out to the west of profile-7 and south of Ain Bu Sukhanah. The length of this profile is 600 m which provides a maximum depth of 117 m in the inversion model. The inversion model was obtained after 5 iterations and 5.9 % error (Figure 4.15). The model shows a very low resistivity area (between 2.2 – 11.0 ohm.m) occupies most of the model except two anomalies of resistivity higher than 13 ohm.m directly below the inline distances of 220 m and 380 m. These anomalies are located at depth 20 m and 28 m respectively. The interpretation of this profile suggested that the very low resistivity zone could be attributed to the Quaternary alluvial sediments except for areas near to the surface which may be represents the soil. Where as zone with higher resistivity it could be clay lenses within the subsurface in the profile area.

Line – 9

The profile was conducted to the west of profile-8 and south of Ain Bu Sukhanah (Figure 4.16) with a length of 600 m. The area in this profile is covered by thick deposits of the aeolian sand (photo 4.8 A& B). The 2-D inversion model was obtained after 11 iterations and 15.9 % error, which is considered the optimum model for interpretation. The model shows a very low resistivity zone with resistivity ranges from 1.0 to 20.0 ohm.m at depth 62 m in the center of the profile. In some areas it reachs the ground

surface as in the distances between 60- 120 m and from 510 -570 m on the inline distance .This low resistivity zone is interpreted as quaternary alluvial sediments saturated by brackish water at depth 62 m. However the low resistivity areas close to the surface could be interpreted as surface soil.

The second zone has a moderate resistivity values ranging from 20.0 – 50.0 ohm m at depth 86 m directly below the horizontal distance of 360 m, which can be attributed to clay layer but the horizontal extent of this layer is not shown by the model. Finally a high resitivity zone with resistivity ranging from 90.0 – 690.0 ohm.m , located at the inline distances between 140 – 320 m and 340 – 500 m, which may be interpreted as dry aeolian sand located at the ground surface.

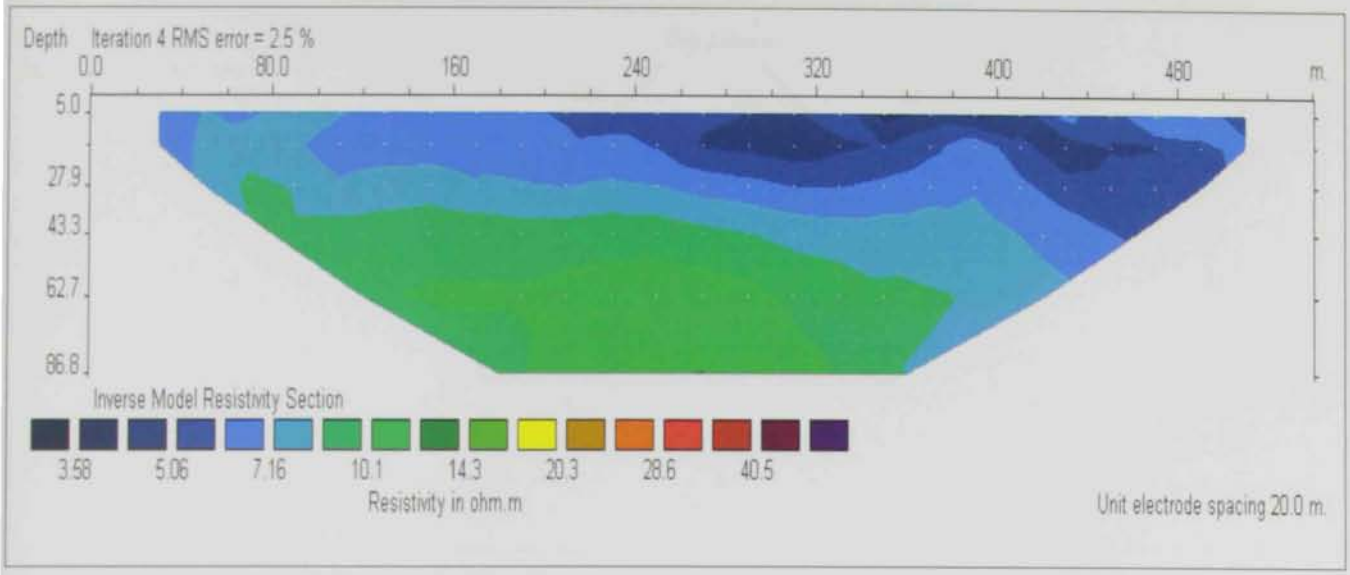

Figure (4.14): Tomographic Image of Line-7.

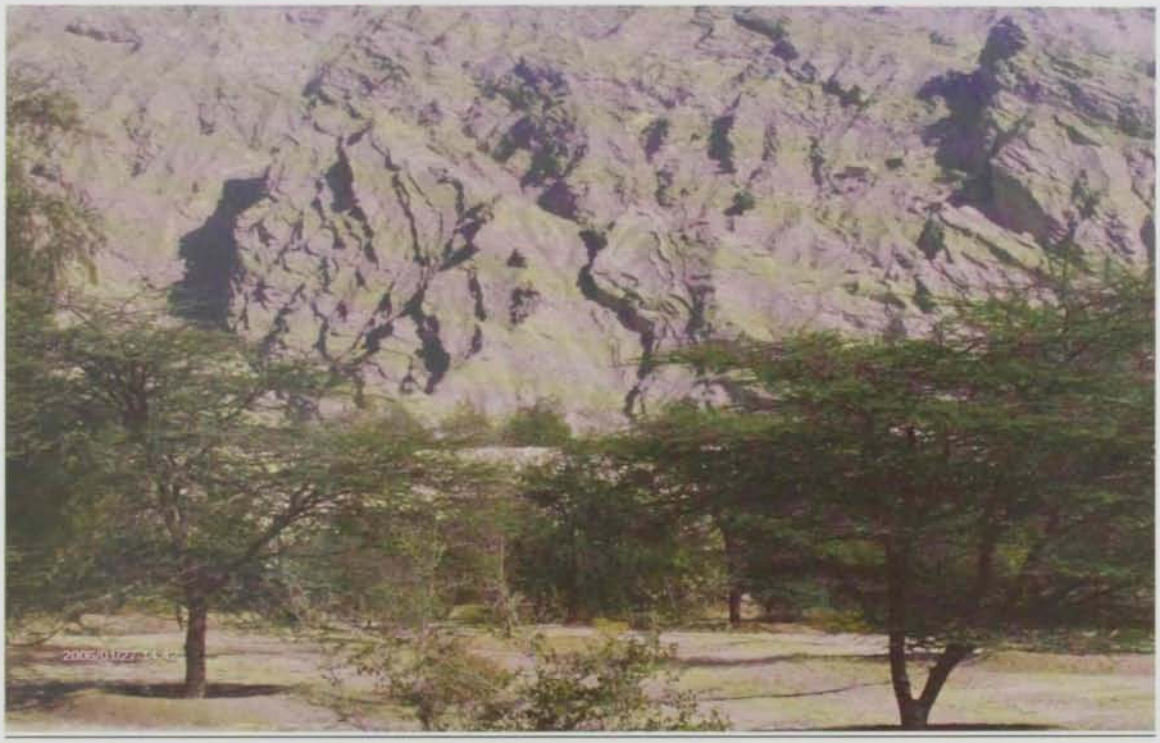

(Photo 4.6) Jabal Hafit at the location of profile – 7.

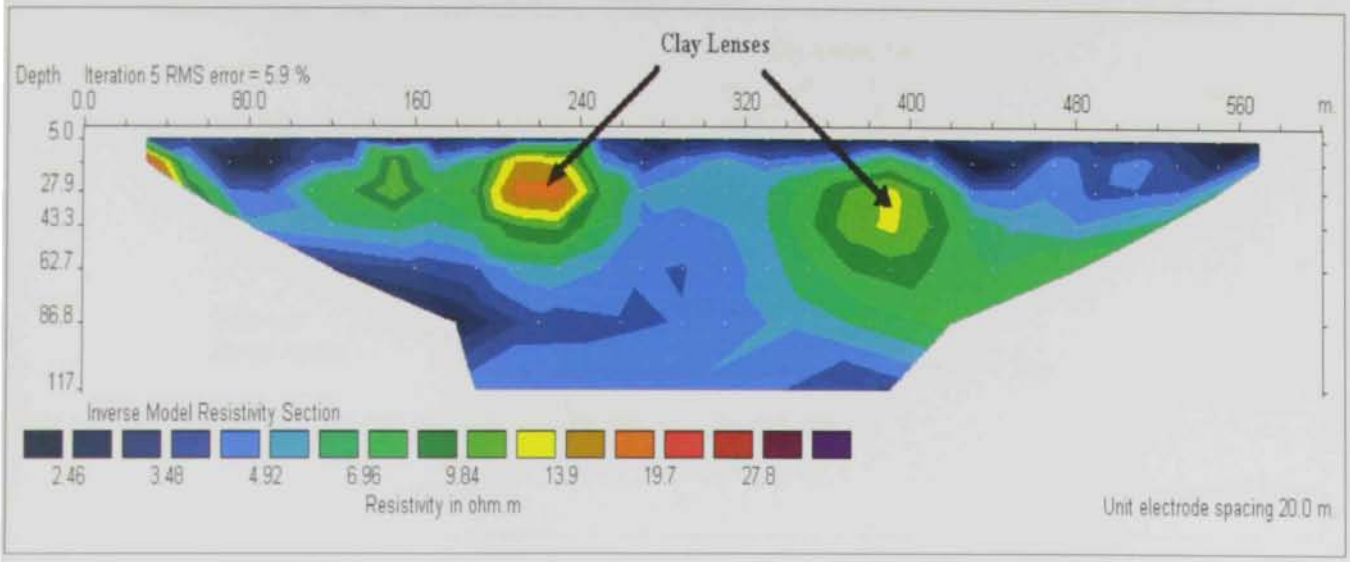

Figure (4.15): Tomographic Image of Line-8

(Photo 4.8) Location of Profile -8 (South of Ain Bu Sukhanah).

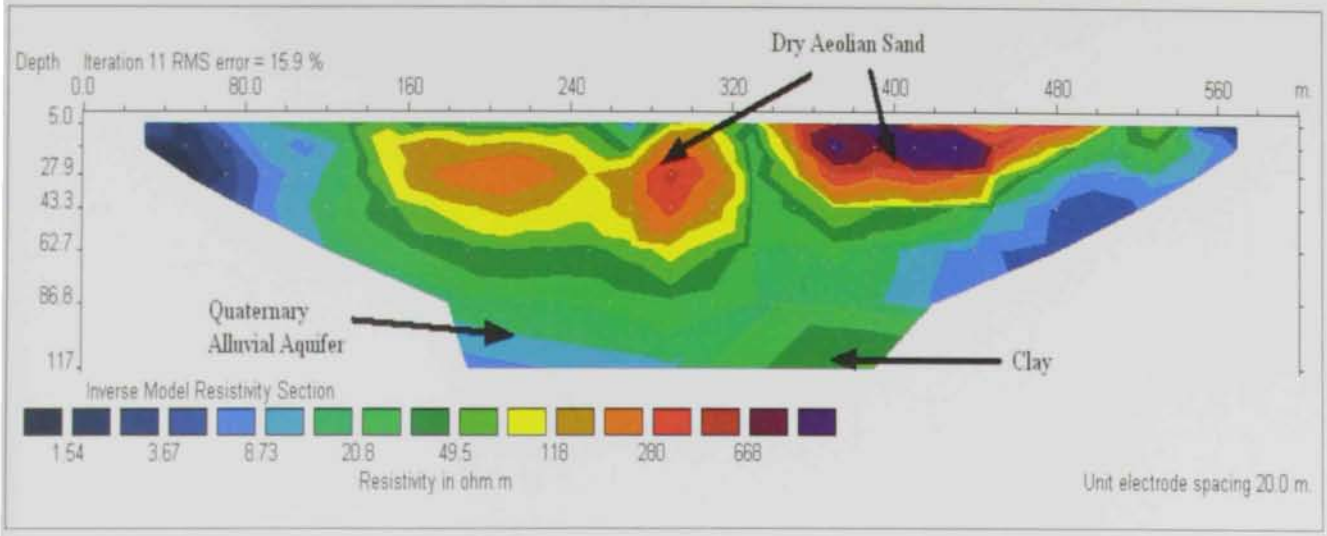

(Figure 4.16): Tomographic Image of Line-9.

A

B

(Photo 4.8 A&B) Field measurements on profile- 9.

CHAPTER 5
Hydrogeochemical Aspects

5.1 Introduction

The objective of this chapter is to analyze the groundwater chemistry of the aquifer systems within the study area in terms of the prevailing natural (climatic, geological and hydrgeological) and man-induced (mainly agricultural) conditions, determining the origin of the groundwater using environmental isotope techniques, and to evaluate the suitability of groundwater for different purposes.

For this study, 53 water samples were collected from 53 governmental and private wells. In addition, 3 samples were collected from different surface water localities in the study area in February, March and April 2006 (Figure 5.1).

The Electrical Conductivity (EC) (μS/cm), salinity (%), temperature (°C) and Total Dissolved Solid (TDS) contents in mg/l were measured directly in the field. The samples were then analyzed for major cations (K^+, Na^+, Mg^+ and Ca^{2+}), major anions (HCO_3^{2-}, SO_4^{2-}, Cl^-, NO_3^-) and trace metals (Sr, Ba, B, Al, Fe and Zn) in the Central Laboratories Unit (CLU), U.A.E University. Analysis of selected 42 water samples for ($\delta^{18}O$, δD) was carried out at the Environmental Isotope Section of the Water Authority of Jordan Laboratories. All chemical data are listed in Appendix B.

5.2 Hydrochemical Characteristics

The main measured physical properties of the groundwater in the study area including, electrical conductivity (EC), total dissolved solids (TDS), hydrogen ion concentration (pH), temperature and chemical properties of the major and some minor constituents are presented .

5.2.1 Physical properties

The quality of water has to agree with the purpose of its intended usage. It must have a suitable physical quality. In this chapter, four criteria will be used in the preliminary assessment of groundwater physical quality. These criteria include electrical

conductivity (EC), total dissolved solids (TDS), hydrogen ion concentration (pH) and temperature.

5.2.1.1 Electrical Conductivity (EC)

Electrical conductivity is an approximate determination of total dissolved salts, which can be made by measuring the electrical conductance of a groundwater sample. Specific electrical conductance defines the conductance of a cubic centimeter of water at a standard temperature of 25°C. It is a function of water temperature, types of ions present and the concentrations of various ions in a water sample (Todd, 1980).

The electrical conductance of water samples collected from the study area varied between 3.79 mS/cm in a farm west of Neima (Well No.9) and 31.0 mS/cm in Ain Bu Sukhanah (Well No.34). The iso-electrical conductance map (Fig 5.2) shows that in the north (Neima Area) the EC values are less than 10 mS/cm , while in Mubazzarah area , the EC values between 15 and 25 mS/cm, and to the west of Jabal Hafit at Ain Bu Sukhanah , the EC values exceed 30 mS/cm. This high EC values is may be resulted from using the groundwater in these areas in agricultural activities.

5.2.1.2 Total Dissolved Solids (TDS)

The total salinity of natural water is a measure of the ion concentration which may be affected by dissolution and evaporation processes. In natural water which contains a variety of ionic and non ionic species, the values of EC are not simply related to TDS. In the study area, the total salinity ranges between 1,910 and 17,400 ppm, with a mean value of 6,714 ppm. The distribution of salinity content is shown in (Figure 5.3).

The salinity increases from east to west in the direction of groundwater flow. The higher salinity content is recorded for the central and western regions (Mubazarah and Ain- Bu Sukhanah areas), whereas at Neima area in the north, it is quite low and increases towards the south.

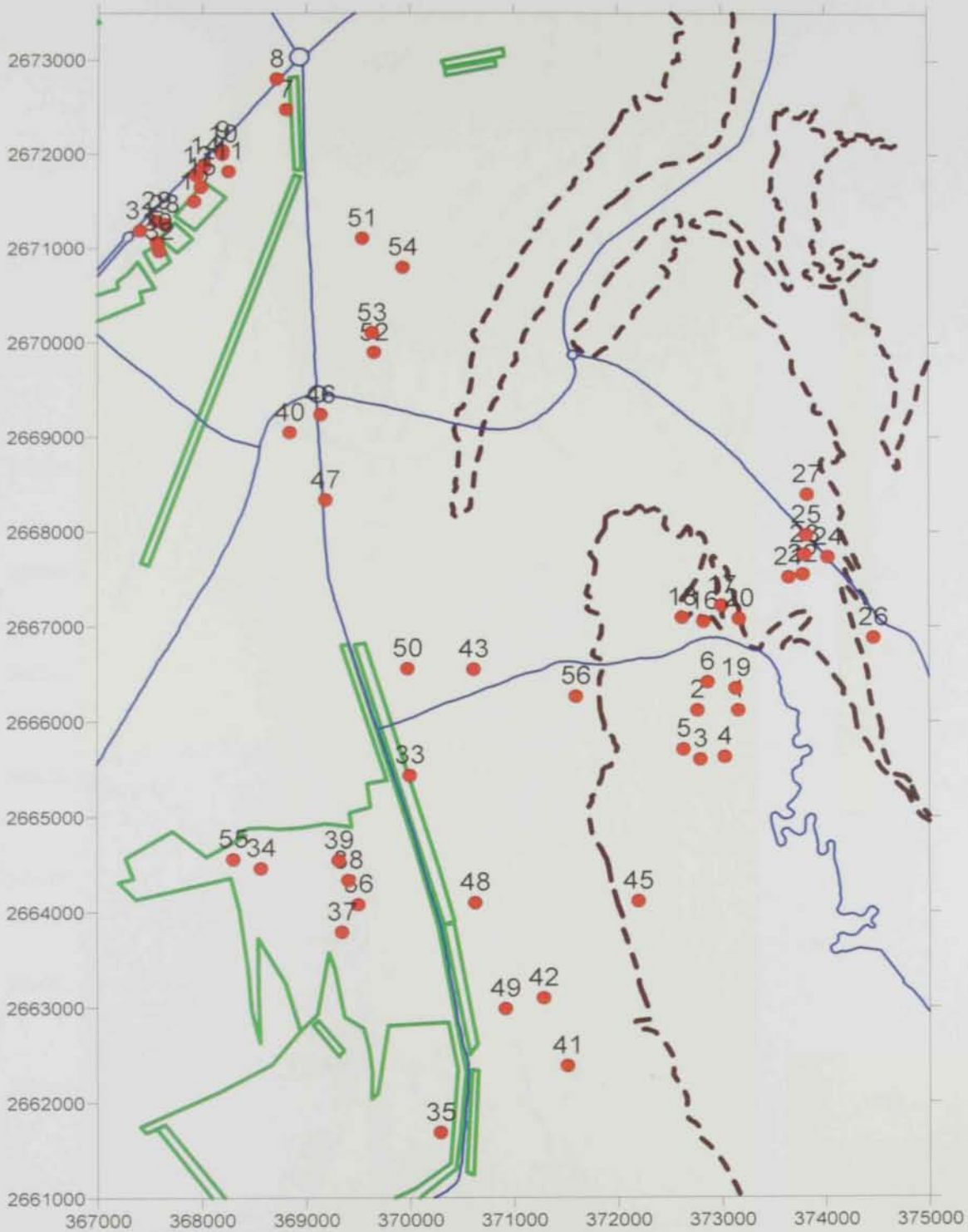

Figure (5.1): Locations of the groundwater samples in the study area.

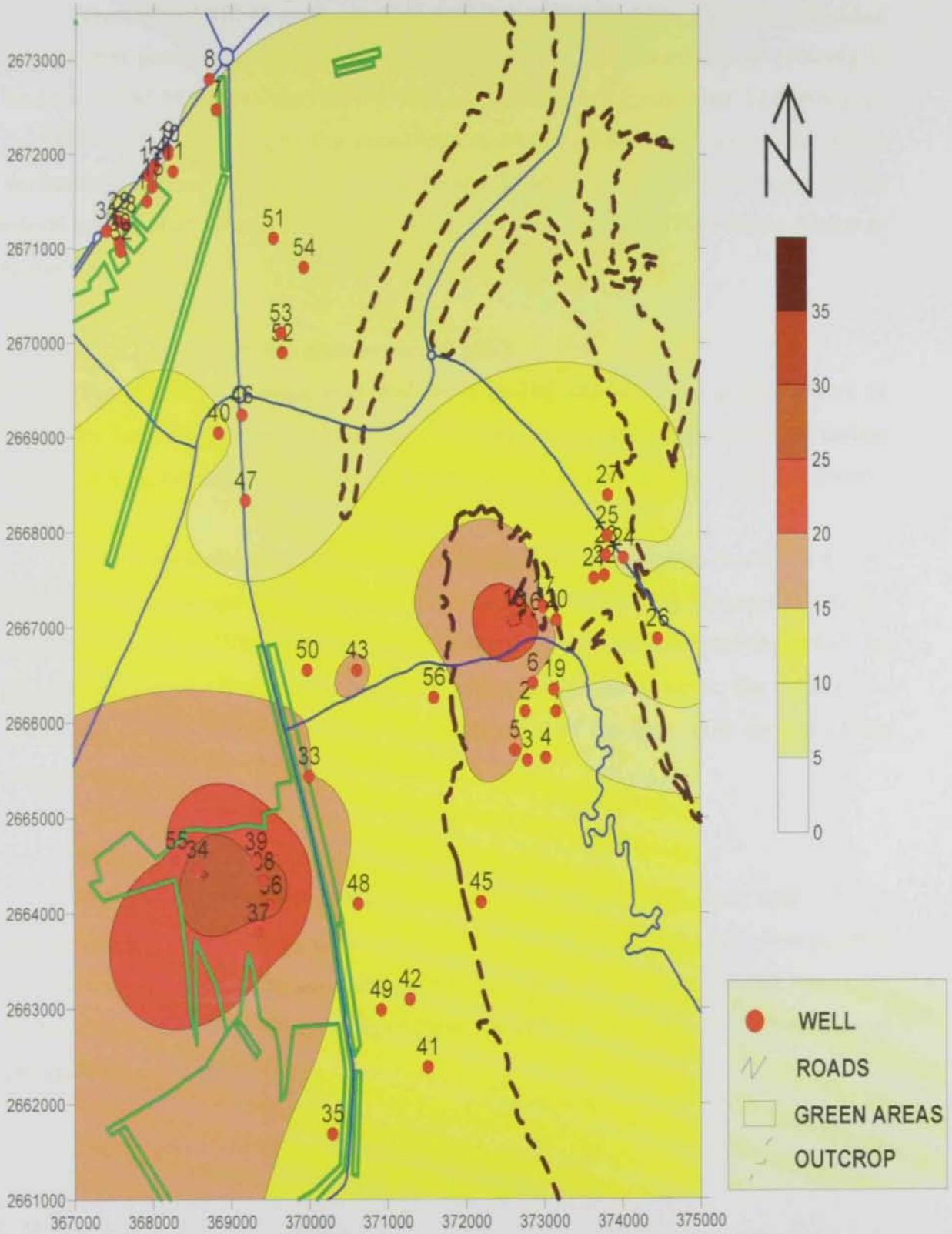

Figure (5.2): Iso-Electrical Conductivity (µS/cm) contour map of groundwater samples collected from the study area.

The USGS/NDC Groundwater Research Project (USGS/NDC,1996) has classified groundwater quality into three main types, namely: fresh: 0-2400 mS/cm (0-1500 mg/l), brackish: 2400-24,000 mS/cm (1500-15,000 mg/l) and saline: greater than 24,000 mS/cm (>15,000 mg/l). According to this classification, all the groundwater samples lie within the brackish interval except wells No 34, 36 and 38 which are in the saline interval. The use of groundwater for irrigation is again the main reason for high TDS values similar to that of EC.

5.2.1.3 Hydrogen Ion Concentration (pH)

The pH value of water is related to its quality and affects to a great extent its suitability for different uses. The pH is controlled by the amount of dissolved carbon dioxide (CO_2), carbonates (CO_3^{2-}) and bicarbonates (HCO_3^-) (Domienico and Schwartz, 1990).

With the exception of the few available readings, the pH varies between 6.45 and 7.66. It should be noted that the acceptable limit of pH for drinking purposes is between 6.5 and 8.5 (WHO, 1971). Inspection of the available data revealed that the pH of the groundwater samples in the study domain is within that range. However, the water in the study area is not suitable for drinking purposes due to the high TDS content of the groundwater.

5.2.1.4 Groundwater Temperature

The temperature of the collected groundwater samples in the study area is varied between 29 °C and 49.1 °C with a mean value of 35.59 °C. Figure (5.4): The temperature increases from west to east, opposite to the direction of groundwater flow. Where as, Mubazarah is characterized by the highest water temperature because of thermal origin of groundwater in that area.

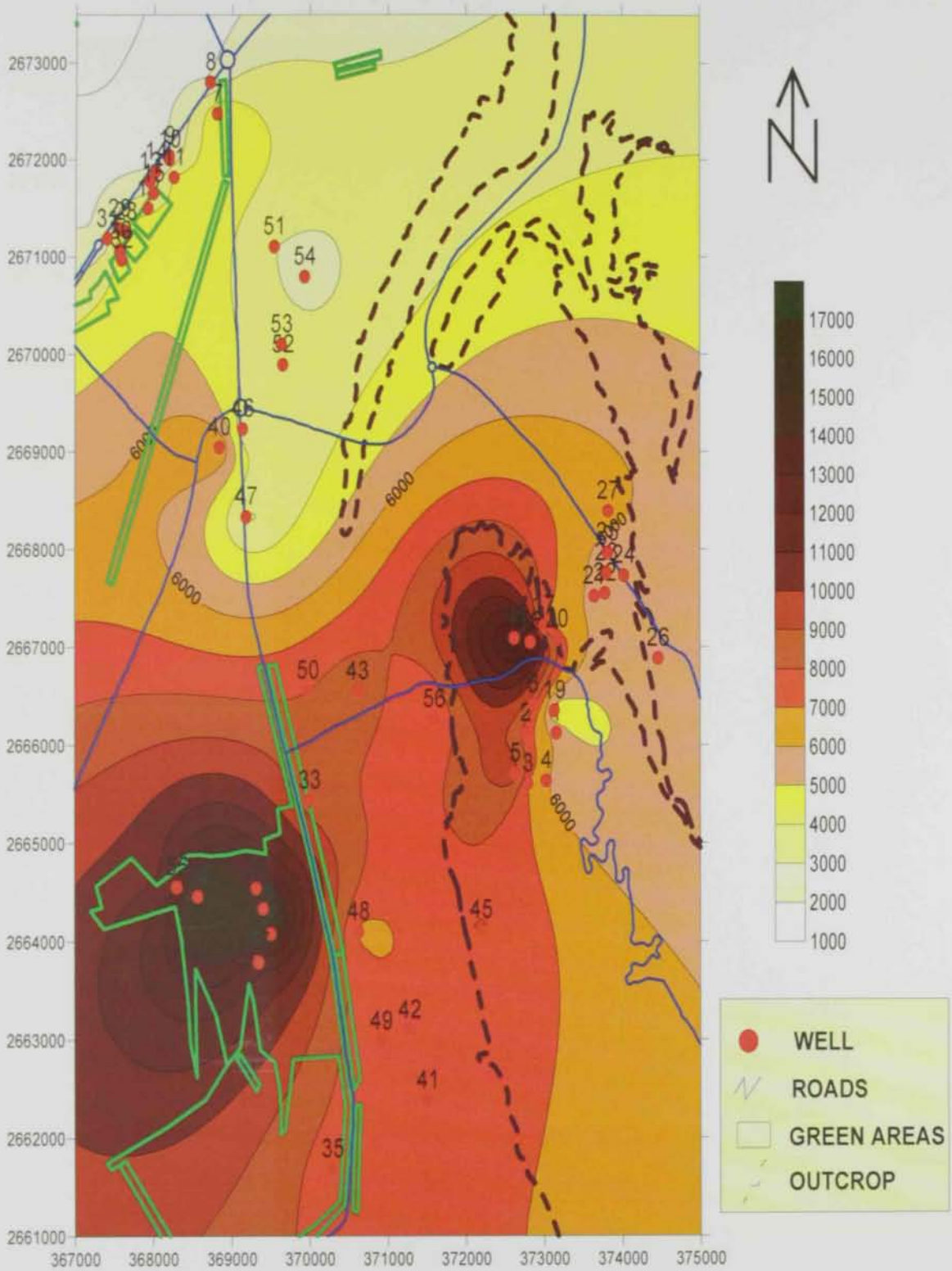

Figure (5.3) Iso-salinity (mg/l) contour map of groundwater in the study area.

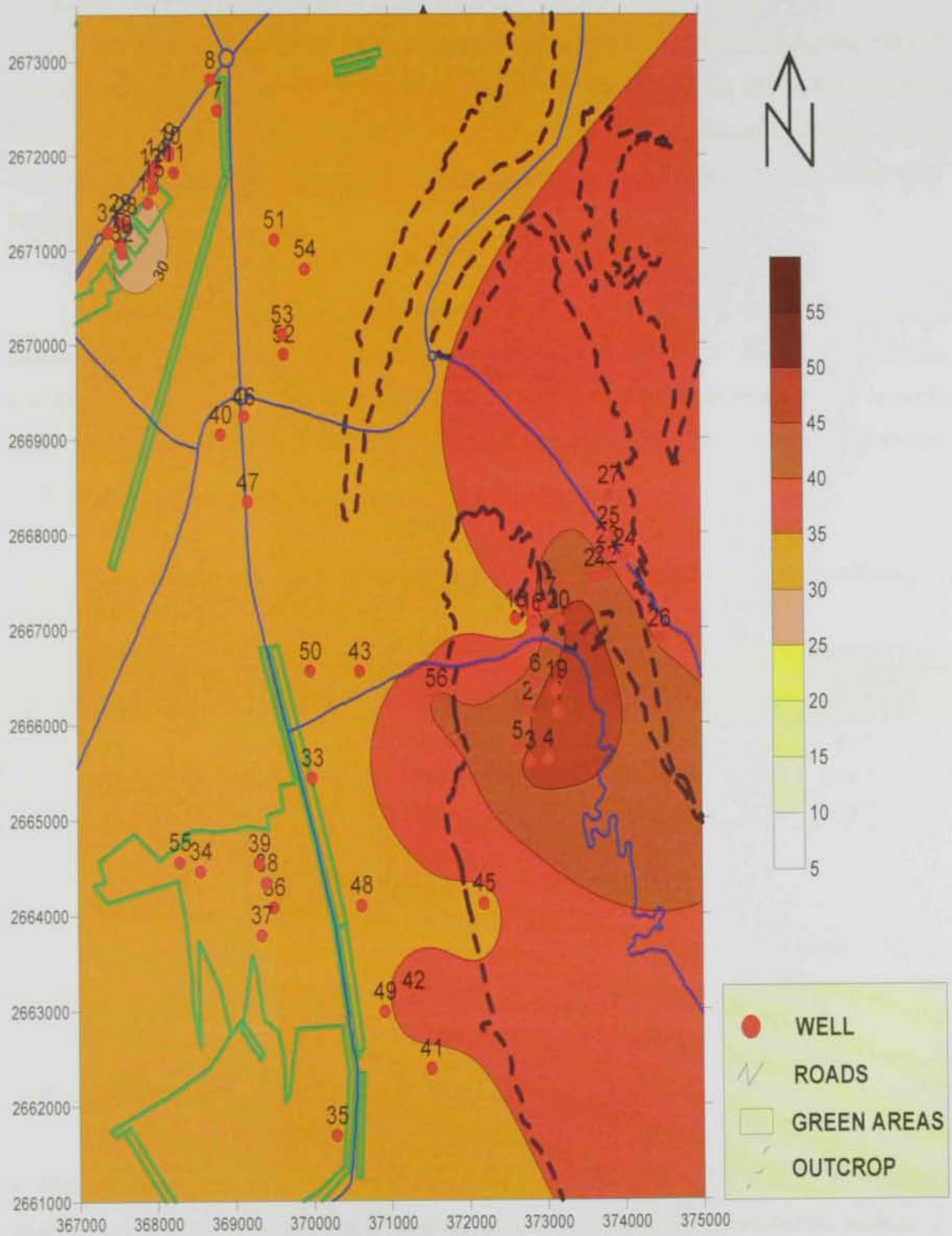

Figure (5.4): Temperature iso-contour map for the study area

5.2.2 Chemical properties

The chemical composition of natural water is controlled primarily by the natural environmental factors to which the water is exposed in the hydrologic cycle. Specifically, the composition of natural water is influenced by the type and amount of soluble products of rock weathering and decomposition and by the terrain traversal by that water (Al-Nuaimi, 2003).

The major cations in water are potassium (K^+), sodium (Na^+), magnesium (Mg^{+2}), calcium (Ca^{+2}) and the major anions are chloride (Cl^-), sulphate (SO_4^{-2}), bicarbonate (HCO_3^{2-}) and nitrate (NO^{3-}). Each of these constituents and their relationship to each other are discussed below. Table (5.1) illustrates statistics about the distribution of theses constituents in the study area.

Table (5.1): Statistical analysis for the parameters of physical properties and major cations and anions in the study area.

					Major Cations				Major Anions			
	pH	Ec	TDS	Temp	Na^+	Ca^+	K^+	Mg^{+2}	Cl^-	SO_4^{-2}	HCO_3^-	NO_3^-
Minimum	6.45	3.79	1910	29.1	137.8	110.7	25.68	120	430	495	65.07	0.08
Maximum	7.66	31	17400	49.1	4954	1813	1657	5173	10000	6280	520.5	95.5
Mean	7.16	12.18	6714	35.59	1888	669.3	115.7	457	3232	1686	202.5	25.8

5.2.2.1 Major cations

The major sequence of cations dominance in groundwater of the study area has the order of: - $Na^+ > Ca^{+2} > Mg^{+2} > K^+$ (Table 5.1 and Appendix (B)).

Sodium (Na^+)

The primary source of most sodium ions (Na+) in natural water is the release of soluble products during the weathering of sodium bearing minerals particularly plagioclase feldspars, which are typical constituents of many igneous rocks. Sodium is also common in evaporites and argillaceous sediments (Davis and DeWiest, 1966)

Sodium ion concentrations in groundwater of the study area ranged from 137.8 ppm North-East Mubazarah (well No. 25) to 4,954 ppm at Ain Bu Sukhanah (well No. 38), with a mean value of 1,888 ppm. The iso-concentration map shows a steady increase in Na^{+} concentrations from east to west (Figure 5.5). Sodium ion concentrations are low at Neima and the northern part of the study area. While Mubazarah and Ain Bu Sukhanah are characterized by high Na^{+} concentrations. The positive relation between sodium and chloride (r^2=0.81) (Figure 5.6) is a strong evidence for extinsively using of brackish groundwater for irrigation.

Calcium (Ca^{+2})

The most common form of calcium in sedimentary rocks is carbonates, particularly as limestone or dolomite, which are dominant in the study area. The dissolution of carbonate minerals and carbonate cement yields calcium to the groundwater.

The calcium ion concentration in groundwater of the study area ranged from 110.7 mg/l at Neima (well No. 47) to 1,813 mg/l at Ain Bu Sukhanah (well No. 34 west of Jabal Hafit). In Figure (5.8), the calcium iso-concentration contour map shows a gradual increase in calcium ion from east to west in the direction of groundwater flow. Calcium ion concentrations are low at Neima and Mubazarah . Where as high calcium ion concentrations encountered in Ain Bu Sukhanah . The calcium abundance is resulted from the limestone dissolution of Jabal Hafit .

Magnesium (Mg^{+2})

The common sources of magnesium in groundwater are dolomite in sedimentary rocks, olivine, biotite, hornblende, and augite in igneous rocks, and serpentine, talc, diopside, and tremolite in metamorphic rocks. In addition, most calcite contains some magnesium, so a solution of limestone commonly yields abundant magnesium as well as calcium (Davis and DeWeist, 1966).

The magnesium ion (Mg^{+2}) concentrations in fresh water are generally less than that of calcium because of low geochemical abundance of magnesium (Mathess, 1982).

The concentration of Mg^{+2} in collected groundwater samples in the study area ranged from 120 to 5,173 ppm, with a mean value of 457 ppm. The Iso-concentration contour map for Mg^{+2} (Figure 5.9) shows a general increase in Mg^{+2} concentrations from east to west. The maximum Mg^{+2} concentrations exist in the western side of Jabal Hafit (Ain Bu Sukhanah). The presence of dolomite in Jabal Hafit could be elevated the magnesium concentration at Ain Bu Sukhanah.

Potassium (K^+)

Potassium content is generally lower than sodium. The natural sources of potassium in water are the igneous rocks as feldspars (orthoclase and microcline), some mica and sedimentary rocks as silicate and clay minerals. Potassium is hardly taken into solution (Davis and DeWiest, 1966). The potassium content ranges between 25.7 ppm at Neima (well No. 10) and 4,953.5 ppm at Ain Bu Sukhanah (well No. 38). In general potassium ion concentrations (Figure 5.10) are low at Neima and Mubazarah areas, while high K^+ concentrations are recognized west of Jabal Hafit at Ain Bu Sukhanah. This high potassium concentration can be attributed to the presence of clay layer, overlained the gypsum aquifer of Ain Bu Sukhanah.

5.2.2.2 Major anions

The sequence of the major anions in the groundwater of the study area has the order of: - $Cl^- > SO_4^{-2} > HCO_3^- > NO_3^-$

Chloride (Cl^-)

The chloride ion (Cl^-) is widely distributed in natural water. Most (Cl^-) in the groundwater is from three sources including ancient seawater entrapped in sediment, dissolution of halite and related minerals, evaporite deposits and solution of dry fallout from the atmosphere especially in the arid region (Davis and DeWesit, 1966).

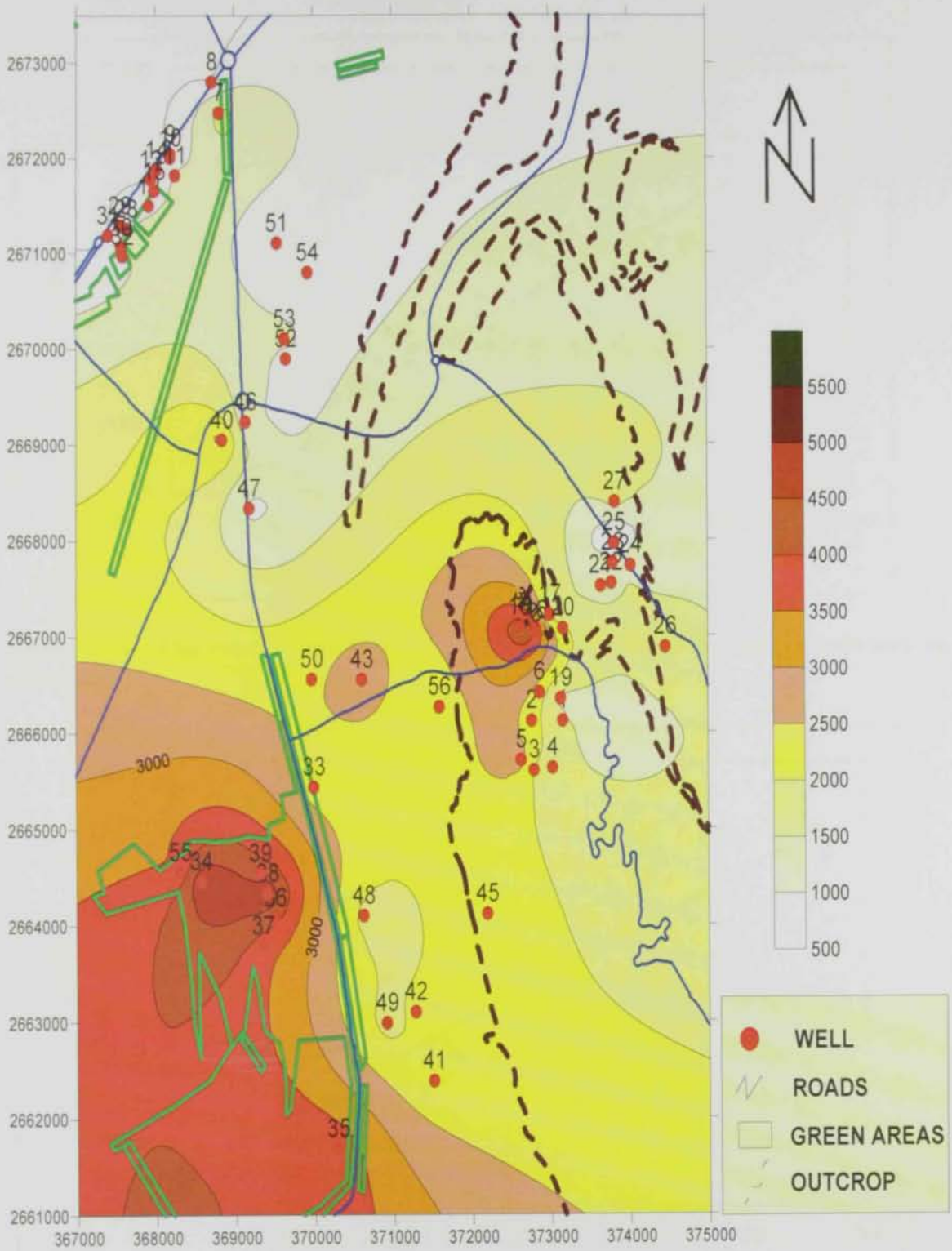

Figure (5.5): Contour Map for Na^+ in the study area.

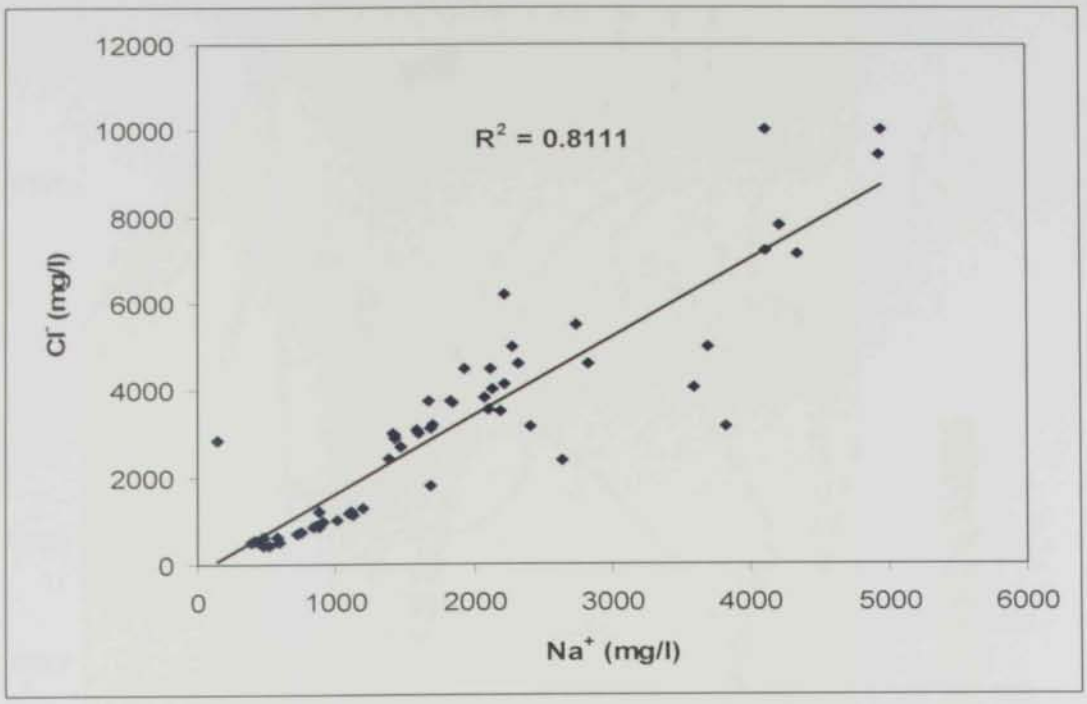

Figure (5.6): The relationship between sodium and chloride for the groundwater in the study area.

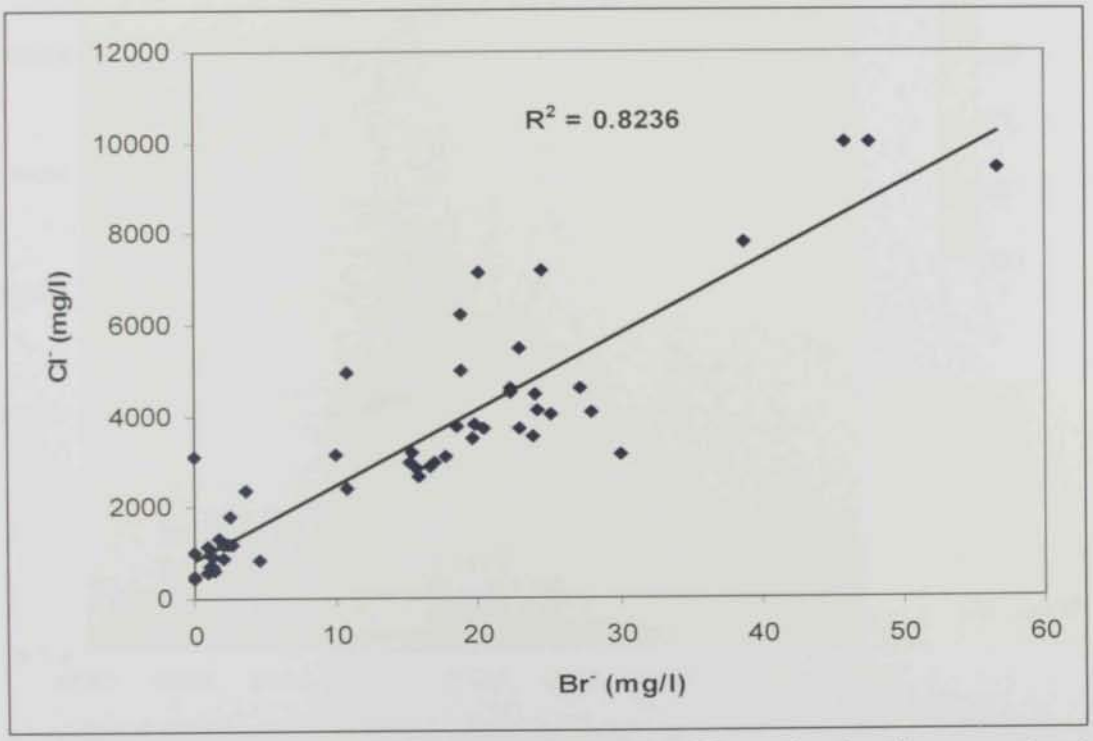

Figure (5.7): The relationship between chloride and bromine for the groundwater in the study area.

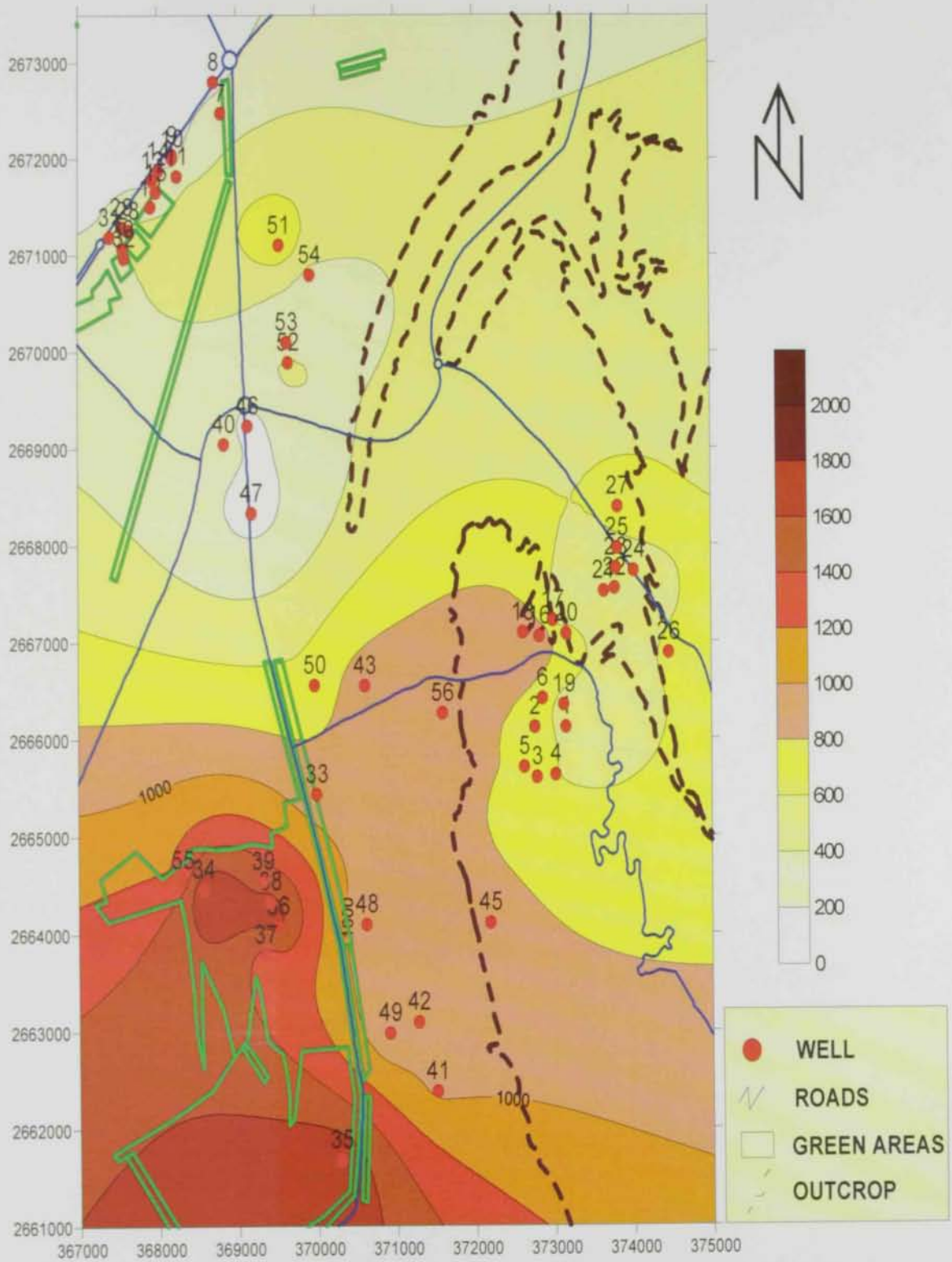

Figure (5.8): Contour Map for Ca^{+2} in the study area.

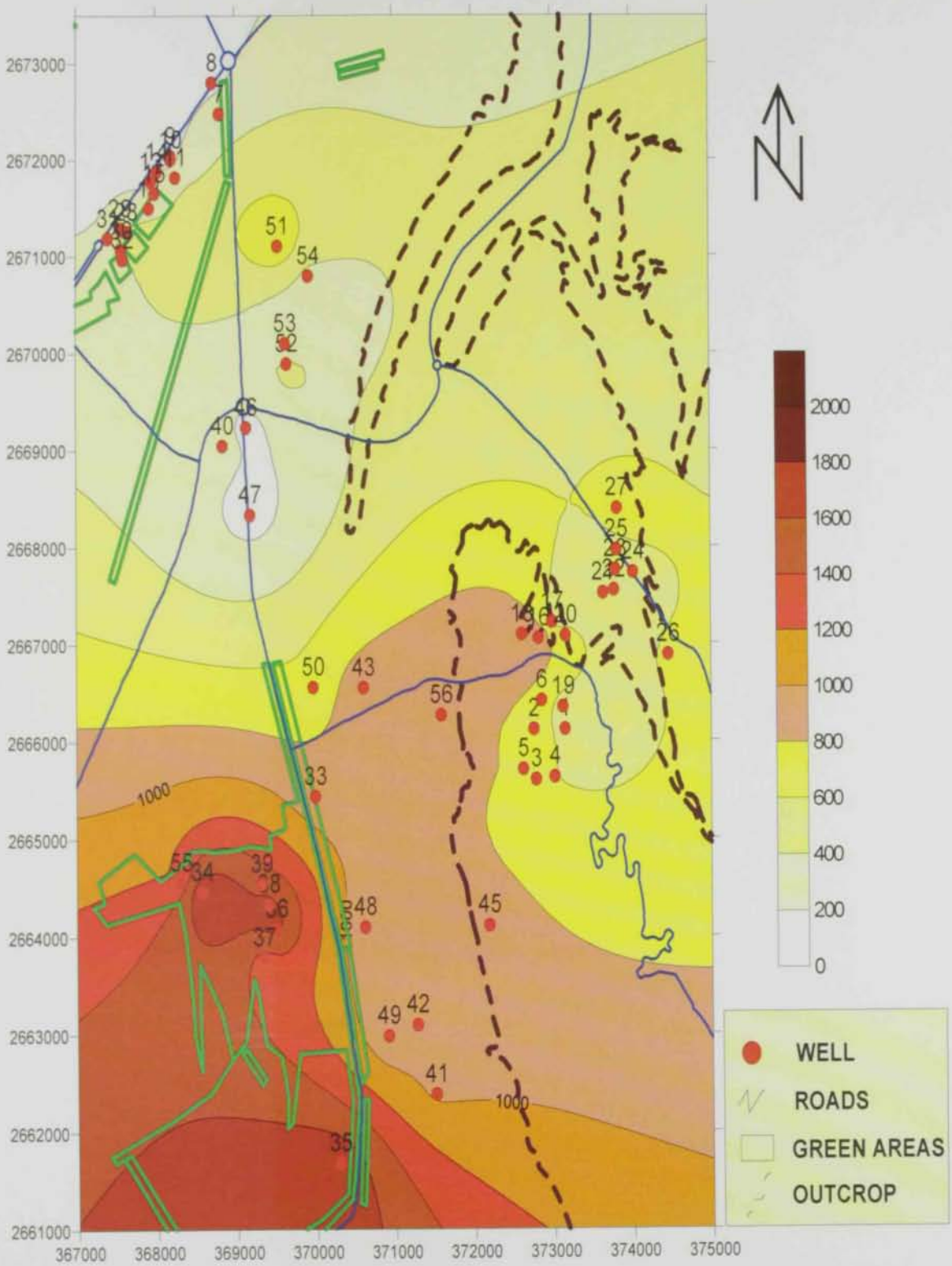

Figure (5.8): Contour Map for Ca^{+2} in the study area.

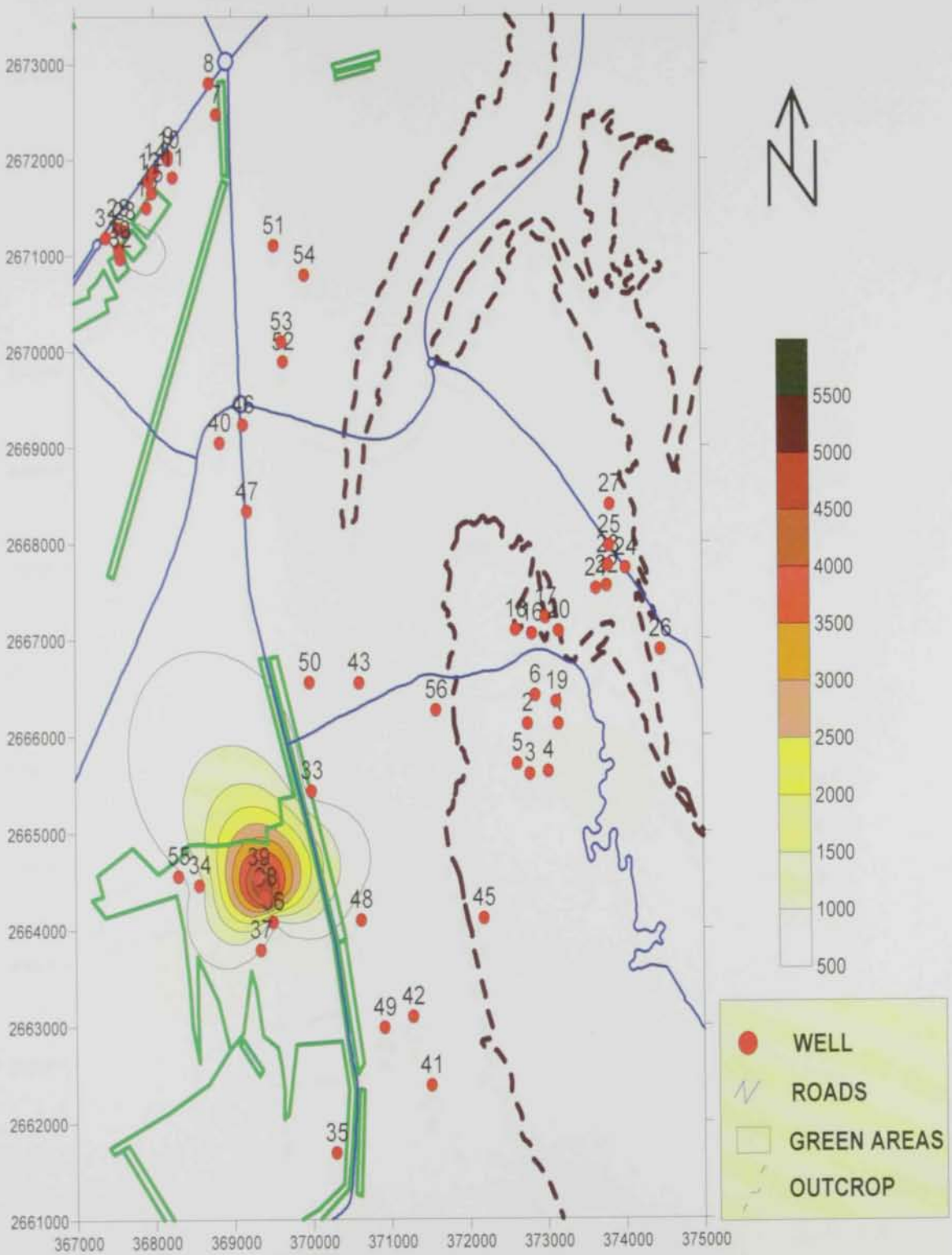

Figure (5.9): Contour Map for Mg^{+2} in the study area.

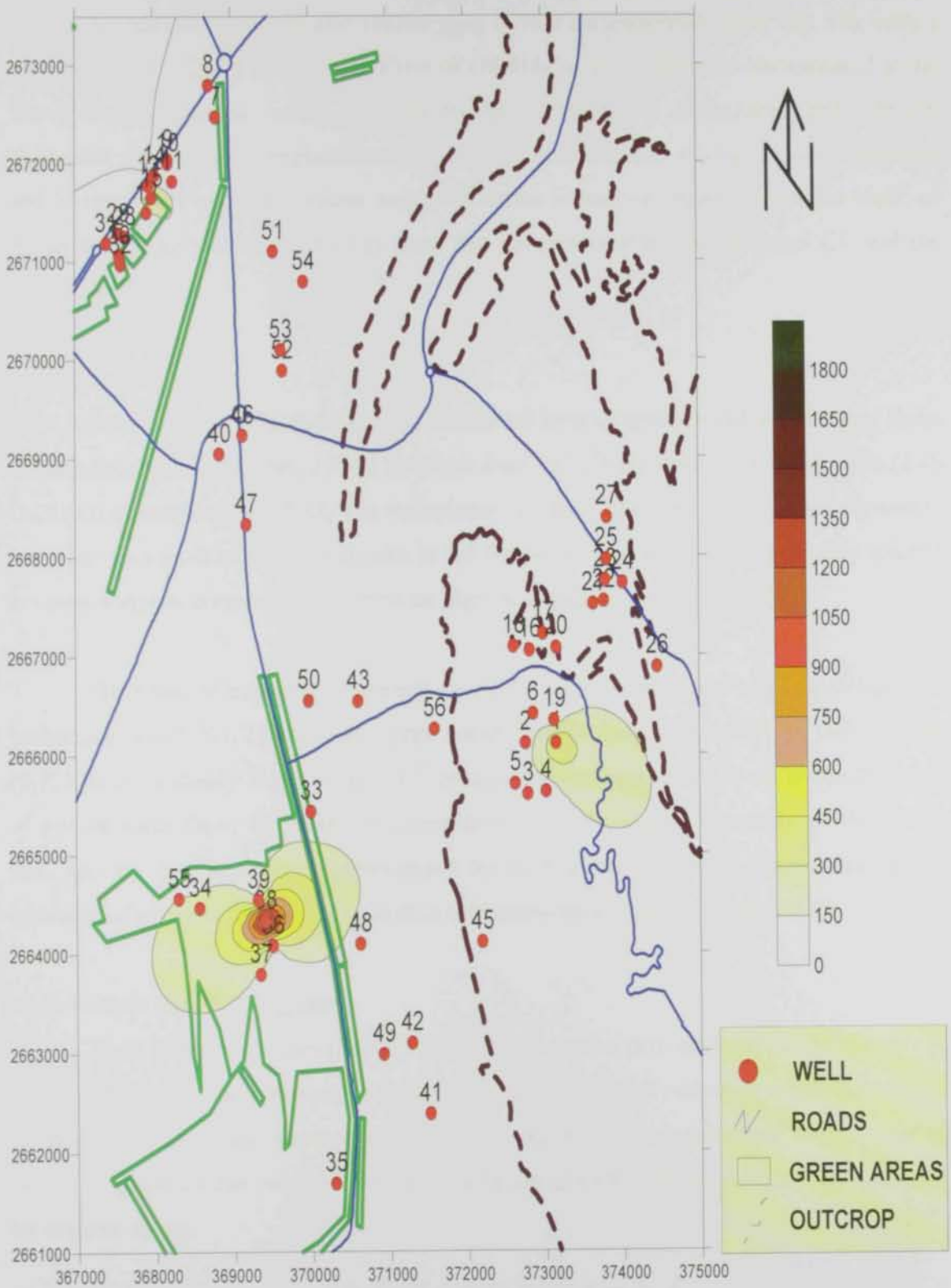

Figure (5.10): Contour Map for K^{+2} in the study area.

The chloride ion concentrations in the study area (Fig 5.11) range between 430 ppm at Neima (well No. 9) and 10,000 ppm in Ain Bu Sukhanah (well No. 38), with a mean value of 3,231.5 ppm. Low values of chloride concentration are encountered at the farms west to Neima, while high values are observed at Mubazarah and Ain Bu Sukhanah. One possible explanation for the high concentration of chloride in Mubazarah and Neima is the entrapped saline water within the limestone sequence of Jabal Hafit, or it can be the agricultural activities from the positive relationship between Cl^- and Br^- (Figure 5.7).

Sulphate (SO_4^{-2})

Sulphate is widely distributed in a reduced form in igneous and sedimentary rocks as metallic sulphides (Hem, 1970). Sulphate ions (SO_4^{-2}) are derived from gypsum (CaS $O_4 2H_2O$) or anhydrite (CaS O_4) in sedimentary rocks. These two minerals are present in the study area as thick beds or streaks in the limestone strata and are sufficiently soluble to cause water in contact with them to be high in sulphate (Garmoon, 1996).

The value of sulphate concentrations in the study area ranged between 495 ppm at Mubazarah (well No. 1) and 6,280 ppm south Ain Bu Sukhanah (well No. 35) . Figure (5.12) shows a steady increase in SO_4^{-2} concentrations from east to west in the direction of groundwater flow. Sulphate ion concentrations are low at Mubazarah; while Neima and Ain Bu Sukhanah are characterized by high concentrations may be due to the presence of gypsum and anhydrite within the limestone sequence of Jabal Hafit.

Bicarbonate (HCO_3^-)

Most bicarbonate ions (HCO_3^-) in groundwater are derived from carbon dioxide in the atmosphere, carbon dioxide in soils and by dissolution of carbonate rocks (Davis and DeWeist, 1966). In the absence of calcareous sediments and carbonate rocks, most of HCO_3^- in groundwater results from the dissolution of carbon dioxide within the soil zone by organic decay.

Bicarbonate concentrations in groundwater of the study area ranged from 65.07 ppm south Mubazarah (well No. 45) to 520.5 ppm south Neima (well No. 47), with a mean value of 202.5 ppm. The iso-concentration map of bicarbonate (Fig. 5.13) shows a steady increase in bicarbonate concentrations in the north-west direction, where Neima is characterized by high bicarbonate concentrations. Dissolution of Jabal Hafit carbonate considered the main source for releasing bicarbonate to the groundwater in the study area.

Nitrate (NO_3^-)

The dissolved nitrogen in form of nitrates (NO_3^-) is the most common contaminant identified in groundwater (Freeze and Cherry, 1979). Nitrate in groundwater generally originates from several natural and man induced sources on land surface. Nitrate or nitrogen has proved to be a health hazard when it occurs in drinking water at concentrations in excess of 10 mg/l (WHO, 1971)

The nitrate content ranges between 0.08 ppm at Mubazarah (well No. 24) and 95.5 ppm west Neima (well No. 30) , with a mean value of 25.8 ppm . Nitrate iso-concentrations map (Fig. 5.14) shows that high values of nitrate are encountered at Mubazarah and west Neima where these areas are highly cultivated. This is related to the intensive use of chemical nitrogen fertilizers in agriculture activities.

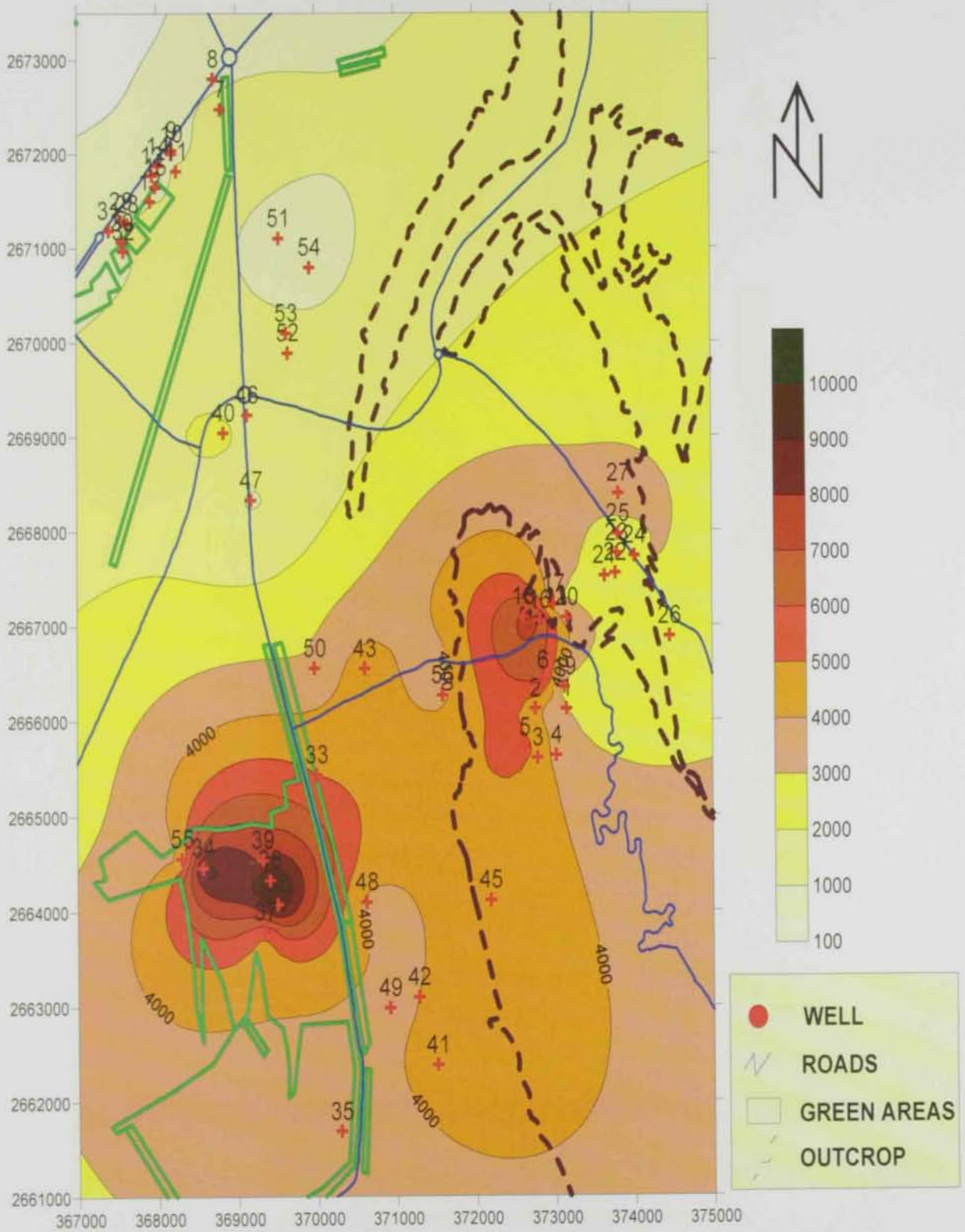

Figure (5.11): Contour Map for Cl^- in the study area.

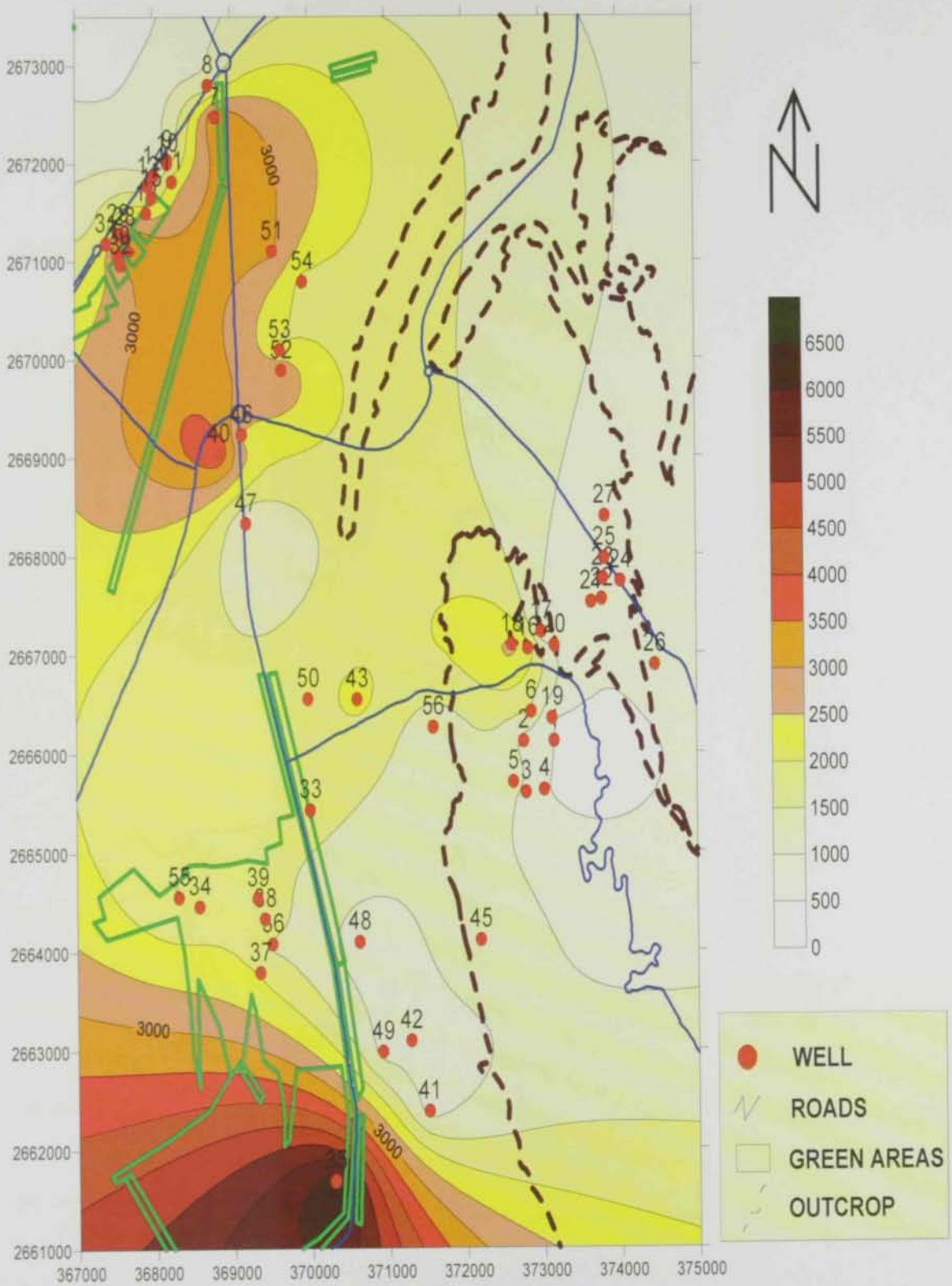

Figure (5.12): Contour map for $SO4^{-2}$ in the study area.

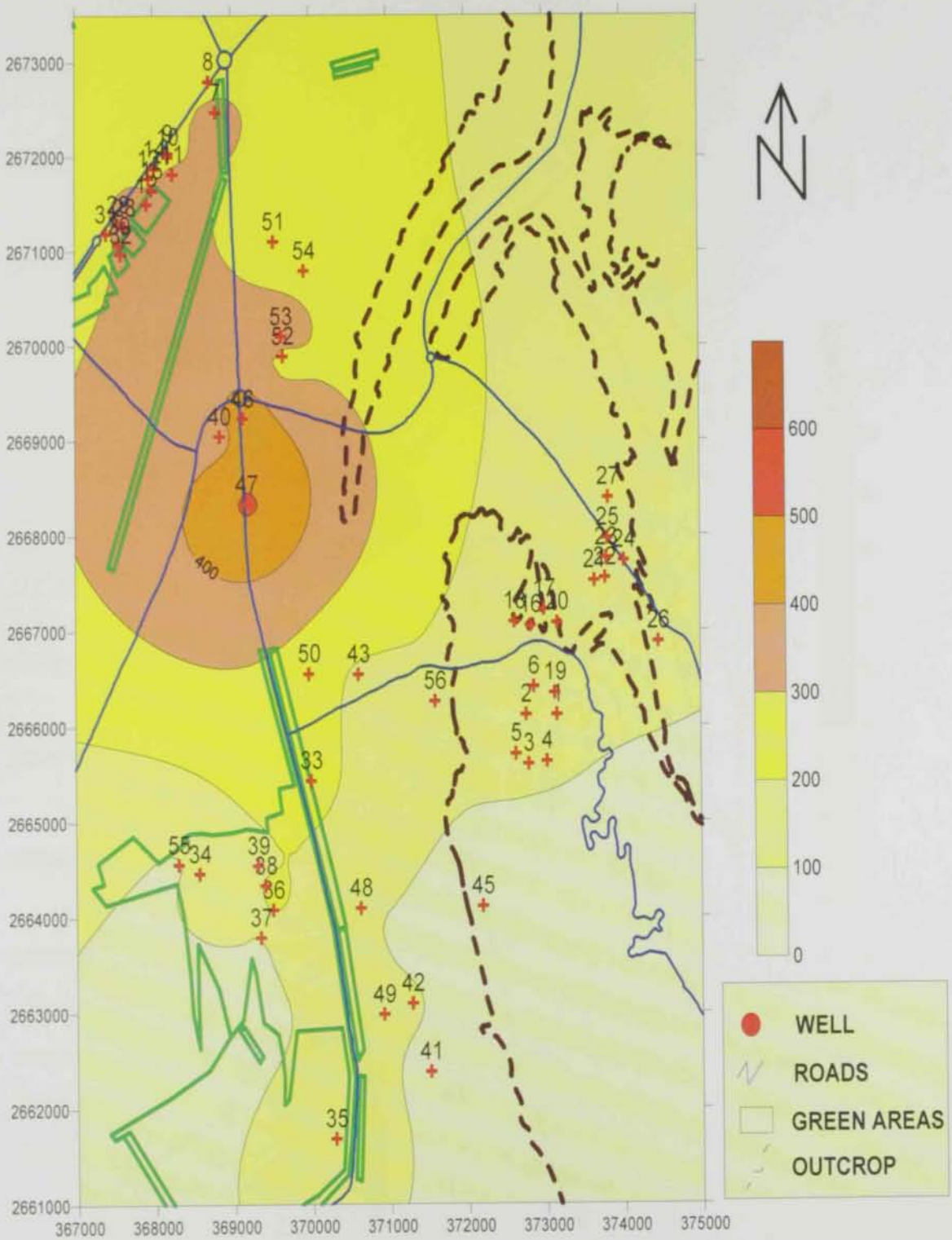

Figure (5.13): Contour map for HCO_3^- in the study area.

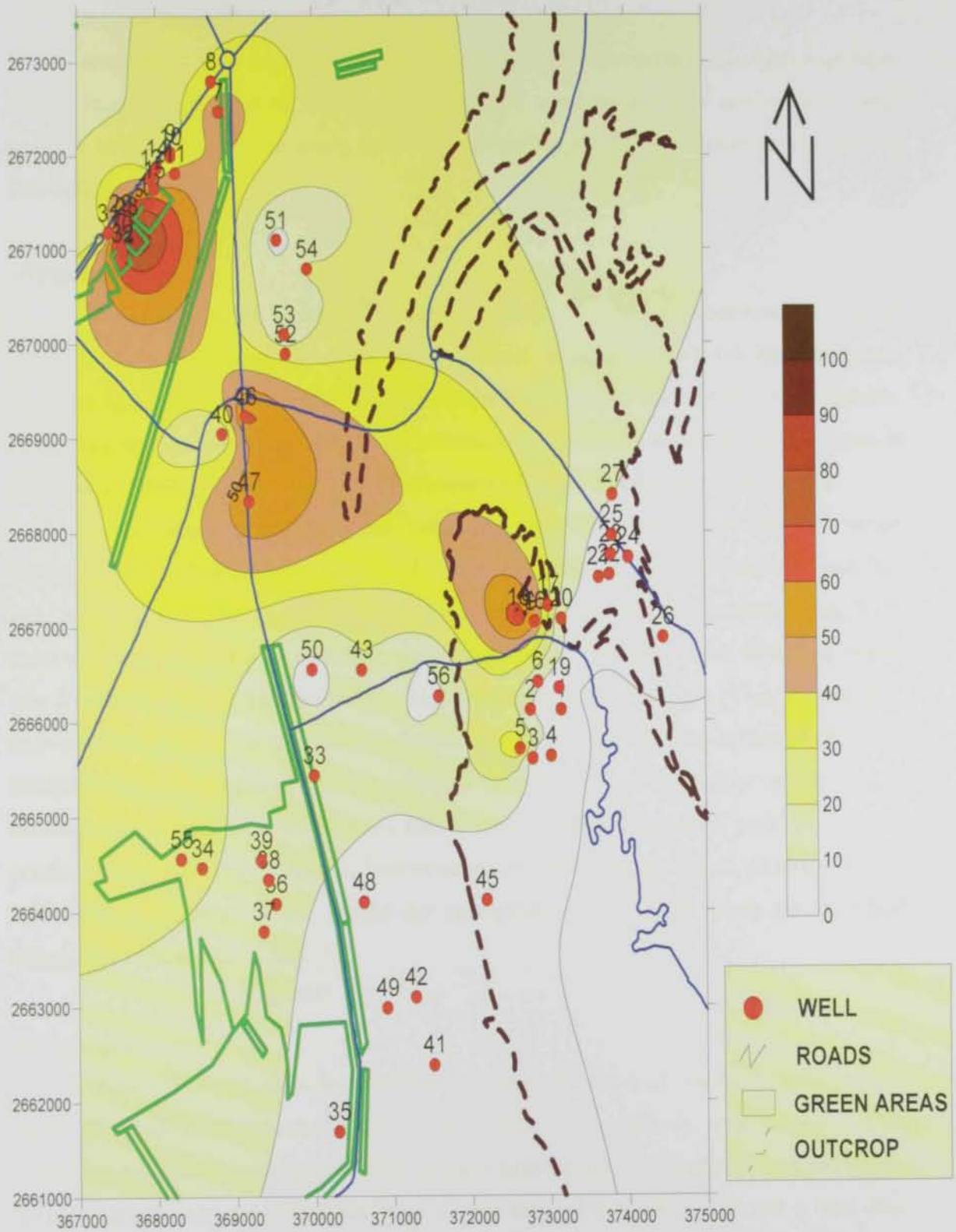

Figure (5.14): Contour map for NO_3^- in the study area.

5.2.2.3 Trace Constituents

Because of their presence in groundwater at high concentrations, which may have serious hazardous effects on human health, several trace metals were analyzed in water samples collected from the study area. The following are brief discussions on each of these elements.

Strontium (Sr)

The chemistry of strontium is similar to that of calcium. Strontium is a fairly common element, replacing calcium or potassium in igneous-rock minerals in minor amounts. The carbonate (strontianite) and the sulfate (celesite) are common in sediments. According to El-Dougdoug (1993), the strontium to calcium ratio in most limestone is less than 1: 1000, although fossils in the limestone tend to be enriched in strontium.

In the study area, strontium concentrations in groundwater samples varied between 5.31 mg/l in Neima (well No. 46) and 68.3 mg/l in Ain Bu Sukhana (well No. 36) , with a mean value of 17.2 mg/l . The iso-concentration map of strontium (Fig. 5.15) shows a steady increase in strontium concentrations in the south-west direction, where Ain Bu Sukhanah is characterized by high strontium concentrations. This strontium is derived mainly from the strontium carbonate ($SrCO_3$) and strontium sulfate ($SrSO_4$).El-Dougdoug (1993) suggested that the celestite mineralization is epigenetic and related to karstification processes. He believes that meteoric water recharged with strontium , produced by weathering of Eocene limestone mixed with sulphate water, produced by the Miocene evaporate sequence, caused the precipitation of celestite along the karstified Oligocene-Miocene boundary.

Barium (Ba)

Barium is an alkaline earth metal occurring in nature as insoluble salts such as barite ($BaSO_4$) and witherite ($BaCO_3$). It is more abundant in igneous rocks than strontium, but that the carbonate rocks contain considerably less barium than strontium. Soluble barium salts are poisonous, with a toxic dose of 0.2 to 0.6 mg/l and a fatal dose of 2.4 grams. Barium considered as undesirable impurity in drinking water; the U.S. mandatory limit is 1.0 mg/l (U.S. Environmental Protection Agency, 1976).

The barium concentrations in the study area ranged between 4.665 µg/l at Ain Bu Sukhanah (well No. 37) and 62.32 µg/l at Mubazarah (well No. 21). Figure (5.16) shows a steady increase in Barium concentrations from west to east. Barium ion concentrations are low at Ain Bu Sukhanah, while Mubazarah and west Neima are characterized by high barium concentrations. This barium abundance can be attributed to the presence of witherite ($BaCO_3$) in Jabal Hafit limestone.

Boron (B)

The most widely distributed mineral of igneous rocks in which boron is an essential constituents is tourmaline. However, it also may be present as an accessory constituent of biotite and the amphiboles. Boron is very important in agriculture, since small amounts are essential to plant growth while greater concentrations of boron in soil and in irrigation water are harmful (U.S. Environmental Protection Agency, 1976).

The boron ion concentration in groundwater of the study area ranged from 0.915 mg/l (well No. 1) to 4.32 mg/l (well No. 18). In Figure (5.17) the boron iso-concentration contour map shows a gradual increase in boron from east to west. Boron concentrations are low at Mubazarah except for few wells. Where as high boron concentrations encountered in Ain Bu Sukhanah and west Neima. These areas are highly cultivated, and it is seems there is a relationship between high boron concentrations and agricultural activities in these areas.

Aluminum (Al)

Although aluminum is the third abundant element in the Earth's outer crust, it rarely occurs in solution in natural water in concentrations greater than a few tenths or hundredths of a milligram per liter. It occurs in substantial amounts in many silicate igneous rock minerals such as the feldspars, the micas and many amphiboles (U.S. Environmental Protection Agency, 1976).

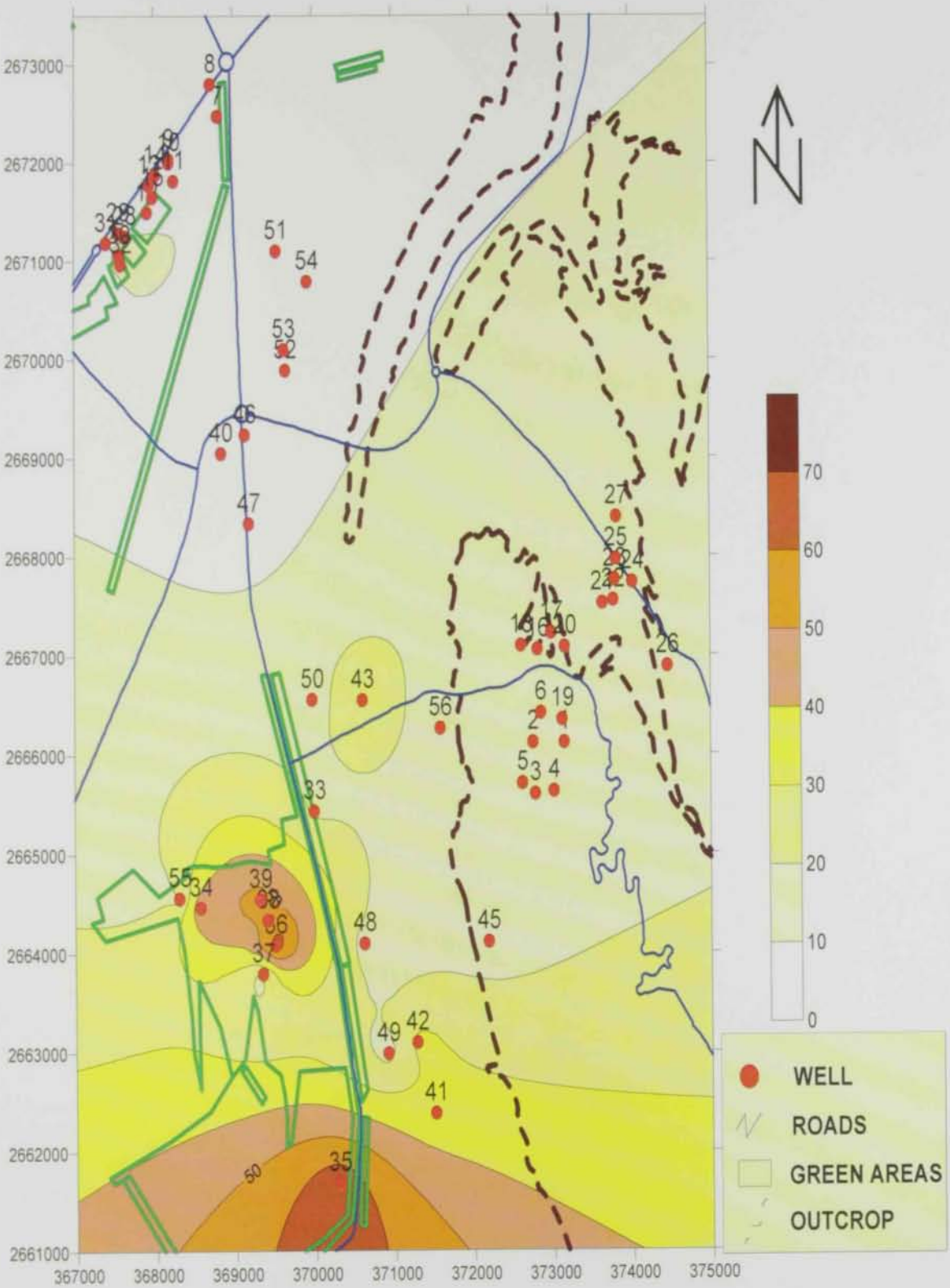

Figure (5.15): Contour Map for Sr^{+} in the study area.

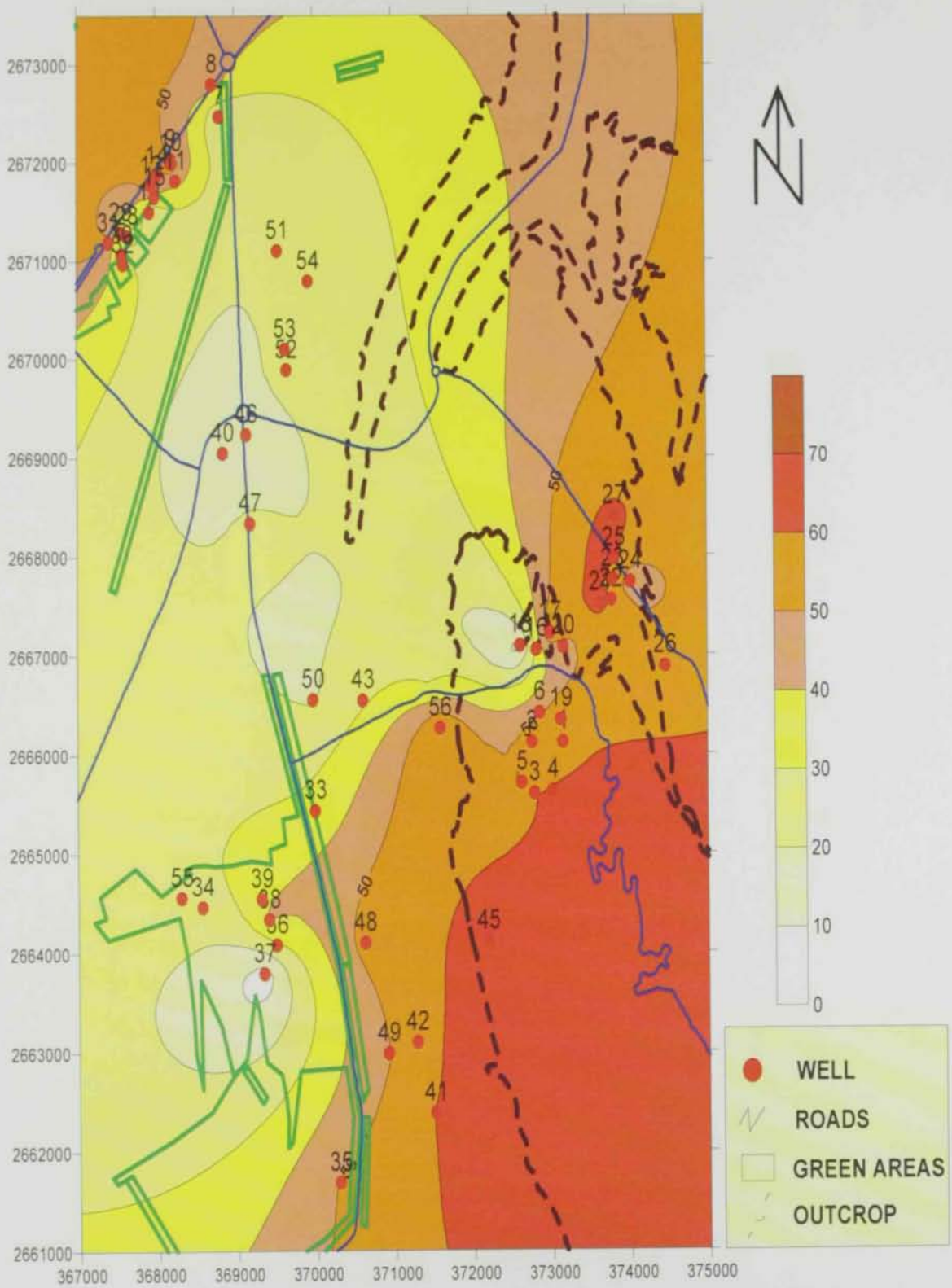

Figure (5.16): Contour Map for Ba in the study area.

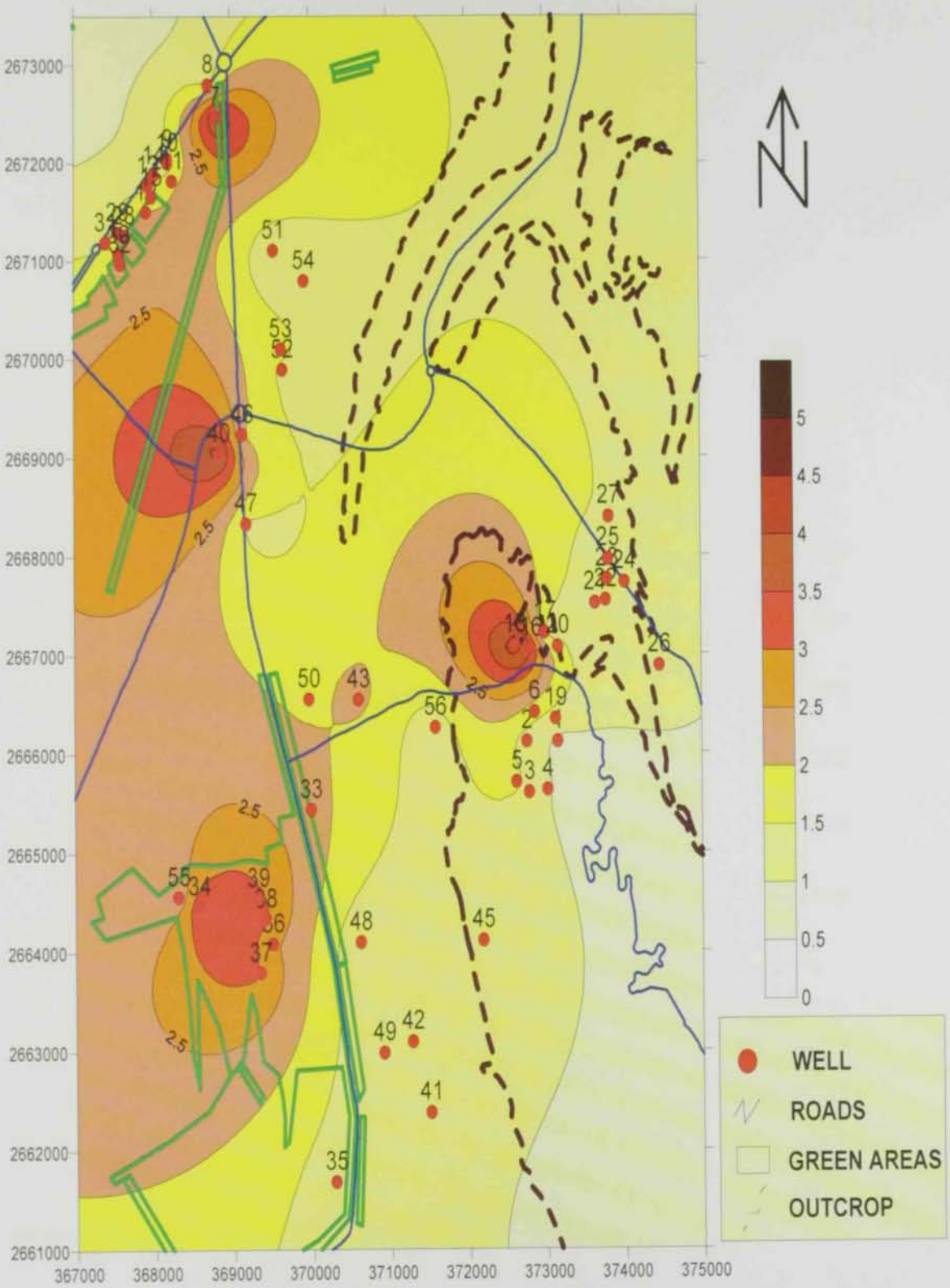

Figure (5.17): Contour Map for B in the study area.

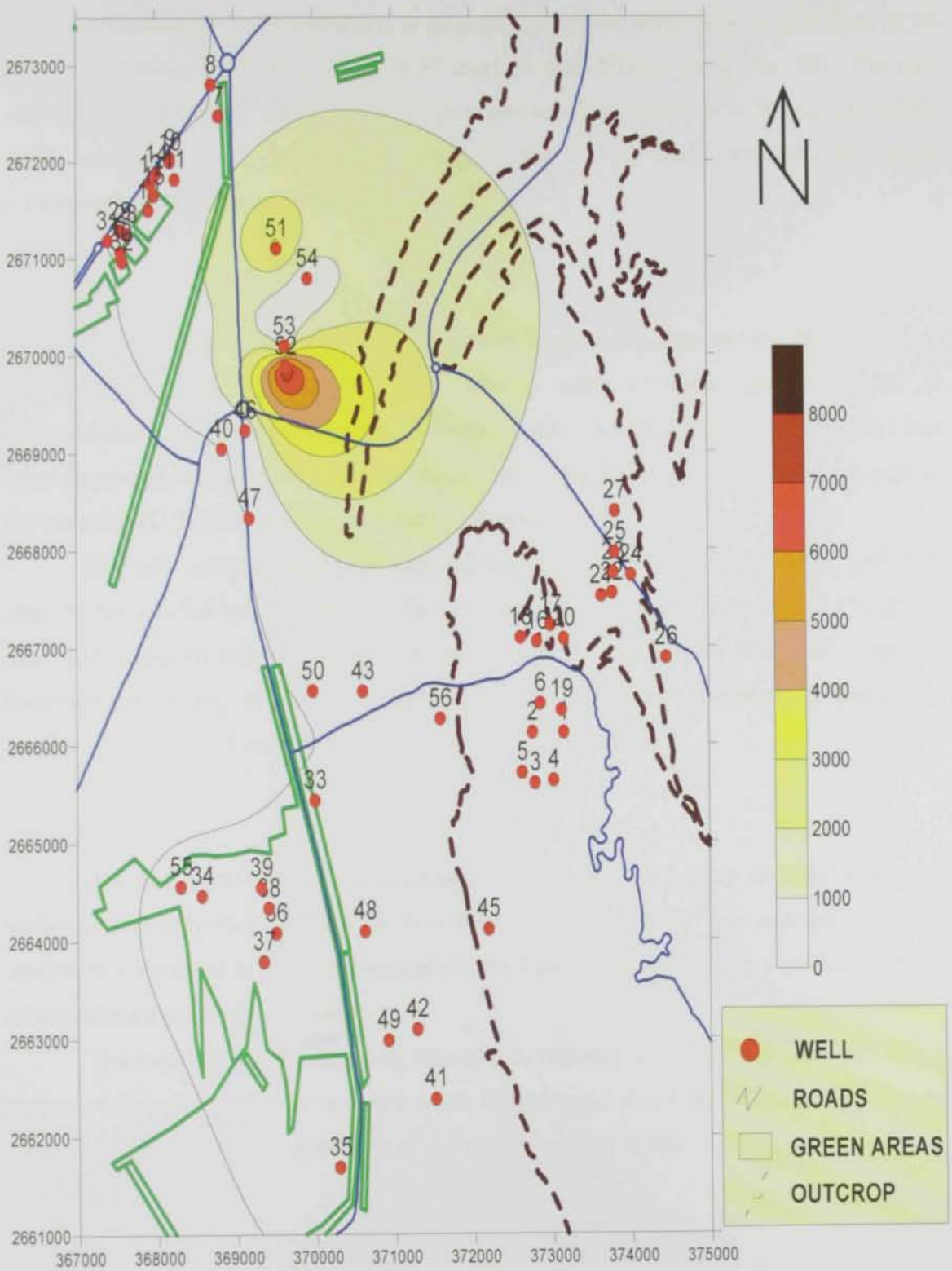

Figure (5.18): Contour Map for (Al) in the study area.

Aluminum ion concentrations in groundwater of the study area ranged from 10.34 µg/l west Neima (well No. 13) to 8.37 mg/l at east Neima (well No. 52). The iso-concentration map (Fig. 5.18) shows a high aluminum concentration in Neima, especially wells number (51, 52, 53 and 55), while in rest of the study area, the aluminum concentrations is less than 90 µg/l.

Iron (Fe)

Igneous rock minerals whose iron content is relatively high include the pyroxenes, the amphiboles, biotite and magnetite. Iron is toxic to some aquatic species at concentrations of 0.32 to 1.00 mg/l. A water quality criterion for iron of 0.3 mg/l has been suggested for domestic uses. For aquatic life, maximum iron content of 1.0 mg/l is the criterion (U.S. Environmental Protection Agency, 1976).

The iron content ranges between 8.2 µg/l at west Neima (well No. 9) and 2.90 mg/l at Ain Bu Sukhanah (well No. 36). Iron iso-concentrations map (Fig. 5.19) shows that high values of iron are encountered at Mubazarah and Ain Bu Sukhanah. The iron concentration is very low in the western side of the study area, because the quaternary aquifer which is the dominant in that area is freely oxygenated.

Zinc (Zn)

Zinc has about the same abundance in crustal rocks as copper or nickel and tends to be substantially more soluble in most types of natural water than are the other two metals. It is essential in plant and animal metabolism, but water is not a significant source of the element in a dietary sense.

The value of zinc in the study area ranges between 2.02 µg/l and 2.28 mg/l. High values of zinc are encountered to the north of Mubzarah and East to Neima. While low zinc concentrations found in the rest of the study area (Fig 5.18).

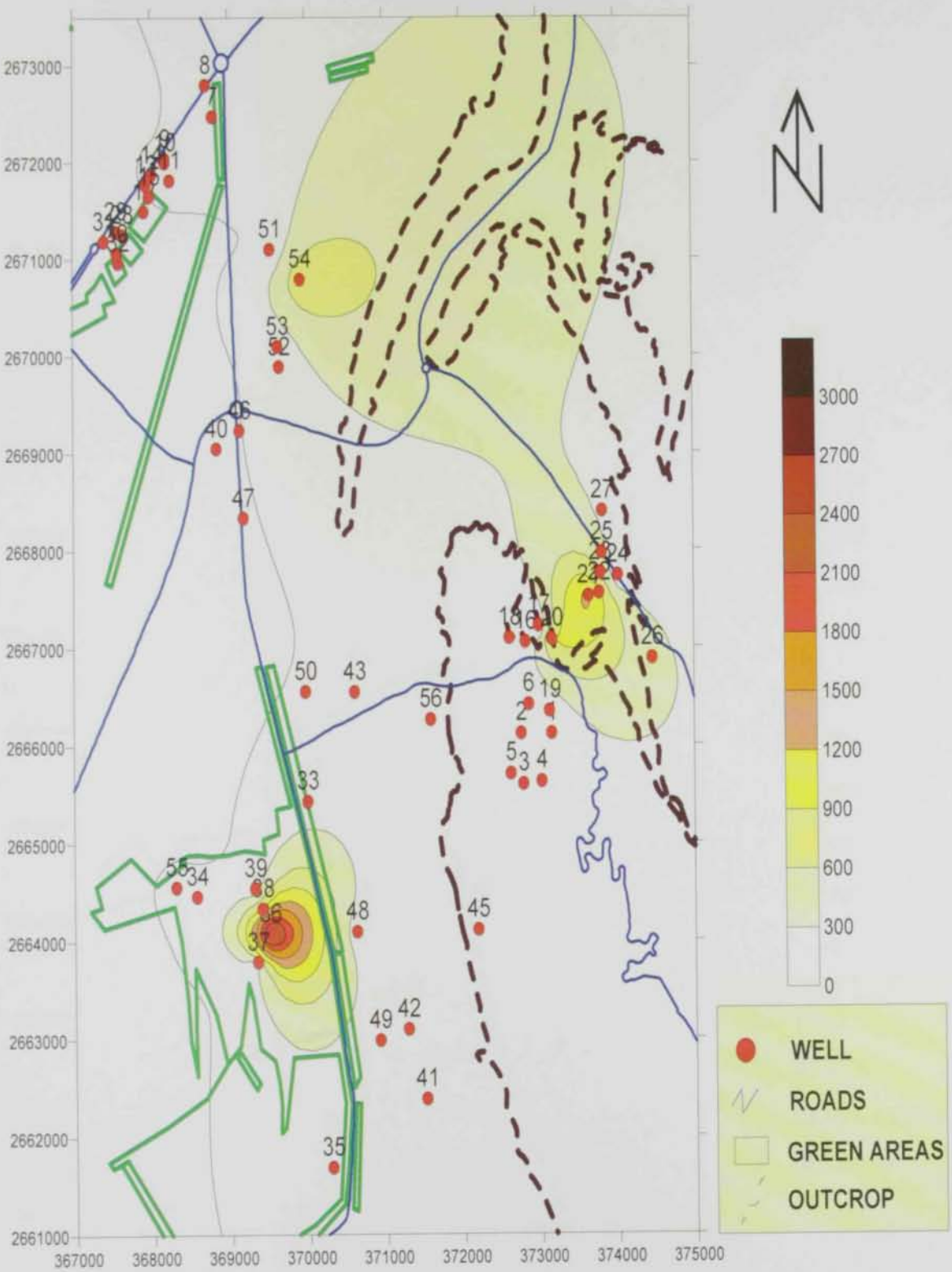

Figure (5.19): Contour Map for Fe in the study area.

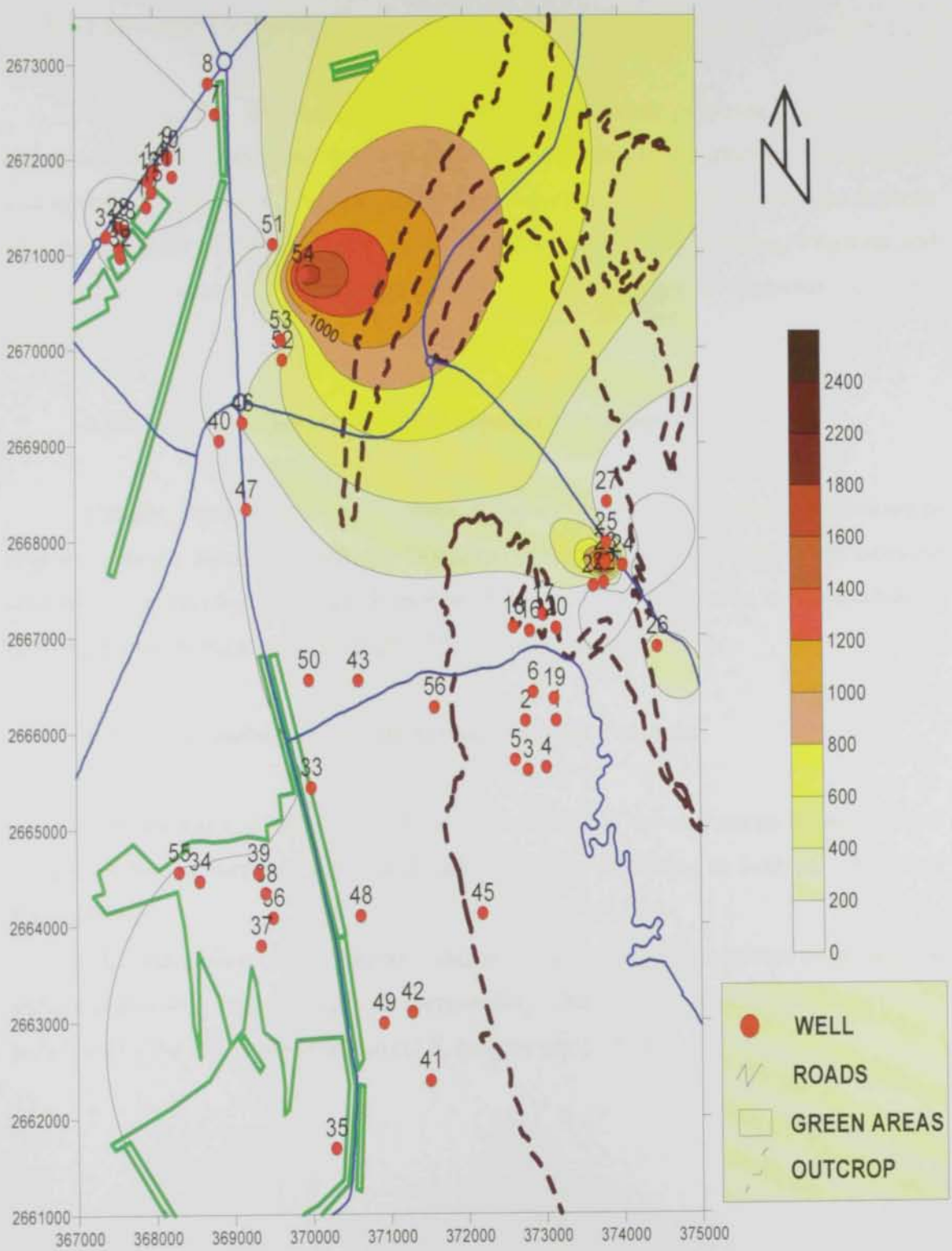

Figure (5.20): Contour Map for Zn in the study area

5.2.3 Groundwater Evaluation

Water quality determines its suitability for different purposes. The following discussion intends to evaluate the suitability of groundwater in the study area to domestic and agricultural purposes. The suitability of groundwater for a particular purpose depends on specific quality criteria. Quality limits of water supplies for drinking, irrigation and industrial uses apply to groundwater because of its extensive development for these purposes (Todd, 1980).

5.2.3.1 Groundwater Quality for Domestic Purposes

Usually, water applied for domestic purposes has certain standard specification as regards to its physical, chemical and biological properties. These standards are intended primarily to protect human health. However, the water in the study area is not suitable for drinking purposes because of the high TDS concentrations.

5.2.3.2 Groundwater Quality for Agricultural Purposes

For evaluation of the suitability of groundwater in the study area for agricultural uses, the effect of water on plants and soil is assessed according to Sodium Adsorption Ratio (SAR).

The sodium-ion concentration is important in classifying irrigation water because sodium reacts with soil to reduce its permeability. The Sodium Adsorption Ratio (SAR) is defined by the following equation (U.S. Salinity staff, 1954):

$$S.A.R = \frac{Na^{+}}{\sqrt{\frac{Ca^{++} + Mg^{++}}{2}}}$$

According to the SAR values (Figure 5.17) and (Table 5.2), the SAR ranged between 1.3 in north-east Mubazarah (well No. 25) and 28.18 at Mubazarah (well No. 18), with a mean value of 14.2. Groundwater in Neima is characterized by limited harmful effect on plants in the north to a moderate harmful effect for plants in the south. In Ain Bu Sukhanah, groundwater can cause moderate to high harmful effects for plants when applied for irrigation. Finally Mubazarah is characterized by groundwater with high to very high damaging risk if it used for irrigation.

Table 5.2 Classification of sodium hazard (Richards, 1969)

Sodium hazard	Value
Low sodium hazard water	Less than 10
Medium sodium hazard water	Between 10 and 18
High sodium hazard water	Between 18 and 26
Very high sodium hazard water	More than 26

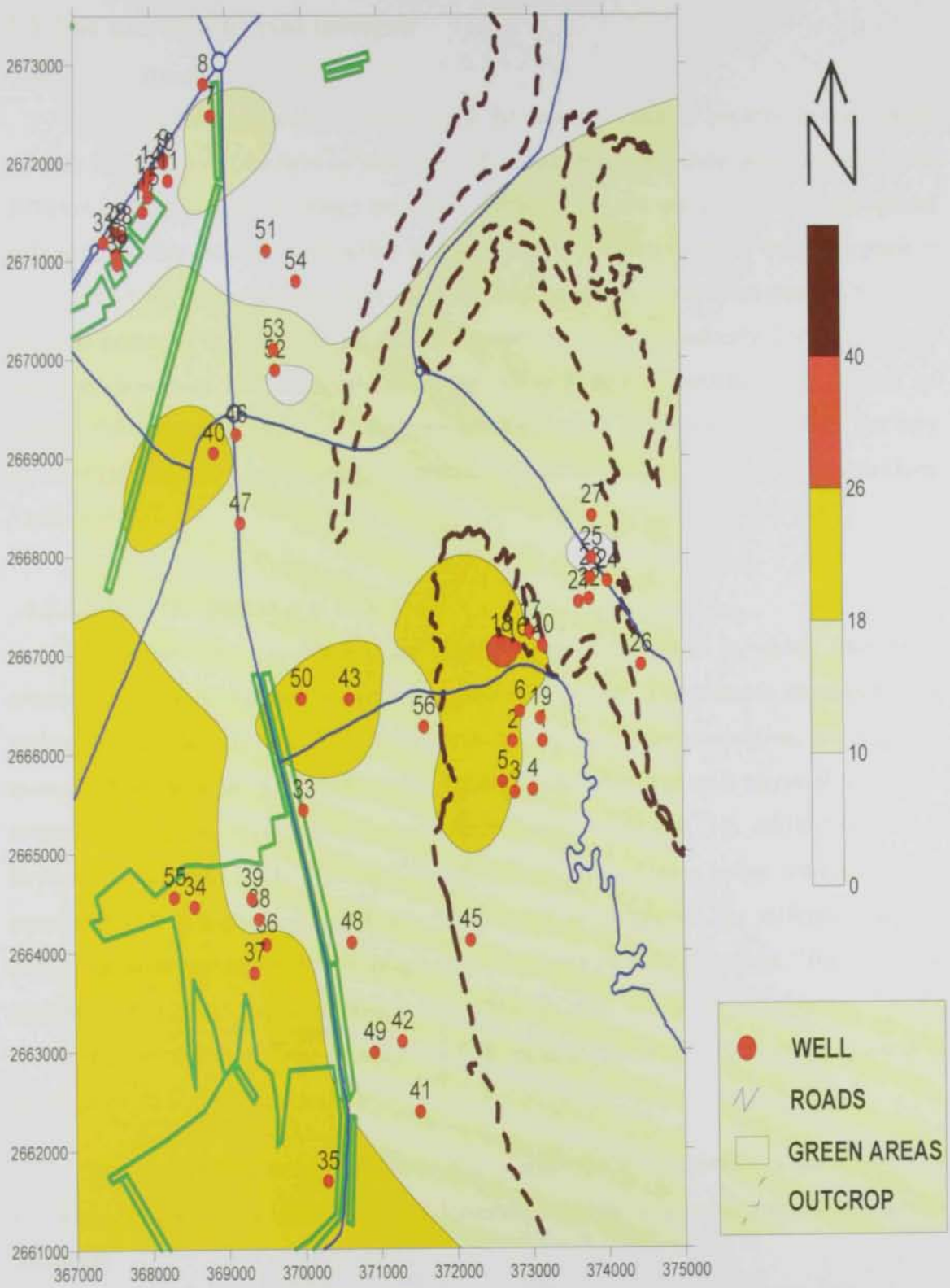

Figure (5.21): Distribution map of the Sodium Adsorption Ratio in the study area.

5.3 The Environmental Isotopes

5.3.1 Introduction

Isotopes of a particular element have the same number of protons in the atomic nucleus but different numbers of neutrons. Thus they have the same atomic number but different atomic weights. Isotopes are called stable if they are not involved in any natural radioactive decay scheme, radioactive if they undergo radioactive decay and radiogenic if they are formed by radioactive decay but do not themselves decay. Radioactive isotopes are used primarily to measure age. Stable isotopes are used to understand the sources of water, or processes that have affected water since it was formed (since it entered an aquifer, for example). Radiogenic isotopes are less widely used in water studies; but they are used primarily for determining the source of specific elements, particularly strontium, (Drever, 1997).

5.3.2 Stable Isotopes of $\delta^{2}H$ & $\delta^{18}O$

Hydrogen and oxygen are the most important elements in which have been observed the natural variations of the isotopic composition. The isotopic composition of hydrogen and oxygen, which are the elements of the water molecules, are variable because their isotopes are fractionated during some chemical and physical processes occurring in nature. Hydrogen has two stable isotopes (^{1}H and ^{2}H), while oxygen has three stable isotopes (^{16}O, ^{17}O and ^{18}O). It is clear that ordinary water molecules have nine different isotopic configurations. The vapor pressures of the different isotopic molecules of water are inversely proportional to their masses, therefore, $^{1}H_2$ ^{16}O has a significantly higher vapor pressure than $^{2}H_2{}^{18}O$. So, water vapor formed by the evaporation of the liquid water is enriched in ^{1}H and ^{16}O, while the remaining water is enriched in ^{2}H and ^{18}O (Drever, 1997).

The isotopic composition of hydrogen is analyzed by the hydrogen gas taken from the water by reduction with Zinc and Uranium at high temperature under a vacuum condition.

$$H_2O + Zn \rightarrow H_2 + ZnO$$

$$2H_2O + U \rightarrow UO_2 + 2H_2 \qquad \text{(IAEA, 1981)}$$

The isotopic composition of oxygen is analyzed through the CO_2 which is in isotopic equilibrium with the water according to the following equation:-

$$C^{16}O_2 + H_2{}^{18}O \rightarrow C^{16}O^{18}O + H_2{}^{16}O \qquad \text{(IAEA, 1981)}$$

The isotopic composition of hydrogen and oxygen are measured on a mass spectrometer with double inlet system and multicollectors system; their values are reported in terms of differences of ^2H / ^1H and $^{18}O/^{16}O$ ratios relative to SMOW (Standard Mean Ocean Water), and are expressed as per mil differences as by the well known symbol "δ^2H ‰ and $\delta^{18}O$ ‰" values. Respectively, positive values of δ^2H and $\delta^{18}O$ indicate enrichment of a sample in ^2H and ^{18}O compared to SMOW, while negative values imply depletion of these isotopes in the sample relative to SMOW (IAEA, 1981).

5.3.2.1 Determination of the δ^2H ‰, $\delta^{18}O$ ‰, and their relationship

For this study, 38 selected groundwater samples were collected from governmental and private active pumping wells. An additional 3 samples were collected from surface water localities in the study area namely, Mubazarah Lake, Ain Bu Sukhanah Lake and the trench well north Ain Bu Sukhanah. The sampled wells are from the fractured limestone, Quaternary alluvial and gypsum aquifers. Groundwater samples were placed in sealed-airtight glass bottles for isotopic analysis.

All samples were collected during February, March and April 2006 for the purpose of this investigation. The spatial distribution of the sampling sites is shown Figure (5.22). Water samples for oxygen isotopic analysis were equilibrated with CO_2 gas at 25°C (Epstein and K. Mayeda, 1953). The CO_2 gas was then cryogenically purified. Water samples for deuterium analysis were reduced to hydrogen gas using metallic zinc (Coleman, et al; 1982) ^2H and ^{18}O contents were determined using a dual-inlet isotope ratio mass spectrometer at the Environmental Isotope Section of the Water Authority of Jordan Laboratories. Both $^2H/^1H$ and $^{18}O/^{16}O$ ratios are expressed in delta values, δ, in units of per mil relative variation with respect to Vienna Standard Mean Ocean Water (VSMOW):

$$\Delta = \frac{1000\,(R_{sample} - R_{standard})}{R_{standard}}$$

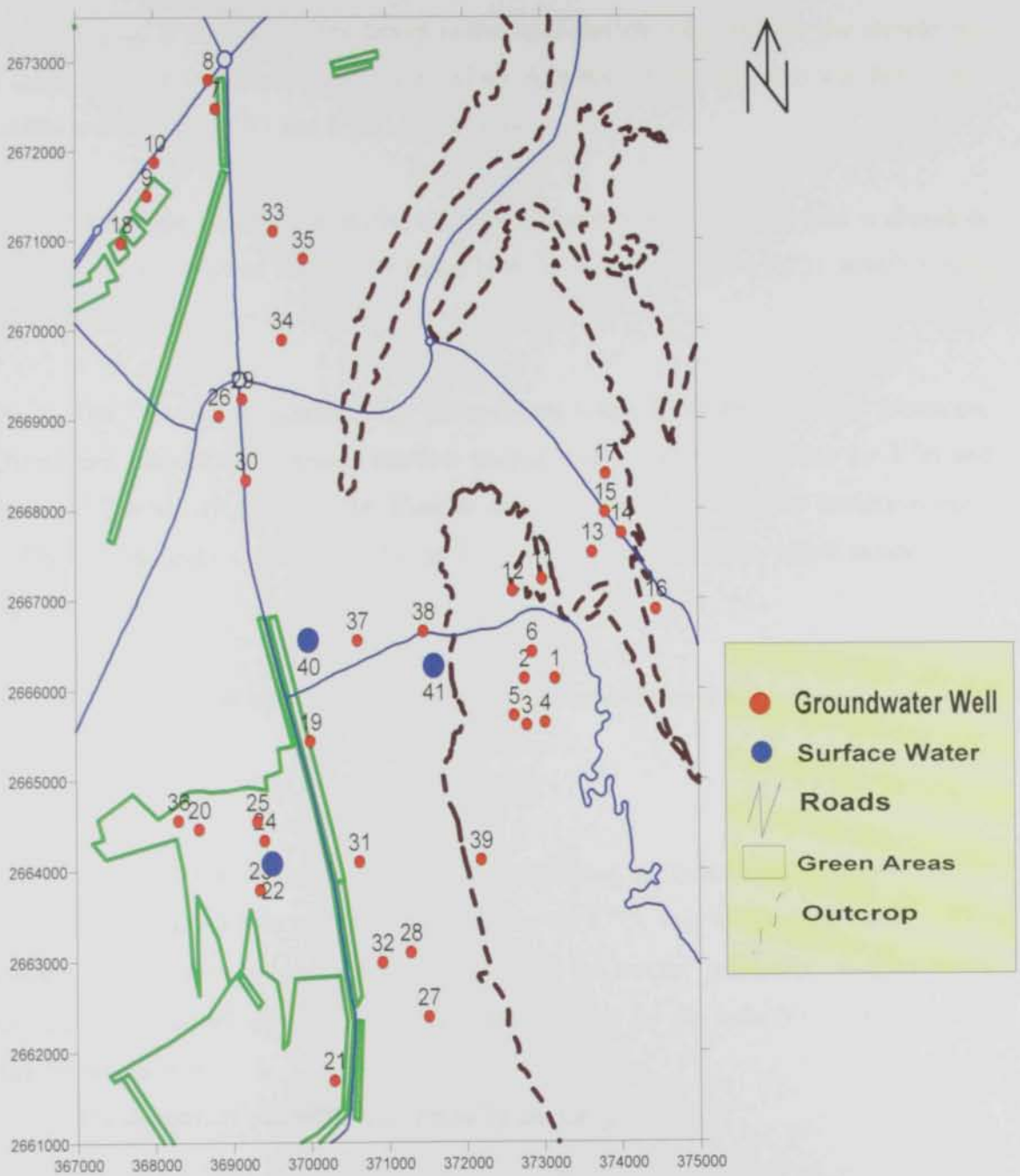

Figure (5.22): Locations of isotopes samples from groundwater wells and surface water.

Where R_{sample} is the ratio of the heavy to the light isotope measured for the sample and $R_{standard}$ is the equivalent ratio for the standard. Analytical reproducibility was better than 0.15‰ and 1‰, for $\delta\ ^{18}O$ and $\delta\ ^{2}H$, respectively.

The stable isotopic composition of the different waters in study area is shown in Appendix B and plotted in the classical δ^2H–$\delta^{18}O$ diagram (Figure 5.23), together with the local meteoric water line LMWL ($\delta^2H = 8\delta^{18}O+15$).

The ^{18}O and ^{2}H contents for groundwater taken from the fractured limestone, Quaternary alluvial and gypsum aquifers ranged from –2.48‰ to 2.06‰ for $\delta^{18}O$ and from –12.7‰ to –10.1‰ for δ^2H. Their arithmetic means and standard deviations are -1.16‰, 1.01‰ and –12.53‰, 2.62‰ for $\delta^{18}O$ and δ^2H respectively, which indicate very high variations.

The local groundwater line (LGWL) for the study area is defined by:

$$\delta^2H = 2.1741\delta^{18}O - 9.9992 \qquad (R^2 = 0.71)$$

The linear correlation means that at equilibrium, the concentration between water and its vapor is about 2 times bigger for δ^2H than for $\delta^{18}O$. This lower slope value (< 8) is connected with the evaporation process, which in nature, generally, happen under nonequilibrium conditions and the isotope fractionation for the ratio ^{18}O / ^{16}O is stronger than for the ratio ^{2}H / ^{1}H.

The deuterium excess is determined by the Craig equation:

$$d = \delta^2H - 2.1741 \times \delta^{18}O$$

The deuterium excess in groundwater ranged from -21.41‰ to 4.51‰ with arithmetic mean and standard deviation of -3.23‰ and 6.04‰, respectively. The distinction of "d" values will give information concerning the origin of vapor masses because the deuterium excess is a parameter which often is associated with evaporation effects (Mook W.G., 2001).

The stable isotopic composition of precipitation is not known for this area, but average stable isotopic composition of meteoric water in UAE is used in this study. In (Figure 5.23), the slope and the intercept values for LGWL are significantly different from those for LMWL indicating that groundwater has undergone considerable evaporation before or during its underground transit. At the Figure (5.23), also shows the "δ" results of the water from the Mubazarah lake; deviates from the LMWL and LGWL, which is taken for the same region. The deviation is resulted from the evaporation process, which is a physical process where the isotopic fractionation occurs (Mook W.G., 2001). The lake water and other water bodies subject to evaporation become enriched in ^{2}H and ^{18}O during the evaporation process.

Referring the results of the isotope ratio measurements on the groundwater samples, it is concluded that isotopic compositions of groundwater, in normal conditions, remains constant with time and that the deuterium excess is less than Craig's value. Also, from the isotopic results of Mubazarah thermal waters (Figure 5.24), seems that $\delta^{18}O$ values are shifted to the positive values compared with local meteoric water from which the thermal springs are derived. The shift is towards $\delta^{18}O$ of the carbonate rocks because at the elevated temperatures at which the oxygen exchange takes place the isotopic fractionation vanishes. The deuterium excess of the thermal spring water, generally, is less than Craig's value. There is no shift for $\delta^{2}H$; this fact reflects that the carbonate rocks contain very little hydrogen which could exchange with the water. The isotope result of the geothermal water indicates that it must be of the "juvenile" water and, probably, contains small amounts of meteoric origin (in sense that Juvenile water has never taken part in the meteoric water cycle). The values for ^{2}H and ^{18}O in Mubazarah area are isotopically light relative to other ground-water samples in the study area, which may reflect recharge on the elevated Jabal.

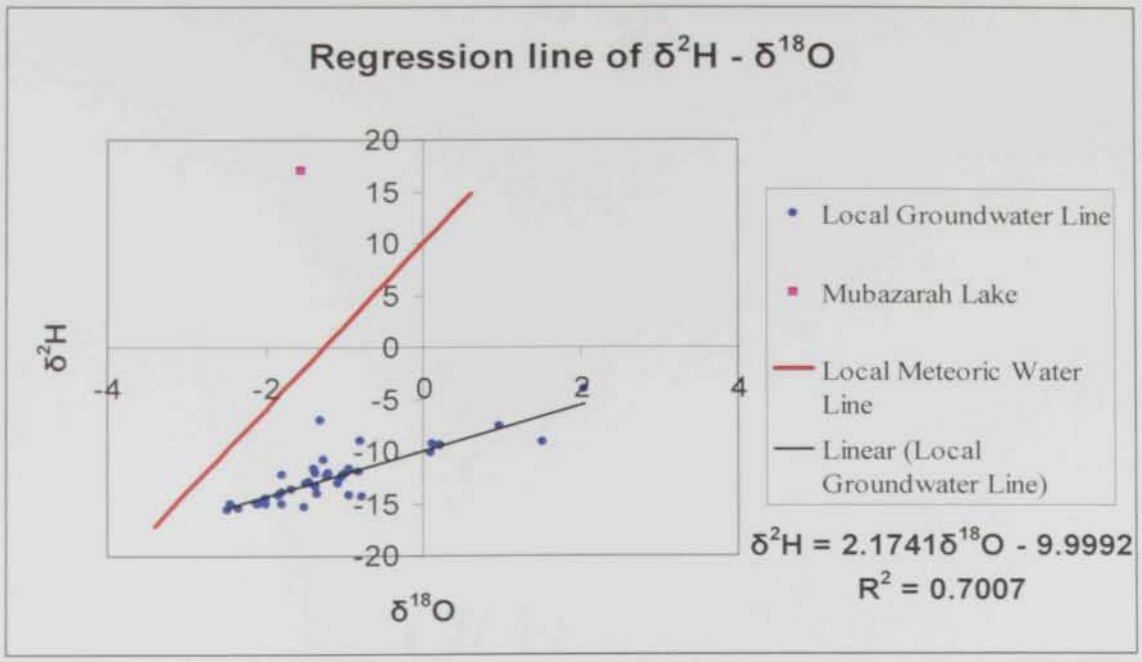

Figure (5.23) Regression line of δ^2H - $\delta^{18}O$ for water samples collected from the study area

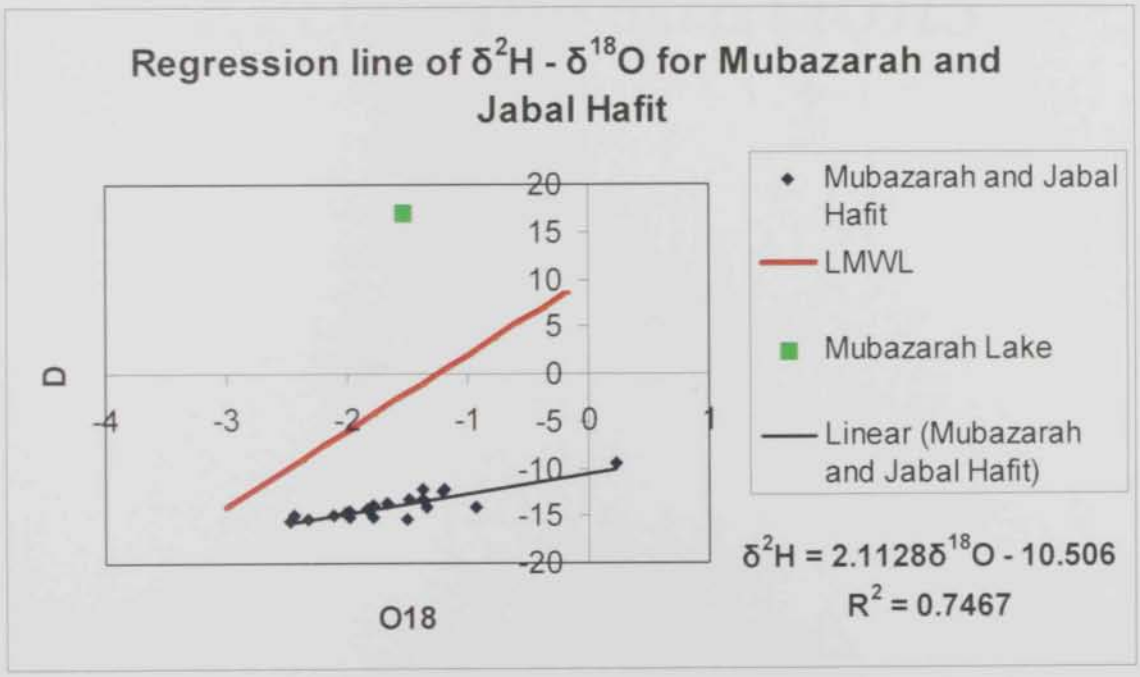

Figure (5.24): Regression line of δ^2H - $\delta^{18}O$ for Mubazarah and Jabal Hafit.

CHAPTER 6
Conclusions and Recommendations

6.1 Conclusions

The following conclusions are based on the literature review, field work, laboratory analysis and office activities conducted during the last three years to study the geology, hydrogeologic systems, hydrogeochemical conditions, the source of thermal water in Mubazarah and the potential effects of pumpage . Based on all the above the following conclusions are made:

6.1.1 Conclusions Based on Climatalogical, Geological and Hydrochemical Studies

I. A detailed assessment of the current water situation in the Emirate shows that the consumption of water continues to increase (currently at 5% annually) and yet the naturally renewable water resources account for only 4% of the total annual water consumption, the remainder being supplied by mining from mostly brackish groundwater resources (79%), the desalination of sea water (17%) and the treatment and re-use of waste water (4%).

II. Groundwater levels continue to fall and have now resulted in the drying up of all the natural falaj systems in Al-Ain, which are now either supported by on site, deep boreholes or imported desalinated water, via long and expensive transmission pipelines. Increasing demands for fresh water in the Eastern Region of the Emirate has resulted in the first inter-emirate transfer of water i.e. the new Fujairah Qidfa desalination plant.

III. Groundwater remains by far the largest source of water and despite its uncontrolled and unregulated use in the past, still accounts for almost 80% of total demands. Given increasing lowering of groundwater levels, and steady trends in increasing salinity, the requirement for its protection and conservation has now reached paramount levels and this issue is currently being addressed at the highest level of government.

IV. Abu Dhabi Emirate's record of treating and re-using both domestic and industrial waste is excellent, with an almost 100% treated and re-use record

in the major cities, but the produced water supplies only 4% of the total consumption.

V. The Hydrogeological situation in the study area is affected by the dominant structural elements, which are north to northwest trending folds associated with northeast-dipping thrust and reverse faults characterized by Jabal Hafit.

VI. The main existing aquifers in study area are Jabal Hafit Limestone aquifer in Mubazarah and eastern Neima, characterized by extensive dolomitization and affected by numerous faults. The Quaternary aquifer, which has minimum thickness on flanks of Jabal Hafit anticline and increases in thickness further west, reaches more than 300 m west of Jabal Hafit, this aquifer is well developed in western Neima. Finally the gypsum aquifer is represented by Ain Bu Sukhanah Spring.

6.1.2 Conclusions Based on Geophysical Studies

In this study, electrical imaging resistivity survey is carried out to investigate the aquifer systems in the study area, the subsurface geology and sequence of strata. Important conclusions of prime concern to the geology and hydrogeology have been derived from the results of this study which can be summarized in the following:-

I. Interpretation of the electrical imaging resistivity profiles indicates the presence of two types of aquifers in the study area. The fractured limestone aquifer in the southeastern and northwestern parts (Mubazarah and east Neima) along the limestone outcrop of Jabal Hafit. The alluvial aquifer that mainly consists of gravel and sand in the eastern part of the study area. However, evidence of the gypsum aquifer which existing in the study area might be intersected by Line-5 at depth of 117 m, this aquifer is overlained by a clay layer, but the horizontal extent of this aquifer is not shown by the model.

II. In Mubazarah, the dissolution of limestone forms a karst aquifer system, characterized by solution channels and caves. The resistivity survey was conducted in this area in order to identify fractured zone with increases porosity. The evidence of faulting as interpreted from modeling of the observed resistivity data is therefore particularly significant since these structures may be the conduits for the thermal fluids.

III. In east Neima (area of the flowing well), the 2-D resistivity results and the water level data suggest that the potential source area(s) for the flowing-well water are the Jabal to the (north/south) east or the area further (north/south) east of the Jabal. The water-level contours clearly indicate a source flowing-well water from the west is not possible.

IV. The thickness of the quaternary alluvial sediments (gravel and sand) is increases in the easterly direction.

V. The salinity of the water bearing formations increases from east to west in the direction of groundwater flow. This is clearly shown by the decreasing of the resistivity values of the profiles towards the west direction.

VI. The boundaries of the aquifers have been estimated and zones with high yield potential have been determined for future development in the area and for choosing the drilling sites.

6.1.2 Conclusions Based on Hydrogeochemical and Environmental Isotopes Studies

I. The total dissolved content of the water shows a general increasing trend from east to west. An area of high total dissolved solids content is encountered in Ain Bu Sukhanah west from Jabal Hafit. This increase of

TDS is attributed to the brine moving upward near Ain Bu Sukhanah. This also attributed to the existence of sabkhas in areas of low elevation west of Jabal Hafit. At locations where the water table is near or at the land surface.

II. The sequence of Cations dominance in groundwater in the study area is in the order of: $Na^{+} > Ca^{2+} > Mg^{+2} > K^{+}$. While the sequence of anions dominance in groundwater in the study area is in the order of: $Cl^{-} > SO_4^{2-} > HCO_3^{2-} > NO_3^{-}$.

III. The presence of celistite ($SrSO_4$) exposures on the eastern side of Jabal Hafit is responsible for the high concentration of Sr in groundwater of the study area.

IV. According to the measured EC and calculated SAR values, groundwater in Neima is characterized by limited harmful effect on plants in the north to a moderate harmful effect for plants in the south. In Ain Bu Sukhanah, groundwater can cause moderate to high harmful effects for plants when applied for irrigation. Finally Mubazarah is characterized by groundwater with high to very high damaging risk if it used for irrigation.

V. Based on the results of the isotope ratio measurements on the groundwater samples, it is concluded that:-

- The values for ^{2}H and ^{18}O in Mubazarah area are isotopically light relative to other groundwater samples in the study area, which may reflect recharge on the elevated Jabal.

- The deuterium excess is less than Craig's value. Also, from the isotopic results of Mubazarah thermal waters, seems that $\delta^{18}O$ values are shifted to the positive values compared with local meteoric water from which the thermal springs are derived. The shift is towards

$\delta^{18}O$ of the carbonate rocks because at the elevated temperatures at which the oxygen exchange takes place the isotopic fractionation vanishes.

- There is no shift for $\delta^{2}H$; this fact reflects that the carbonate rocks do not contain sufficient hydrogen which could exchange with the water. The isotope result of the geothermal water indicates that it must be of the "juvenile" water and, probably, contains small amounts of meteoric origin (in sense that Juvenile water has never taken part in the meteoric water cycle).

6.2 Recommendations

In order to better understand the groundwater resources in the Mubazarah area, and to better explain the flowing-well phenomena, additional work is required. The groundwater resource in the area should be better understood because it is a potential source for aiding in the development of the area (Mubazarah and Ain Bu Sukhanah) as a major tourist destination. The water because of its special characteristics is used to develop a spa and used for enhancing estatic beauty of the area by supporting additional vegetation in the area. Specifically, the following is recommended:

- A large and expensive program of commissioning new desalination plants is required in order to keep up with the increasing demands for drinking water, since the yields of existing potable wellfields is declining.

- A comprehensive water resources database for information regarding well locations, meteorological data, water quality and water levels should be developed. This database should be accessible by researchers and scientists in the different fields of water resources.

- A monitoring system for groundwater levels and quality should be established, maintained and updated.

- A series of wells should be drilled between the flowing well and Mubazarah, the purpose of these wells would be to verify the source area for the flowing well water. Once complete the wells should be included in the monitoring network for the area.

REFERENCES

REFERENCES

1) **Abdelghany, O., (under preparation).** Contribution to the Late Cretaceous/Tertiary Stratigraphy West of the Northern Oman Mountains.

2) **Abou El-Enin H.S., (1993).** Structurally controlled features in Jabal Hafit. Bull. Geog. Soc., Kuwait, V.151, p 1-63.

3) **Abu Dhabi Water & Electric Authority (ADWEA), (2001).** Master Plan for Water System of Abu Dhabi Emirate 2000-2010; Tebodin Final report for ADWEA.

4) **Al Naumi , H.S., (2003).** Hydrogeological and geophysical studies on Al Jaww plain, Al Ain area , United Arab Emirates. M.Sc Thesis, United Arab Emirates University, 4p.

5) **Al-Saiy, A.K., (2002).** Petrology, Geochemistry and Framework of Sedimentation of the Quaternary Aquifer Rocks North of Al-Ain, UAE. M.Sc. Thesis, Faculty of Sciene, Suez Canal University., Egypt.

6) **Alshamsei, M.H., (1993).** Drainage basins and flash flood hazards in Al-Ain area, United Arab Emirates, M.Scthesis, UAE University, UAE.

7) **Alsharhan, A.S., Rizk, Z.A., Nairn, A.E.M., Bakhit, D.W., and AlHajari, S.A., (2001).** Hydrogeology of an Arid Region: The Arabian Gulf and Adjoining Areas, Elsevier, Publishing Company, New York. 331p.

8) **Baghdady, A.R., (1998).** Petrography, mineralogy and environmental impacts of the sand dune fields of the greater Al-Ain area , United Arab Emirates University , PhD.thesis , Faculty of Science, Ain Shams University , Egypt .

9) **Bakhit, D.W.M., (1998).** Environmental and Management problems in hydrology of the United Arab Emirates. Ph.D Thesis. University of South Carolina , Columbia, 407 p.

10) **Barker, R.D., (1981).** The offset system of electrical resistivity sounding and its use with a multicore cable. Geophys. Prosp, v. 29: 128-143.

11) **Brook, M.C., (2003)**, History & Current Status of Municipal Wellfields in the Eastern Region of Abu Dhabi Emirate, 1979-2002. Vol I & 11

12) **Brook, M.C, Al Houqani, H, Dawoud, M., (2005).** The Opportunities for Water Resources Management in the Emirate of Abu Dhabi, United Arab Emirates. In Proceedings of 7th Gulf Water Conference, Kuwait, 2005.

13) **Brook, M.C., (2005)** Development of a Groundwater Monitoring Network for Abu Dhabi Emirate.

14) **Cherif. O.H and El-Deeb. W.Z., (1984).** The Middle Eocene-Oligocene of the northern Hafit area, south Al-Ain city, U.A.E. Geol. Mediterr., 11/2.p207-217.

15) **Coleman, R.G., (1981).** Tectonic setting for ophiolite obduction in Oman. Journal of Geophyiscal Research, V 86. No B4. p 2497-2508.

16) **Coleman, M.L. Shepherd, T.J. Durham, J.J. Rouse, J.E. and Moore, G.R., (1982),** Reduction of Water with Zinc for Hydrogen Isotope Analysis, Anal. Chem., pp. 993–995.

17) **Dahlin,T. and Loke, M.H., (1998).** Resolution of 2D Wenner resistivity imaging as assessed by numerical modelling, Journal of Applied Geophysics, 38, 237-249.

18) **Daily W. and Owen E., (1991).** Crosshole resistivity tomography. Geophysics 56, p 1228–1235.

19) **Dawoud, M.A., Farbridge, R., Wonderen, J. van, Brook, M.C. 7 Al Houqani, H., (2005).** An ARCGIS database for water supply/demand modeling and management in Abu Dhabi Emirate, UAE. *WASTA Seven Gulf Water Conference Proceedings*: Water in the GCC towards integrated Management: 575-592, Kuwait.

20) **Davis, S. N. and De Weist, R. J., (1966).** Hydrogeology. John Wiley and Sons, New York, 108p.

21) **Domenico, P.A., and Schwartz, F.W., (1990).** Physical and chemical hydrology: John Wiley and Sons, New York, 824 p.

22) **Drever, J.L., (1997).** The Geochemistry of Natural Waters: Surface and Groundwater Environments, 3rd ed., Prentice Hall, New Jersey, 436 p.

23) **EAD, (2001).** Abu Dhabi Water Resources Statistics, 2001

24) **EAD, (2002).** Abu Dhabi Water Resources Statistics, 2002

25) **EAD, (2003).** Abu Dhabi Water Resources Statistics, 2003

26) **EAD/Mott Macdonald International (MMI), (2004).** Preliminary Assessment of the Water Situation in the Eastern and Central Regions of Abu Dhabi Emirate.

27) **El-Dougdoug, A., (1993)**, Origin of unconformity-bound celestite minerlization, Jabal Hafit, Al-Ain area, United Arab Emirates: M.E.R.C, Ain Shams University, Earth Science Serr., V.7,pp. 209-222.

28) **El-Shami, F., (1990)**, The hydrogeochemistry of the spring of Ain Bu Sukhanah , U.A.E. Arab Gulf Journal of Scientific Research, V.8 , no. 1, pp 34 -36 .

29) **Embabi, N.S. and El Sharkawy, F.M., (1989)**. Landform systems of the United Arab Emirates from space images. 1st symp. Remote Sens., UAE University, Al-Ain, UAE, p7-28.

30) **Embabi, N.S., (1991)**. Dune types and patterns in the United Arab Emirates using Landsat TM-Data. 24th Intern. Symp. On Remote Sensing of Environment, Rio Dejaneiro, Brazil, p27-31.

31) **Enivronmental Protection Agency., (1976).** Water Quality Criteria, EPA R3 73033, Governmental Printing Office, Washington, D.C.

32) **Epstein, S and Mayeda,K., (1953),** Variation of 18O Content of Waters from Natural Sources, Geochim. Cosmochim. Acta, pp. 213–224.

33) **Garamoon, H.K., (1996).** Hydrogeological and geomorphological studies on the Abu Dhabi-Dubai-Al Ain triangle, UAE. Unpublished Ph.D. thesis, Geol. Dep., Fac. Sci., Ain Shames University, Egypt, 127p

34) **Geoconsult and Bin Ham Well Drilling Establishment (1985).** Project 21/81, Drilling of deep water wells at various locations in the UAE, V3, Ministry of Agriculture and Fisheries. Water and Soil Department. , unpublished report. P87.

35) **Gibb, S.A and partners., (1970) .** Water resources survey, supplement to interim report, subsurface investigation in Al-Ain area: Development and Public works, Abu Dhabi, p 608.

36) **Glennie, K.W., Bouef , M.G.A., Huhger Clarke, M.W., Moody Stuart, M., Pillar, W.F.H. and Reinhardt, B.M., (1974)** . Geology of the Oman Mountains. Koninklijk Nederlands Geol. Genootshap. (Transactions of the Royal Dutch Geological and Mining Soc), p 31-423.

37) **Griffiths D.H. and Barker R.D., (1993).** Two-dimensional resistivity imaging and modeling in areas of complex geology. Journal of Applied Geophysics, 29, 211-226.

38) **Griffiths D.H., Turnbull J. and Olayinka A.I., (1990),** Two-dimensional resistivity mapping with a computer- controlled array. First Break 8, 121-129.

39) **Griffiths, D.H. and Turnbull, J., (1985).** A multi-electrode array for resistivity surveying. First Break 3 (No. 7), 16-20.

40) **GTZ/Dornier Consult/ADNOC,. (2005).** Status Report Phases 1Xa, 1Xb and 1Xc for Groundwater Assessment Project Abu Dhabi.

41) **Hamdan , A.A.,and Anan, H.S., (1989).** The Paleocene tecto-sedimentary events of Jabal Malaqet., East of Al-Ain., West of the Northern Oman Mountains. M.E.R.C., Ain Shams Univ., Earth Sci. Ser., (3), p209-224.

42) **Hamdan,A.A., and El-Deeb, W.Z., (1990).** Stratigraphy of the Paleogene succession of Jabal Malaqet, West of the Northern Oman Mountains., Fac. Sci., UAE University.,(2) p30-39 .

43) **Hamdan , A.A. and Bahr, S.A., (1992).** Lithostratigraphy of the Paleogene succession of northern Jabal Hafit., Al-Ain area., UAE., M.E.R.C., Ain Shams Univ., Earth Sci. Ser., (6) , p201-224 .

44) **Hamdan , A.A.,and Anan, H.S., (1993).** Cretaceous / Tertiary boundary in the United Arab Emirates. M.E.R.C, Ain Shams Univ., Earth Sci. Ser., (7), p 223-231.

45) **Hunting Geology and Geophysics Ltd,. (1979).** Report on mineral survey of the U.A.E., Al-Ain area, V.9, p29.

46) **Hutchinson, C.B., ed., (1996).** Groundwater resources of Abu Dhabi Emirate: U.S. Geological Survey Administrative Report, 136 p., prepared for the National Drilling Company.

47) **HydroConsult,. (1987).** Reconnaissance report and development proposals, Abu Dhabi, (UAE) Eastern Region water resources: Government of Abu Dhabi, Ministry of Petroleum and Mineral Resources report. 126 p.

48) **Imes, J.L., Hutchinson, C.B., Signor, D.C., Tamayo, J.M., Mohamed, F.A., and Hadley, D.G., (1994).** Ground-water resources of the Liwa Crecent area, Abu Dhabi Emirate: U.S. Geological Survey Administrative Report 94-001, 138 p., prepared for the National Drilling Company.

49) **Inman, J.R., Ryu, J. and Ward, S.H. (1973).** Resistivity inversion. Geophysics, v. 38: 1088-1108.

50) **Kastning, E. H., (1977).** Faults as positive and negative influences on ground-water flow and conduit enlargement in Dilamarter, R. R., and Csallany, S. C., editors, Hydrologic problems in karst regions, U. S., Bowling Green, Kentucky, Western Kentucky University, p. 193-201.

51) **Keller G.V. and Frischknecht F.C., (1966).** Electrical methods in geophysical prospecting. Pergamon Press Inc.

52) **Khalifa, M.A,. (1997).** Hydrogeology of the geothermal fractured rock well field at Jabal Hafit, Abu Dhabi Emirate: Proceedings of the Third Gulf Water Confer, Muscat, Sultanate of Oman., pp. 125-140.

53) **Khalifa, M.A,. (2003).** Geohydrology and the source of Flowing well water in Al-Neima area, Al, Abu Dhabi Emirate, UAE. National Drilling Company and United States Geological Survey. p9.

54) **LaBrecque D., Miletto M., Daily W., Ramirez A. and Owen E., (1996).** The effects of 'Occam' inversion of resistivity tomography data.Geophysics 61, p 538–548.

55) **Lippard , S.J., Shelton, A.W.,and Gass, I.G., (1986).** The ophiolite of northern Oman. The Geological Society of London, Memoir no. 11, 178 p.

56) **Li Y.G. and Oldenburg D.W., (1992).** Approximative inverse mapping in DC resistivity problems. Geophysical Journal International 109, p 343–362.

57) **Loke, M.H., (1997).** RES2DINV ver. 3.3 for Windows 3.1, 95, and NT, Advanced Geosciences, Inc., pp. 66.

58) **Loke M.H. and Barker R.D., (1996) a.** Rapid least-squares inversion of apparent resistivity pseudosections using a quasi-Newton method. Geophysical Prospecting, 44, pp 131-152.

59) **Loke M.H. and Barker R.D., (1996) b.** Practical techniques for 3D resistivity surveys and data inversion. Geophysical Prospecting, 44, 499-523.

60) **Loke M.H. and Barker R.D., (1995).** Least-squares deconvolution of apparent resistivity pseudosections. Geophysics 60, 1682–1690.

61) **Maddy, D. V., Editor,. (1993).** Ground-water Resources of Al Ain area, Abu Dhabi Emirate, U. S. Geological Survey Administrative Report 93-001, 332 p.

62) **Matthess, G. (1982).** The properties of groundwater. New York. John Wiley and Sons. 215-255 p.

63) **Meinzer, O.E,. (1923).** The occurrence of groundwater in United States, with discussionof principles: U.S.Geological Survey. Water Supply, p 489.

64) **Ministry of Agriculture and Fisheries,. (1993)**. Climatological data, V 3, 1979-80to 1991-92: Department of Soil and Water, MAF, UAE, 442p.

65) **Mook W.G., (2001).** Environmental Isotopes in the hydrological cycle (Principles and applications),Unesco, Paris 2001.

66) **Mott MacDonald, (2004).** Preliminary Assessment of the Water Situation in the Eastern & Central Regions of Abu Dhabi, Final Report to UAE Offsets Group.

67) **National Atlas of United Arab Emirates, (1993).** UAE University. , Al-Ain., UAE.

68) **NDC & USGS, (1993).** Groundwater Resources of Abu Dhabi Emirate.

69) **NDC & USGS, (1996).** Groundwater Resources of Abu Dhabi Emirate.

70) **Patton, T.L and O'Connor, S.J., (1988).** Cretaceous flexural history of Northern Oman Mountains foredeep., United Arab Emirates ., AAPG Bull., (72)., p797-809

71) **Park S.K. and Van G.P., (1991).** Inversion of pole-pole data for 3-D resistivity structure beneath arrays of electrodes. Geophysics 56, 951–960.

72) **Qanim, A. Hameed and Saef Al-Qaydi., (2001).** Urban development in Al-Ain. Abu Dhabi: Cultural Foundation Publications.

73) **Rizk, Z.S., (1999).** A review article on water resources in the United Arab Emirates. Unpublished Article, Department of Geology, Faculty of Science-Menoufia University, Shebin El Kom, Egypt, 10p.

74) **Rizk, Z.S., and El Etr, H.A., (1997).** Hydrogeology and hydrogeochemistry of some springs in the United Arab Emirates. Arab Jour. Sci. Eng., King Fahd University for Petroleum and Minerals, Dhahran, Saudi Arabia, v.22 (1c), p.95-111.

75) **RSB. (2004).** Regulation and Supervision Bureau for the Water and Electricity Sector in the Emirate of Abu Dhabi. Water Quality Regulations, Document ED/R01/001 (revision 2)

76) **Sasaki Y. (1994).** 3-D resistivity inversion using the finite-element method. Geophysics 59, 1839–1848.

77) **Shima H. (1992).** 2-D and 3-D resistivity imaging reconstruction using crosshole data. Geophysics 55, 682–694.

78) **Shankland and Cox, (1986).**

79) **Smith N.C. and Vozoff K. (1984).** Two-dimentional DC resistivity inversion for dipole-dipole data. IEEE Transactions on Geoscience and Remote Sensing, GE - 22, 21-28.

80) **Stable Isotope Hydrology, Deuterium and Oxygen-18 in the Water Cycle, (1981).** Technical Reports Series No. 210, IAEA, Vienna, Austria.

81) **Stringfield, V. T., and Le Grand, H. E., (1966).** Hydrology Of limestone terrains in the coastal plain of the southeastern United States: U. S.; Geological society of America, Special paper, v. 93, 45 p.

82) **Todd, D.K., (1980).** Groundwater hydrology: John Wiley and Sons, Icn., New York, U.S.A., 535 p.

83) **Toth, D.K., (1980).** A theoritical analysis of groundwater flow in small drainage basins: J.Geophysics .Res. 68 .p4795 - 4812.

84) **U. S. Salinity Laboratory Staff, (1954).** Diagenesis and improvement of saline and alkali soils: U. S. Dept. Adri., Agricultural Handbook no. 60, pp. 60-160.

85) **Warburton, J., Burnhill, T.J., Garham , R.H., and Isaac, K.P., 1990 .** The evolution of the Oman Mountains forland basin . In Robertson, A.H.F., Searle. M.P., and Ries, A.C.(edits). The Geology and tectonics of the Oman Region. Geol .Soc. London Spec. Publ., V.49, p419-427.

86) **Warrak, M., 1987**. Synchronous deformation of neoautochthonous sediments of the Northern Oman Mountains, 5th Conf. SPE., Bahrain, p129-136.

87) **Whittle, G.L., and Alsharhan, A.S . (1994).** Dolomitization and Certification of the Early Eocene Rus Formation in Abu-Dhabi, UAE sed. Geol., V.92. p273-285

88) **White, W. B., (1977),** Conceptual models for carbonate aquifers: Revisited in Dilamarter, R. R., and Csallany, S. C., editors, Hydrologic problems in karst regions, U. S., Bowling Green, Kentucky, Western Kentucky University, p. 176-187

89) **WHO (World Health Organization), (1971)**. International standards for drinking water, 3rd edition: Geneva, Swizerland.

90) **Woodward, D.G., and Menges, C.M., (1991)**, Application of uphole data from petroleum seismic surveys to ground water investigations, Abu Dhabi, United Arab Emirates. Geoexploration,.V.27 , p193-212 .

APPENDICES

			Results (mg/l)							Results (mg/l)																				
Sample ID	North	East	CO3-2	HCO3-	Cl-	NO3-	Br-	SO4-2	PH	Ca	K	Mg	Na	Sr	B	Al	As	Ba	Cd	Co	Cr	Cu	Fe	Mn	Mo	Ni	P	Pb	V	Zn	SiO2
1	2666116	373162	ND	111.80	3089.00	3.22	17.80	495.00	ND	565.74	465.00	157.00	1584.90	13.81	0.92	40.34	ND	56.43	ND	ND	ND	ND	61.17	ND	ND	ND	ND	ND	7.53	2.58	ND
2	2666116	372769	ND	120.00	4130.00	9.69	24.20	841.00	ND	668.85	77.56	196.75	2214.00	14.77	1.27	34.87	ND	55.56	ND	ND	ND	ND	9.73	ND	ND	ND	ND	ND	10.12	78.98	ND
3	2665601	372797	ND	109.80	4494.00	2.37	22.30	690.50	ND	673.88	74.06	176.07	1933.00	15.45	1.10	42.22	ND	59.64	ND	ND	ND	ND	40.90	19.60	ND	ND	ND	ND	8.19	ND	ND
4	2665628	373032	ND	109.80	3755.00	5.79	18.50	528.80	ND	600.30	63.68	142.26	1677.90	15.22	1.03	40.18	ND	60.52	ND	ND	ND	ND	86.62	ND	ND	ND	ND	ND	12.80	6.80	ND
5	2665707	372635	8.00	122.00	5480.00	39.10	22.90	1418.00	ND	777.05	97.24	265.23	2745.60	15.03	1.69	42.19	ND	48.68	ND	ND	ND	ND	123.60	6.64	ND	ND	ND	ND	6.84	ND	ND
6	2666412	372868	ND	122.00	6212.00	11.70	18.80	1471.00	ND	701.12	80.85	245.26	2219.50	15.22	1.70	27.81	ND	47.85	ND	ND	ND	ND	27.79	ND	ND	8.27	ND	ND	8.04	4.38	ND
7	2672475	368809	ND	337.50	1811.00	47.90	2.56	3512.00	ND	299.33	71.57	323.40	1686.90	8.30	4.06	48.16	ND	20.38	ND	ND	7.67	ND	37.89	ND	ND	18.03	ND	ND	5.27	3.05	ND
8	2672800	368718	ND	252.10	444.00	33.20	ND	1171.00	ND	150.91	26.34	232.67	477.54	6.39	1.39	18.56	ND	44.29	ND	ND	15.97	ND	23.71	ND	ND	10.40	ND	ND	3.18	ND	ND
9	2672040	368196	ND	276.50	430.00	24.20	ND	1001.00	ND	155.42	29.77	258.55	515.62	6.95	1.26	18.51	ND	49.31	ND	ND	19.00	ND	8.20	ND	ND	9.20	ND	ND	3.68	3.45	ND
10	2672002	368196	ND	268.40	558.00	34.90	0.98	1346.00	ND	123.31	25.68	219.85	424.53	5.67	1.14	19.04	ND	60.35	ND	ND	20.85	ND	51.92	ND	ND	9.17	ND	ND	3.27	61.03	ND
11	2671817	368257	ND	317.20	1192.00	43.30	2.71	2250.00	ND	352.89	48.99	398.90	1110.70	9.20	1.89	17.81	ND	42.20	ND	ND	11.14	ND	ND	ND	ND	11.31	ND	ND	3.77	93.56	ND
12	2671498	367925	ND	317.20	976.00	64.90	1.18	2298.00	ND	351.32	48.31	391.98	914.69	9.16	2.06	19.33	ND	27.88	ND	ND	12.19	ND	ND	ND	ND	12.19	ND	ND	3.65	ND	ND
13	2671773	367950	ND	290.80	615.00	36.00	1.10	1382.00	ND	150.36	28.28	239.26	480.42	5.92	1.34	10.34	ND	56.85	ND	ND	17.38	ND	ND	ND	ND	9.40	ND	ND	3.30	4.55	ND
14	2671875	368023	ND	292.80	492.00	27.40	ND	1084.00	ND	203.60	32.70	276.73	588.81	7.07	1.42	14.11	ND	46.78	ND	ND	15.93	ND	ND	ND	ND	10.95	ND	ND	3.35	4.65	ND
15	2671651	367991	ND	305.00	720.00	55.20	1.11	1704.00	ND	261.72	389.02	329.65	726.42	8.07	1.71	17.93	ND	33.59	ND	ND	15.39	ND	ND	ND	ND	10.95	ND	ND	3.03	12.39	ND
16	2667049	372828	ND	154.53	7198.00	50.98	24.50	2315.00	ND	987.97	107.25	427.91	4113.90	17.68	3.57	51.62	ND	34.68	ND	ND	5.80	ND	42.89	ND	ND	ND	ND	ND	ND	24.31	ND
17	2667217	373001	ND	113.87	3110.00	ND	ND	698.00	ND	522.34	43.81	191.21	1685.00	13.46	1.31	36.79	ND	58.59	ND	ND	ND	ND	22.81	ND	ND	ND	ND	ND	4.70	14.79	ND
18	2667089	372621	ND	150.47	7130.00	67.00	20.10	2620.00	ND	981.42	105.54	493.11	4335.60	19.88	4.32	30.23	ND	6.22	ND	ND	7.66	ND	51.58	ND	ND	7.00	ND	ND	ND	30.57	ND
19	2666346	373136	ND	113.87	2416.00	1.19	10.80	498.00	ND	520.86	42.10	120.30	1389.80	13.21	1.29	42.91	ND	58.75	ND	ND	ND	ND	88.43	ND	ND	ND	ND	ND	ND	3.63	ND
20	2667077	373169	ND	126.07	3550.00	9.05	23.90	931.00	ND	665.40	60.49	213.28	2110.00	14.16	1.65	53.76	ND	44.36	ND	ND	ND	ND	932.00	ND	ND	ND	ND	ND	ND	142.78	ND
21	2667516	373648	ND	101.67	2975.00	3.37	16.97	571.50	ND	507.90	59.60	156.61	1424.10	13.47	1.28	65.00	ND	62.32	ND	ND	ND	ND	1354.10	22.24	ND	10.28	ND	ND	ND	4.77	ND
22	2667546	373785	ND	105.73	2895.00	7.44	16.60	533.50	ND	497.80	54.50	150.51	1432.00	14.25	1.25	32.87	ND	59.18	ND	ND	ND	ND	ND	ND	ND	ND	ND	ND	ND	69.10	ND
23	2667755	373802	ND	113.87	2675.00	0.72	15.90	544.00	ND	544.94	61.10	153.55	1464.20	14.10	1.27	30.51	ND	57.32	ND	ND	ND	ND	ND	ND	ND	ND	ND	ND	ND	2277.00	ND
24	2667728	374026	ND	113.87	2998.50	0.08	16.97	568.00	ND	574.64	60.52	148.88	1416.40	14.00	1.07	35.01	ND	43.97	ND	ND	ND	ND	36.22	ND	ND	ND	ND	ND	ND	118.45	ND
25	2667960	373818	ND	113.87	2830.00	4.08	15.60	557.00	ND	584.28	64.57	143.56	137.80	13.90	1.10	19.32	ND	62.13	ND	ND	ND	ND	ND	ND	ND	ND	ND	ND	ND	194.44	ND
26	2666881	374464	ND	113.87	2997.50	4.85	15.20	633.00	ND	618.21	61.35	158.74	1607.10	13.98	1.20	24.63	ND	55.51	ND	ND	ND	ND	ND	ND	ND	ND	ND	ND	ND	284.10	ND
27	2668387	373827	ND	122.00	3205.00	10.18	15.31	705.00	ND	627.46	68.33	187.15	1706.00	15.31	1.43	29.36	ND	61.86	ND	ND	ND	ND	ND	ND	ND	ND	ND	ND	ND	98.60	ND
28	2671255	367641	ND	378.20	1003.00	88.25	ND	3371.00	ND	439.10	51.70	587.01	1009.50	9.67	2.20	22.54	ND	36.20	ND	ND	ND	ND	ND	ND	ND	ND	ND	ND	ND	6.82	ND
29	2671288	367561	ND	337.53	845.00	70.40	4.58	2809.00	ND	324.27	47.99	434.13	839.59	9.61	1.73	23.32	ND	28.28	ND	ND	13.74	ND	ND	ND	ND	ND	ND	ND	ND	61.95	ND
30	2671064	367571	ND	325.33	1305.00	95.50	1.72	4190.00	ND	479.80	61.54	588.02	1196.90	11.95	2.26	27.11	ND	23.66	ND	ND	7.90	ND	ND	ND	ND	17.97	ND	ND	ND	ND	ND
31	2671185	367407	ND	260.27	500.00	27.90	ND	1835.00	ND	250.83	32.79	250.56	386.54	7.14	1.38	17.28	ND	52.35	ND	ND	14.42	ND	ND	ND	ND	12.63	ND	ND	ND	9.32	ND
32	2670967	367592	ND	317.20	900.00	72.96	1.21	2810.00	ND	367.66	51.85	476.36	858.23	10.41	2.17	21.00	ND	34.68	ND	ND	10.94	ND	ND	ND	ND	14.71	ND	ND	ND	20.43	ND
33	2665432	370005	ND	235.87	4999.00	17.20	18.80	1712.00	ND	866.49	63.24	269.79	2275.40	18.39	2.19	33.00	ND	33.00	ND	ND	ND	ND	ND	ND	ND	ND	ND	ND	ND	2.02	30.38
34	2664459	368572	ND	142.33	9420.00	ND	56.60	1746.00	ND	1812.80	179.54	673.65	4927.30	48.70	3.44	70.86	ND	24.38	ND	ND	ND	ND	25.02	45.08	ND	ND	ND	ND	ND	6.15	25.37
35	2661682	370294	ND	122.00	3140.00	ND	30.00	6280.00	ND	1764.40	124.90	443.77	3824.80	67.28	1.26	49.49	ND	50.59	ND	ND	ND	ND	138.93	ND	ND	ND	ND	ND	ND	17.66	25.75
36	2664078	369508	ND	211.47	9995.00	ND	45.90	1415.00	ND	1650.90	131.28	543.45	4116.00	68.31	2.57	49.83	ND	28.68	ND	11.81	ND	ND	2902.60	1551.00	ND	ND	ND	ND	ND	7.24	48.43
37	2663788	369350	ND	93.53	4970.00	ND	10.80	1960.00	ND	1318.30	115.11	434.93	3698.20	16.82	3.04	35.22	ND	4.67	ND	ND	ND	ND	247.22	63.91	ND	ND	ND	ND	ND	104.93	19.70
38	2664332	369412	ND	207.40	10000.00	ND	47.70	1930.00	ND	1676.30	1656.80	5172.80	4953.50	48.76	3.09	61.74	ND	40.85	ND	ND	ND	ND	888.70	150.67	ND	ND	ND	ND	ND	12.63	37.90
39	2664541	369320	ND	178.93	7798.00	ND	38.80	1687.00	ND	1502.00	131.60	4829.10	4218.00	54.02	3.10	51.62	ND	ND	ND	ND	ND	ND	151.13	120.36	ND	ND	ND	ND	ND	5.44	44.59
40	2669045	368848	ND	353.80	2385.00	19.00	3.58	3990.00	ND	300.88	79.02	364.43	2633.80	8.98	4.21	19.73	ND	12.11	ND	ND	ND	ND	ND	ND	ND	ND	ND	ND	ND	3.59	41.53
41	2662381	371516	ND	89.47	4485.00	5.94	24.10	825.00	7.05	968.88	99.10	247.15	2114.20	32.93	1.11	47.73	ND	60.38	ND	ND	ND	ND	33.79	ND	ND	ND	ND	ND	ND	55.97	ND
42	2663094	371288	ND	105.73	4010.00	4.31	25.10	911.00	6.96	970.80	97.22	251.12	2129.30	32.94	1.18	51.66	ND	56.91	ND	ND	ND	ND	18.58	ND	ND	ND	ND	ND	ND	89.24	ND
43	2666546	370619	ND	183.00	4610.00	19.70	22.30	2130.00	7.01	942.00	122.30	325.31	2822.70	29.46	2.11	62.57	ND	28.79	ND	ND	35.88	ND	ND	ND	ND	ND	ND	ND	ND	28.33	ND
44	2666646	371469	ND	187.07	3500.00	9.51	19.70	1750.00	7.00	900.69	97.75	266.74	2192.90	15.53	1.68	53.82	ND	31.85	ND	ND	ND	ND	ND	ND	ND	ND	ND	ND	ND	38.45	ND
45	2664112	372200	ND	65.07	4580.00	2.70	27.20	1420.00	6.45	877.21	96.91	284.67	2322.30	15.43	1.32	82.98	ND	62.29	ND	ND	ND	ND	63.55	ND	ND	ND	ND	ND	ND	11.72	ND
46	2669233	369146	ND	471.73	1130.00	64.00	1.00	2430.00	7.51	131.84	79.39	187.40	1123.50	5.31	2.03	16.77	ND	13.43	ND	ND	ND	ND	ND	ND	ND	ND	ND	ND	ND	221.67	ND
47	2668331	369193	ND	520.53	860.00	61.00	2.00	940.00	7.40	110.69	67.61	190.85	879.80	6.51	1.41	19.56	ND	21.72	ND	ND	ND	ND	ND	ND	ND	ND	ND	ND	ND	24.60	ND
48	2664095	370632	ND	105.73	3715.00	4.50	23.00	770.00	7.20	839.98	89.60	213.04	1846.40	16.36	1.09	84.12	ND	53.31	ND	ND	ND	ND	111.75	ND	ND	ND	ND	ND	ND	83.61	ND
49	2662982	370921	ND	105.73	3725.00	4.50	20.50	825.00	7.14	842.43	87.45	218.24	1826.50	16.47	1.09	61.82	ND	49.38	ND	ND	ND	ND	116.31	ND	ND	ND	ND	ND	ND	125.43	ND
50	2666553	369984	ND	248.07	3150.00	5.00	10.00	1815.00	7.26	668.81	107.88	338.71	2405.00	15.12	1.91	39.45	ND	19.27	ND	ND	ND	ND	ND	ND	ND	ND	ND	ND	ND	34.35	ND
51	2671104	369546	ND	203.33	620.00	5.50	1.50	3085.00	6.80	756.31	41.77	336.18	580.18	8.60	1.01	3309.70	ND	20.86	ND	ND	ND	ND	29.62	20.34	ND	ND	ND	ND	ND	9.92	ND
52	2669890	369660	ND	248.07	1195.00	27.00	2.00	3040.00	6.96	486.57	53.75	219.72	885.83	8.21	1.40	8365.60	ND	23.52	ND	ND	ND	ND	107.75	ND	ND	ND	ND	ND	ND	424.18	ND
53	2670099	369640	ND	390.40	1166.00	10.60	2.40	1948.00	7.45	160.72	69.84	196.66	1097.40	5.42	1.62	20.44	ND	21.32	ND	ND	ND	ND	107.17	47.05	ND	ND	32.73	ND	ND	24.90	ND
54	2670793	369936	ND	252.13	722.00	21.20	1.20	1836.00	7.11	332.89	47.79	179.56	743.27	7.62	1.33	164.37	ND	24.05	ND	ND	ND	ND	857.02	56.94	ND	ND	ND	ND	ND	1802.30	ND
55	2664554	368307	8.00	89.47	4060.00	23.40	28.00	1465.00	7.66	1244.10	152.87	415.80	3595.40	19.39	2.06	97.42	ND	27.66	ND	ND	ND	ND	56.28	17.41	ND	ND	ND	ND	ND	3.01	ND
56	2666261	371601	ND	113.87	3800.00	8.20	19.80	1100.00	7.60	823.66	90.73	259.15	2076.10	14.57	1.21	43.15	ND	61.04	ND	ND	ND	ND	16.97	ND	ND	ND	ND	ND	ND	3.80	ND

APPENDIX B

Sample N	Stable Isotopes		Type of	CO-Ordinates		Location
	δD‰	δO18	Sample	Longtitude	Latitude	
1	-15.01	-2.44	Water Well	2666116	373162	Almubazara (Well # 16)
2	-14.68	-2.01	Water Well	2666116	372769	Almubazara (Well for Children Swimming Pool)
3	-15.65	-2.48	Water Well	2665601	372797	Almubazara (Well # 13)
4	-15.45	-2.33	Water Well	2665628	373032	Almubazara (Well in Resort Area)
5	-13.16	-1.49	Water Well	2665707	372635	Almubazara (Well # 12)
6	-14.26	-1.83	Water Well	2666412	372868	Almubazara (Well # 10)
7	-11.7	-1.39	Water Well	2672475	368809	Mohier Ali House (Zakher)
8	-12.21	-1.79	Water Well	2672800	368718	Abdullah S,Alkhaili House (Zakher)
9	-7.05	-1.29	Water Well	2671498	367925	Fadel Alshamsi Farm
10	-10.83	-1.25	Water Well	2671875	368023	Mohd Alamri Farm
11	-13.95	-1.78	Water Well	2667217	373001	Almubazara (Well # 24)
12	-9.5	0.23	Water Well	2667089	372621	Almubazara (Well # 19)
13	-15.09	-1.98	Water Well	2667516	373648	Almubazara (Behind President Palace)
14	-14.89	-2.12	Water Well	2667728	374026	Opposite Almubazara (well # 3)
15	-15.09	-1.99	Water Well	2667960	373818	Opposite Almubazara (well # 6)
16	-14.45	-1.99	Water Well	2666881	374464	Opposite Almubazara (well # 2)
17	-15.12	-1.79	Water Well	2668387	373827	Opposite Almubazara (well # 8)
18	-11.66	-0.93	Water Well	2670967	367592	Zakher Farms
19	-12.14	-0.97	Water Well	2665432	370005	Al-Ain Alfaida
20	-9.36	0.12	Water Well	2664459	368572	Al-Ain Alfaida (Protective Area)
21	-15.03	-2.09	Water Well	2661682	370294	Al-Ain Alfaida (Towards Al-Wagan)
22	-10.17	0.11	Surface Pool	2664078	369508	Al-Ain Alfaida (Duck lake)
23	-12.55	-1.03	Water Well	2663788	369350	Al-Ain Alfaida
24	-9.17	1.53	Water Well	2664332	369412	Al-Ain Alfaida
25	-4.13	2.06	Water Well	2664541	369320	Al-Ain Alfaida
26	-13.02	-1.45	Water Well	2669045	368848	House in Neima
27	-13.73	-1.67	Water Well	2662381	371516	Jebel Hafeet (Well # 5)
28	-13.34	-1.37	Water Well	2663094	371288	Jebel Hafeet (Well # 4)
29	-12.15	-1.19	Water Well	2669233	369146	Forrest opposite Al-Ain Alfaida
30	-11.98	-0.82	Water Well	2668331	369193	Flowing Well (Resistivity Profile # 1)
31	-7.61	0.98	Water Well	2664095	370632	Beside Zayed Center for New Muslims
32	-12.3	-1.02	Water Well	2662982	370921	Beside Zayed Center for New Muslims
33	-12.43	-1.21	Water Well	2671104	369546	Almubazara
34	-15.31	-1.51	Water Well	2669890	369660	Almubazara (Beside Resistivity Profile # 3)
35	-14.11	-1.34	Water Well	2670793	369936	Bottom of Jabel Hafeet
36	-12.16	-1.37	Water Well	2664554	368307	Beside Basco Factory
37	-14.33	-0.77	Water Well	2666546	370619	House in Neima
38	-13.09	-1.08	Water Well	2666646	371469	House in Neima
39	-14.19	-0.94	Water Well	2664112	372200	Forrest opposite Al-Ain Alfaida
40	-8.95	-0.79	Surface Pool	2666553	369984	Trench in Al-Ain Alfaida (Surface Water)
41	17	-1.54	Surface Pool	2666261	371601	Almubazara (Surface Water)

وبناءاً على الدراسات الحقلية و المعملية و المكتبية على المنطقة، يمكن تلخيص نتائج الدراسة الحالية في النقاط التالية:

- تتكون الظواهر الأساسية في منطقة العين من الجبال و السهول و الكثبان الرملية.
- تمثل الصخور في منطقة الدراسة العصور الممتدة من عصر الأيوسين إلى العصر الحديث، حيث أن مكاشف الصخور الجيرية المتكسرة يمكن رؤيتها في تركيب جبل حفيت. كما أن معظم المنطقة مغطاة برسوبيات العصر الرباعي
- وجود ثلاثة أنواع من الخزانات المائية في المنطقة، الأول موجود في منطقة الميزرة وشرق منطقة النعمة على الحدود الغربية لجبل حفيت ويتكون من الصخور الجيرية المتكسرة من عصر الأيوسين حيث أنه يمثل خزان جيد للمياه الجوفية في تلك المنطقة. الثاني موجود إلى الغرب من منطقة النعمة ويتكون من ترسبات العصر الرباعي ويزيد سمك هذا الخزان في الاتجاه الغربي ، وأخيراً رسوبيات الجبس ممثلة في منطقة العين الفايضة.
- المياه الجوفية الموجودة في المنطقة غير صالحة للشرب وذلك لارتفاع ملوحتها ووجود الترسبات العالقة و علو تراكيز العناصر الكيميائية فيها، وذلك نتيجة للمياه المالحة الموجودة في تكوين جبل حفيت وتفاعلها مع الصخور الموجودة في المنطقة، ونتيجة أيضا لعوامل التبخر.
- المياه الجوفية الموجودة في منطقتي الميزرة والعين الفايضة غير صالحة للاستخدام في الزراعة، بناءاً على نتائج قياسات التوصيل الكهربائي ونسبة ادمصاص الصوديوم، إلا إذا تم خلطها مع مصدر مياه آخر كمياه المجاري المعالجة.
- أوضحت النتائج الجيوفيزيائية الوضع الطبقي للمنطقة، والتي لها انعكاسات مباشرة على الوضع الهيدرولوجي لخزانات منطقة الدراسة، كما أوضحت أماكن الربط بين الخزانات الموجودة في تلك المنطقة.
- أظهرت نتائج دراسة النظائر المستقرة لعنصري الهيدروجين والأكسجين أنها أخف في منطقة الميزرة مقارنة بالمناطق الأخرى في منطقة الدراسة مما يدل على أن جبل حفيت هو مكان التغذية الرئيسي للخزانات المائية الجوفية الموجودة في المنطقة، والتي تتم عادة عن طريق مياه الأمطار. كما أظهرت أيضاً أن جبل حفيت يحتوي على مياه جوفية تكونت أثناء تكون الجبل وتختلف في خواصها عن مياه الأمطار.

ملخص الرسالة

شهدت دولة الإمارات في السنوات الماضية نهضة تنموية شاملة غير مسبوقة أثرت في مختلف أوجه الحياة فيها. وبالرغم من الفوائد والمستويات العالية من الرفاهية التي حققتها تلك النهضة في فترة زمنية قصيرة نسبياً، إلاّ أنها شكلت ضغوطاً على الموارد الطبيعية، خاصة موارد المياه والطاقة.

وقد أولت الدولة اهتماماً بالغاً بتنمية البنية التحتية في قطاعات الصحة والتعليم والعمران والزراعة ، ولم يستثنى قطاع السياحة والترفيه من هذه التنمية ، حيث قامت بإنشاء الكثير من الحدائق والمنتزهات والمسطحات الخضراء التي يقصدها الكثير من المواطنين والمقيمين على أرض الدولة.

وتعد منطقة المبزرة (موضوع الدراسة) والتي تقع جنوب مدينة العين عند سفح جبل حفيت، واحدة من أجمل المناطق السياحية في الإمارات بعد التوجيهات السامية لصاحب السمو الشيخ زايد بن سلطان آل نهيان "طيب الله ثراه" والذي أوصى بعد تفجر المياه من آبارها بتحويل هذه المنطقة إلى منطقة سياحية و الاستفادة من هذه المياه والتي دلت المسوحات الجيولوجية فيها إلى وجود المياه بعمق 320 – 600 قدم تحت سطح الأرض، وبإمكانية إنتاجية تصل إلى 25.000 الف جالون في الساعة، وتتفاوت درجة العذوبة هذه المياه ما بين 1.9 الى 17.4 ألف جزء من المليون، ولذلك تم استغلالها في إقامة المزارع وزراعة أشجار النخيل والعشب الأخضر لتحويل هذه المنطقة الجبلية المهجورة التي لم يكن يعرفها أحد إلى منتجع سياحي جميل صار يشهد مئات الزوار يومياً من مختلف أنحاء الإمارات ومن الدول المجاورة، نظراً للفوائد العلاجية والصحية التي تتمتع بها هذه المياه على الرغم من عدم صلاحيتها للشرب والاستهلاك الآدمي.

وفي هذه الدراسة، تم تقييم مصادر المياه الجوفية في منطقة المبزرة ، كما تم مقارنتها بمصادر المياه الجوفية الأخرى الموجودة في منطقة جبل حفيت بوجه عام وخاصة منطقتي العين الفايضة و النعمة من حيث النوعية وأماكن تواجدها ونوعية الخزانات الجوفية الموجودة. ولتحقيق هذا الغرض تم استخدام طريقة المسح الجيوفيزيائي الكهربي ودراسة هيدروجيوكيمياء المنطقة استناداً إلى العينات التي أخذت من الآبار الموجودة في المنطقة، بالإضافة إلى دراسة النظائر المشعة المستقرة لبعض العينات، كما تم الرجوع لبعض الدراسات السابقة عن جيولوجيا وهيدروجيولوجيا المنطقة.

جامعة الإمارات العربية المتحدة
عمادة الدراسات العليا
برنامج ماجستير علوم موارد المياه

عنوان الرسالة

التصوير الجيوكهربي، استقصاءات هيدروكيمياء والنظائر المشعة المستقرة لمنطقة المبزرة ، العين – دولة الإمارات العربية المتحدة

إسم الباحث

فارس ميرغني فتح الله محجوب

المشرفون

م	الاسم	الوظيفة
1	د .أحمد مراد	رئيس قسم الجولوجيا - أستاذ مساعد في جيولوجيا المياه - قسم الجيولوجيا - كلية العلوم – جامعة الإمارات العربية المتحدة.
2	د .أحمد المحمودي	أستاذ مساعد في الجيوفيزياء – مركز دراسات المياه – جامعة الملك فيصل – المملكة العربية السعودية.
3	د .حيدر بكر	أستاذ تطبيقات الجيوفيزياء – أستاذ مساعد في الجيوفيزياء - – قسم الجيولوجيا - كلية العلوم – جامعة الإمارات العربية المتحدة.